Enhanced Air Traffic Flow and Capacity Management under Trajectory Based Operations considering traffic Complexity

MARC MELGOSA

Aeronautical Engineer

Advisors

DR. XAVIER PRATS I MENÉNDEZ

DR. ANDRIJA VIDOSAVLJEVIC

Doctorate program in Aerospace Science and Technology

Department of Physics - Aerospace Engineering Division

Technical University of Catalonia - BarcelonaTech

A dissertation submitted for the degree of

International Doctor of Philosophy

February 2023

Enhanced Air Traffic Flow and Capacity Management under Trajectory Based Operations considering traffic Complexity

Author
Marc Melgosa

Advisor
Dr. Xavier Prats i Menéndez
Dr. Andrija Vidosavljevic

Reviewers
Dr. Andrea Ranieri
Dr. Yan Xu

Thesis committee
Dr. Andrea Ranieri
Dr. Yan Xu
Dr. Leïla Zerrouki

Doctorate program in Aerospace Science and Technology
Technical University of Catalonia - BarcelonaTech
February 2023

PhD. Thesis made in:
Department of Physics - Aerospace Engineering Division
Esteve Terradas, 5
08860 Castelldefels (Barcelona), Spain

Als meus pares, Maria Rosa i Francesc.
A la Raquel.

Contents

List of Figures

Figures in Appendices

List of Tables

List of Publications

The list of publications resulting from this PhD. work is given in inverse chronological order as follows:

- M. Melgosa, L. Zerrouki, P. Terzioski, P. Olivella, and A. Vidosavljevic. 2020 (Jun.). Capacity Management based on the Integration of Dynamic Airspace Configuration and Flight Centric ATC solutions using Complexity. *In: 9th International Conference for Research in Air Transportation. ICRAT*: Eurocontrol/FAA.
- M. Melgosa, X. Prats, Y. Xu, and L. Delgado. 2019 (Sep.). Enhanced demand and capacity balancing based on alternative trajectory options and traffic volume hotspot detection. *In: Proceedings of the 38th Digital Avionics Systems Conference (DASC)*: IEEE/AIAA.

Acknowledgements

Tot i que diuen que fer un doctorat és una tasca solitaria, jo he tingut la sort i el privilegi de sentir-me acompanyat en tot moment. Hi ha hagut un seguit de persones que m'han ajudat i m'han donat el seu suport i companyia a les quals vull donar les més sinceres gràcies.

Primer de tot voldria donar les gràcies al Dr. Xavier Prats. Va ser ell qui em va *rescatar* i em va donar l'oportunitat de dedicar-me a la recerca i gaudir cada dia de la feina que faig. També va ser ell qui em va encoratjar a començar el doctorat. No és d'extranyar, doncs, que en Xevi hagi estat el meu director de tesi i a qui li vull agraïr la seva infinita paciència, els seus consells professionals i personals i les grans revisions que ha fet de la tesi. Moltes gràcies per tot Xevi. In addition, I would like to thank Dr. Andrija Vidosavljevic for his great contribution as co-advisor of this PhD. Many thanks for your advice, for your time, for hosting me twice at Toulouse and for the uncountable time you dedicated to me. I will never thank sufficiently what you did for me.

I am grateful to Dr. Andrea Ranieri and Dr. Yan Xu for their willingness to review this PhD dissertation and their participation as members of the committee. Their valuable insights and constructive feedback have greatly enhanced the quality of my final document. I also extend my sincere thanks to Dr. Leïla Zerrouki for her participation in the committee too. Thank you for your time and dedication.

No em puc oblidar de mencionar els meus companys i amics de la universitat. Aquesta tesi la vaig començar compartint el despatx 121 amb el Dr. Ramon Dalmau, el Dr. Yan Xu i Dr. Leonardo Camargo. Gràcies Ramon per la teva ajuda, el teu suport i la teva amistat. Sempre m'has ajudat quan ho he necessitat, personal i professionalment. I quins grans moments hem passat a Tamariu i amb la Gitan. Many thanks Yan for the time we spent together, I enjoyed a lot and I learned from you. Indeed, this thesis builds upon your previous work, and it would not have been possible without your contributions. I will never forget the time I spent in China with you. Gracias Leo por nuestras charlas y por ser el más *bacano* del despacho. Més tard van arribar el Dr. Raul Saez, la Homeyra Khaledian i la Dra. Jovana Kuljanin. Gràcies Raul per ajudar-me amb els meus infinits dubtes ràpids. I am grateful to Homeyra for being an incredible person and providing a listening ear during my difficulties. And what shall I say about Jovana (or Mrs. Thanks)? Many thanks for always bringing a positive attitude and being ready to offer help whenever needed. Your support is greatly appreciated.

Me gustaría mencionar a Luis Delgado, quien me dió valiosos consejos al principio del doctorado y, sí, acabaremos el paper que tenemos a medias.

Fora de l'ambit acadèmic vull fer una menció als de Fraga, Raul i Geno. Gràcies per cedir-me el despatx on s'ha escrit part d'aquesta tesi però també per animar-me i ajudar-me a desconectar quan ho he necessitat. I clar, no em puc oblidar del Bifi, el gosset que m'ha fet companyia quan ha estat amb mi.

També voldria donar les gràcies als meus pares, Maria Rosa i Francesc. Tot el que he aconseguit us ho dec a vosaltres i a l'absoluta confiança i dedicació que m'heu dedicat. Sou part d'aquesta tesi. Moltes gràcies per ser-hi.

Per últim, vull donar les gràcies a la persona que més m'ha ajudat i que sempre està al meu costat, la Raquel. La paraula infinita és queda curta quan penso en la paciència que has tingut amb mi. Quantes vegades hem endarrerit el viatge a Nova York? Posem ja la data? De nou, moltes gràcies. No existiria aquesta tesi sense tu.

Barcelona, Febrer de 2023
Marc Melgosa

Abstract

The Air Traffic Flow and Capacity Management (ATFCM) aims at maintaining the forecast traffic demand below the estimated capacity in airports and airspace sectors. The purpose is to maintain the workload of the air traffic controllers under safe limits and avoid overloaded situations. Since the air traffic demand has recovered values close to those achieved before the COVID-19 pandemic, the ATFCM processes still require improvements in order to avoid the significant flight delays experienced some years ago.

At present, the demand and the capacity management initiatives are deployed separately. Given a forecast traffic demand, the different air navigation service providers allocate their air traffic control resources providing the airspace sectorisations. Then, the network manager addresses the remaining overloads by allocating delay using the Computer-Assisted Slot Allocation (CASA) algorithm based on a ration-by-schedule principle. It should be noted that some ad-hoc flights might be re-rerouted or limited in cruise altitude in order to avoid congested airspace by submitting a new flight plan. Hence, the previously chosen sectorisations may be not optimum once the demand management initiatives are deployed. Moreover, the flexibility of the airspace users is limited since they cannot express their preferences. Furthermore, the demand and the capacity are currently measured using entry counts as proxy of the air traffic control workload, which is rather easy to measure or estimate. Yet, this metric cannot evaluate the difficulty to handle different traffic patterns inside the sectors leading to the use of capacity buffers.

This PhD focuses on overcoming the limitations of the current ATFCM system outlined before by the introduction of complexity metrics (instead of entry counts) in order to measure the traffic load, the better consideration of the airspace users preferences allowing the possibility of submitting alternative trajectories to avoid congested airspace, and the holistic integration of the demand and capacity management into the same optimisation problem.

First, the integration of two capacity management initiatives, i.e. Dynamic Airspace Configurations (DAC) and Flight Centric Air Traffic Control (FCA), is studied proving some benefits when such integration is dynamic. Next, a new concept of operation is proposed where the airspace users have the option of submitting alternative trajectories and the network manager is the responsible for the demand management (delay allocation and choice of the used trajectory) and the capacity management (selection of the airspace sectorisation), considering a network-wide optimisation. This concept of operations is mathematically modelled with two Demand and Capacity Balancing (DCB) models addressing only demand management and three holistic DCB

models where the demand and the capacity management measures are considered together in the same optimisation problem.

A first model aims at choosing the best trajectory and delay allocation per flight while analysing the traffic load with entry counts at traffic volume level. It is solved in a realistic case study using the historical regulations providing a 76.84% of reduction in the arrival delay if compared to the current system.

One of the three holistic DCB models formulated in this PhD, i.e. the one that uses complexity metrics and includes the optimisation of the opening scheme by choosing the used configurations, is studied in detail. This model is addressed with a new Hybrid method introduced in this PhD based on Simulated Annealing and Dynamic programming. In a first case study, this new method is compared with the exact method solved by Gurobi providing better performance principally when the difficulty of the problem increases. In a second case study a sensitivity study of the parameter that models a penalty for different consecutive configurations is conducted. Finally, a big scale scenario is solved with the Hybrid method providing a 74.01% less of arrival delay and a 28.47% less in the cost of open sectors compared with a baseline scenario representing the best conditions of the current system.

Resumen

La gestión de los flujos de tráfico y de la capacidad (ATFCM) tiene como objetivo mantener la demanda de tráfico prevista por debajo de la capacidad estimada de los aeropuertos y los sectores del espacio aéreo. El propósito es mantener la carga de trabajo de los controladores de tráfico aéreo por debajo de unos niveles seguros y evitar situaciones de sobrecarga. Dado que la demanda de tráfico aéreo ha recuperado valores cercanos a los anteriores a la pandemia de COVID-19, los procesos de ATFCM todavía requieren de mejoras para evitar los altos valores de retraso experimentados hace algunos años.

Actualmente, las iniciativas de gestión de la demanda y las iniciativas de gestión de la capacidad se implementan por separado. Ante una demanda de tráfico prevista, los diferentes proveedores de servicios de navegación aérea asignan sus recursos de control de tráfico aéreo proporcionando las sectorizaciones del espacio aéreo. Después, el administrador de la red trata las sobrecargas restantes mediante la asignación de retrasos utilizando el algoritmo de asignación de franjas horarias asistido por ordenador (CASA) basado en un principio de ordenación por orden de llegada. Cabe señalar que a algunos vuelos también se les puede cambiar de ruta o limitar la altitud de crucero para evitar la congestión del espacio aéreo requiriendo de un nuevo plan de vuelo. Así pues, las sectorizaciones elegidas anteriormente pueden no ser óptimas una vez que se implementen las iniciativas de gestión de la demanda. Adicionalmente, la flexibilidad de los usuarios del espacio aéreo es limitada ya que no pueden expresar sus preferencias. Además, la demanda y la capacidad se miden actualmente contando el número de llegadas como proxy de la carga de trabajo del control del tráfico aéreo ya que es bastante fácil de medir o estimar. Sin embargo, esta métrica no puede evaluar la dificultad de controlar diferentes patrones de tráfico dentro de los sectores lo que conduce al uso de márgenes de capacidad.

Este PhD se centra en superar las limitaciones del sistema de ATFCM actual descritas anteriormente mediante la introducción de métricas de complejidad (en lugar del número de llegadas) para medir la carga de tráfico, la mejor consideración de las preferencias de los usuarios del espacio aéreo permitiendo la posibilidad de la presentación de trayectorias alternativas para evitar la congestión del espacio aéreo, y la integración holística de la gestión de la demanda y de la capacidad en un mismo problema de optimización.

Primero, se estudia la integración de dos iniciativas de gestión de la capacidad, la configuración dinámica del espacio aéreo (DAC) y el control del tráfico aéreo centrado en el vuelo (FCA), demostrando algunos beneficios cuando dicha integración es dinámica. A continuación, se pro-

pone un nuevo concepto operacional donde los usuarios del espacio aéreo tienen la opción de presentar trayectorias alternativas y el administrador de la red es el responsable de la gestión de la demanda (asignación de retrasos y elección de la trayectoria utilizada) y la gestión de la capacidad (selección de la sectorización), considerando una optimización de toda la red. Este concepto operacional se modela matemáticamente con dos modelos de equilibrio de la demanda y la capacidad (DCB) que abordan sólo la gestión de la demanda y tres modelos holísticos donde las medidas de gestión de la demanda y de la capacidad se consideran conjuntamente en el mismo problema de optimización.

Un primer modelo tiene como objetivo elegir la mejor asignación de trayectoria y retraso por vuelo mientras se analiza la carga de tráfico con el número de llegadas a nivel de volumen de tráfico. Se resuelve un caso de estudio realista utilizando las regulaciones históricas proporcionando un 76.84 % de reducción en el retraso en la llegada si se compara con el sistema actual.

Uno de los tres modelos holísticos de DCB formulados en este PhD se estudia en detalle, en concreto el que utiliza métricas de complejidad y optimiza las sectorizaciones del espacio aéreo escogiendo entre un conjunto de configuraciones disponibles. Este modelo se trata con un nuevo método híbrido presentado en este PhD basado en el recocido simulado y la programación dinámica. En un primer caso de estudio, se compara este nuevo método con el método exacto resuelto con Gurobi proporcionando un mejor rendimiento principalmente cuando aumenta la dificultad del problema. En un segundo caso de estudio se realiza un estudio de sensibilidad del parámetro que modela una penalización para diferentes configuraciones consecutivas. Finalmente, se resuelve un escenario a gran escala con el método Híbrido proporcionando un 74.01 % menos de retraso en la llegada y un 28.47 % menos en el coste de la sectorización resultante en comparación con un escenario de referencia que representa las mejores condiciones del sistema actual.

Resum

La gestió dels fluxos de trànsit i de la capacitat (ATFCM) té com a objectiu mantenir la demanda de trànsit prevista per sota de la capacitat estimada dels aeroports i els sectors de l'espai aeri. El propòsit és mantenir la càrrega de treball dels controladors de trànsit aeri sota uns nivells segurs i evitar situacions de sobrecàrrega. Com que la demanda de trànsit aeri ha recuperat valors propers als anteriors a la pandemia de COVID-19, els processos d'ATFCM encara necessiten de millores per tal d'evitat els alts valors de retard obtinguts en anys anteriors.

Actualment, les iniciatives de gestió de la demanda i les iniciatives de gestió de la capacitat es duen a terme de manera separada. Donada una previsió de demanda de trànsit, els diferents proveïdors de serveis de navegació aèria assignen els seus recursos de control del trànsit aeri proporcionant les sectoritzacions de l'espai aeri. Després l'administrador de la xarxa tracta les sobrecàrregues restants mitjançant l'assignació de retards utilitzant l'algoritme d'assignació de franges horàries assistit per ordinador (CASA), que es basa en l'ordenació per ordre d'arribada. Cal senyalar que a alguns vols també se'ls pot canviar la ruta o se'ls pot restringit l'altitud del creuer per tal d'evitar zones congestionades requerint la presentació d'un nou pla de vol. Així doncs, les sectoritzacions prèviament escollides poden ser no òptimes una vegada s'implementin les iniciatives de gestió de la demanda. A més, la flexibilitat dels usuaris de l'espai aeri és limitada ja que no poden expressar les seves preferències. Altrament, la demanda i la capacitat es mesuren actualment comptant el nombre d'arribades com a proxy de la càrrega de treball del control del trànsit aeri, ja que és bastant fàcil de mesurar o estimar. No obstant això, aquesta mètrica no pot evaluar la dificultat de gestionar diferents patrons de trànsit dins els sectors, la qual cosa condueix a la utilització de marges de capacitat.

Aquest PhD es centra en superar les limitacions de l'actual sistema d'ATFCM indicades anteriorment mitjançant la introducció de mètrics de complexitat (en lloc del número d'arribades) per a mesurar el trànsit, la millor consideració de les preferències dels usuaris de l'espai aeri permetent la possibilitat d'utilitzar trajectories alternatives per a evitar la congestió de l'espai aeri, i la integració holística de la gestió de la demanda i de la capacitat en el mateix problema d'optimització.

Primer, s'estudia la integració de dues iniciatives de gestió de la capacitat: la configuració dinàmica de l'espai aeri (DAC) i el control del trànsit aeri centrat en el vol (FCA). S'obtenen beneficis especialement quan la integració és dinàmica. Després, es proposa un nou concepte operacional on els usuaris de l'espai aeri tenen l'opció de proposar trajectories alternatives i l'administrador

de la xarxa és el responsable de la gestió de la demanda (assignació de retards i elecció de la trajectòria utilitzada) i de la capacitat (selecció de la sectorització de l'espai aeri) considerant l'optimització de tota la xarxa. Aquest concepte operacional es formula matemàticament amb dos models d'equilibri de demanda i la capacitat (DCB) que aborden només la gestió de la demanda i tres models holístics on la gestió de la demanda i de la capacitat es consideren conjuntament en el mateix problema d'optimització.

Un primer model es centra en escollir la millor trajectòria i assignació de retard per vol, mentre que el trànsit s'avalua mitjançant el número d'arribades als volums de trànsit. Es resol un cas d'estudi realista on s'utilitzen les regulacions històriques aconseguint un 76.84% menys de retard a l'arribada si es compara amb els sistema actual.

Un dels tres models holístics de DCB formulats en aquest PhD s'estudia en detall, en concret el que utilitza mètriques de complexitat i optimitza les sectoritzacions de l'espai aeri escollint entre un seguit de configuracions disponibles. Aquest model es tracta amb un nou mètode híbrid presentat en aquest PhD i que combina la simulació del recuit i la programació dinàmica. En un primer cas d'estudi, aquest nou mètode es compara amb el mètode exacte resolt amb Gurobi proporcionant un millor rendiment principalment quan la dificultat del problema augmenta. En un segon cas d'estudi es realitza un estudi de sensibilitat del paràmetre que modela una penalització per a diferents configuracions consecutives. Finalment, es resol un escenari a gran escala amb el mètode híbrid proporcionant un 74.01% menys de retard a l'arribada i un 28.47% menys en el cost de la sectorització resultant en comparació amb un escenari de referència que representa les millors condicions del sistema actual.

Notation

$\mathcal{F}$	Set of flights
$\mathcal{T}$	Set of instants of time
$\mathcal{P}$	Set of periods of time
$\mathcal{T}^p \subset \mathcal{T}$	Set of instants of times in the period $p, \forall p \in \mathcal{P}$
$\mathcal{T}_k^v \subset \mathcal{T}$	Set of instants of times when trajectory k can potentially arrive at the traffic volume v, $\forall k \in \mathcal{K}, \forall v \in \mathcal{V}$
$\mathcal{K}$	Set of all trajectories
$\mathcal{K}_f \subset \mathcal{K}$	Set of trajectories for flight $f, \forall f \in \mathcal{F}$
$\mathcal{V}$	Set of traffic volumes
$\mathcal{V}_k$	Set of traffic volumes that the trajectory k crosses
$\mathcal{S}_{\mathrm{E}}$	Set of elementary sectors
$\mathcal{S}_{\mathrm{C}}$	Set of collapsed sectors
$\mathcal{S} = \mathcal{S}_{\mathrm{E}} \cup \mathcal{S}_{\mathrm{C}}$	Set of operating sectors
Λ	Set of configurations
Λ^s	Set of configurations that contain the operating sector $s, \forall s \in \mathcal{S}$
$\mathcal{E}^s$	Set of elementary sectors in operating sector $s, \forall s \in \mathcal{S}$
$\mathcal{S}^{s_{\mathrm{E}}}$	Set of operating sectors that contains the elementary sector $s_{\mathrm{E}}, \forall s_{\mathrm{E}} \in \mathcal{S}_{\mathrm{E}}$
$\mathcal{S}_a^p$	Set of active operating sectors during the period $p, \forall p \in \mathcal{P}$
$\underline{\mathcal{T}}_k^v$	First instant of time when the trajectory k can arrive at traffic volume v
$\overline{\mathcal{T}}_k^v$	Last instant of time when the trajectory k can arrive at traffic volume v
J_k	Total cost of trajectory $k, \forall k \in \mathcal{K}$
J_{F_k}	Cost of fuel of trajectory $k, \forall k \in \mathcal{K}$
J_{D_k}	Cost of arrival delay of trajectory $k, \forall k \in \mathcal{K}$
J_{T_k}	Cost of trip time of trajectory $k, \forall k \in \mathcal{K}$
R_k	Cost of route charges for trajectory k, $\forall k \in \mathcal{K}$
$\bar{J}_k$	Cost of the initial submitted trajectory of the flight associated with trajectory $k, \forall k \in \mathcal{K}$
$\bar{J}_{\mathrm{F}_k}$	Cost of fuel of the initial submitted trajectory of the flight associated with trajectory $k, \forall k \in \mathcal{K}$
$\bar{J}_{\mathrm{D}_k}$	Cost of arrival delay of the initial submitted trajectory of the flight associated with trajectory $k, \forall k \in \mathcal{K}$
$\bar{J}_{\mathrm{T}_k}$	Cost of time of the initial submitted trajectory of the flight associated with

	trajectory $k, \forall k \in \mathcal{K}$
$\bar{R}_k$	Cost of route charges of the initial submitted trajectory of the flight associated with trajectory k, $\forall k \in \mathcal{K}$
r_k^v	Estimated time of arrival of trajectory k at traffic volume v, $\forall k \in \mathcal{K}, \forall v \in \mathcal{V}$
v_k^*	The next traffic volume that the trajectory k crosses after v
$\underline{\mathcal{V}_k}$	First traffic volume that the trajectory k crosses
$\overline{\mathcal{V}_k}$	Last traffic volume that the trajectory k crosses
α_k	Arrival delay unit cost for trajectory k, $\forall k \in \mathcal{K}$
β_k	Fuel unit cost for trajectory k, $\forall k \in \mathcal{K}$
F_k	Trip fuel used in trajectory k, $\forall k \in \mathcal{K}$
T_k	Trip time of trajectory k, $\forall k \in \mathcal{K}$
D_k	Ground delay of trajectory k, $\forall k \in \mathcal{K}$
$\bar{T}_k$	Trip time of the initial submitted trajectory of the flight associated with trajectory k, $\forall k \in \mathcal{K}$
$\bar{J}_k$	Cost of operating the initial submitted trajectory of the flight associated with trajectory k, $\forall k \in \mathcal{K}$
$H^{t,s}$	Complexity threshold of sector s at time t, $\forall t \in \mathcal{T}$, $\forall s \in \mathcal{S}$
$H^{p,v}$	Entry count threshold of traffic volume v during the period p, $\forall v \in \mathcal{V}$, $\forall p \in \mathcal{P}$
$\theta^{p,s}$	Cost of opening sector s during the period p, $\forall p \in \mathcal{P}$, $\forall s \in \mathcal{S}$
ρ	Penalty cost of allocating one elementary sector to a different operating sector

List of Acronyms

ACC	Area Control Center
AFP	Airspace Flow Program
AIRAC	Aeronautical Information Regulation and Control
ANSP	Air Navigation Service Provider
ASM	Airspace Management
ATC	Air Traffic Control
ATCO	Air Traffic Controller Officer
ATFCM	Air Traffic Flow and Capacity Management
ATM	Air Traffic Management
ATS	Air Traffic Services
AU	Airspace User
B&B	Branch and Bound
CARATS	Collaborative Actions for Renovation of Air Traffic Systems
CASA	Computer-Assisted Slot Allocation
CDM	Collaborative Decision Making
CG	Complexity Generator
CI	Cost Index
COTTON	Capacity optimisation in trajectory-based operations
CTOP	Collaborative Trajectory Options Program
CWP	Controller Working Position
DAC	Dynamic Airspace Configurations
DAS	Dynamic Airspace Sectorisation
DCB	Demand and Capacity Balancing
DDR2	Demand Data Repository 2
ECAC	European Civil Aviation Conference
ENAC	Ecole Nationale de l'Aviation Civile
ETFMS	Enhanced Tactical Flow Management System
FABEC	Functional Airspace Block Europe Central
FCA	Flight Centric Air Traffic Control
FI	Flight Intention
FMP	Flow Management Positions
FMS	Flight Management System
FP	Flight Plan
GANP	Global Air Navigation Plan
GDP	Ground Delay Program

ICAO	International Civil Aviation Organization
ICO	Improved Configuration Optimizer
ILP	Integer Linear Programming
LB	Lower Bound
LP	Linear Programming
MAGHP	Multi-Airport Ground-Holding Problem
MILP	Mixed Integer Linear Programming
MINLP	Mixed Integer Nonlinear Programming
MIP	Mixed Integer Program
MPL	Maximum Payload
NextGen	Next Generation Air Transportation System
NLP	Nonlinear Programming
NM	Network Manager
PHARE	Programme for Harmonised ATM Research in EUROCONTROL
PI	Performance Indicator
RAD	Route Availability Document
RBS	Ration-by-Schedule
SAGHP	Single-Airport Ground Holding Problem
SES	Single European Sky
SESAR	Single European Sky ATM Research
TBO	Trajectory Based Operations
TMI	Traffic Management Initiative
TMV	Traffic Monitoring Value
TOS	Trajectory Options Set
TV	Traffic Volume
UB	Upper Bound
UDPP	User-Driven Prioritisation Process

I
Introduction

The Air Traffic Management (ATM) system is recurrently performing with overloaded airspace and/or airports. In such situations, Air Traffic Flow and Capacity Management (ATFCM) measures are typically deployed in order to maintain the forecast demand below the forecast capacity by the allocation of delay (EUROCONTROL, 2017). For example, the 9.6% of the European flights were delayed by en-route ATFCM measures in 2018 (EUROCONTROL, 2018). This value, increased to the 9.9% in 2019, although the total en-route ATFCM delay fell by the 9.0%, and 2019 was the second highest year with respect to en-route ATFCM delay since 2010 (EUROCONTROL, 2020a). Due to the COVID-19 outbreak at the beginning of 2020, the air traffic experienced in 2020 and in the first half of 2021 a historical minimum. Nevertheless, the situation at the end of 2022 is recovering the values from before the COVID-19 pandemic. The majority of European states experienced a prosperous summer, but the network is still disrupted by the Russian invasion of Ukraine (EUROCONTROL, 2022). Thus, the improvement of ATFCM models and methodologies remains as one of the big challenges in current ATM research in order to protect the ATM system from overloaded traffic situations, but also aiming to make operations as efficient as possible in response to the increasing concerns in the environmental impact of the air transportation.

ICAO (2016) defines ATM as: *The dynamic, integrated management of air traffic and airspace including air traffic services, airspace management and air traffic flow management — safely, economically and efficiently — through the provision of facilities and seamless services in collaboration with all parties and involving airborne and ground-based functions.* Hence, the main ATM services are typically divided in:

- Air Traffic Services (ATS), which includes Alert Services, Flight Information Services and Air Traffic Control (ATC) services. ATC aims at maintaining a minimum separation between aircraft (when airborne or at ground) and at maintaining an orderly and expeditious flow of air traffic (ICAO, 2001). ATC services are provided by one or a pair of Air Traffic Controller Officers (ATCOs) within a volume of airspace called *sector*.

- ATFCM, that aims at balancing the demand and the capacity by optimising the utilization of the available resources and coordinating appropriate actions in order to improve the quality of service and the performance of the ATM system (Network Manager, 2018).
- Airspace Management (ASM), which is focused at the strategic scope and it consists in the design of the airspace as efficiently as possible in order to satisfy the needs of the different users, both civil and military. The design of new routes, procedures and new sector configurations are among the main functions of ASM.

This thesis is mainly focused on the ATFCM activities and aims at improving current Demand and Capacity Balancing (DCB) processes.

I.1 Current ATFCM

In the context of ATFCM, three main stakeholders are identified:

1. the Airspace Users (AUs), as airlines, flight operators or military/state aircraft, who generate the traffic *demand*;
2. the Air Navigation Service Providers (ANSPs), in charge of providing air traffic services (ATS) and manage the airspace, who provide *capacity* ; and
3. the Network Manager (NM), which has the global picture and can be in charge of balancing demand and capacity in the entire network.

The main objective of ATFCM is to keep the forecasted traffic demand below the available capacity at the airports and in the airspace sectors. Different ATFCM processes are deployed, from the most strategic planning to the execution of the operations, and the NM considers the best available information at each planing horizon for the demand and capacity forecasting.

I.1.1 Demand management

In the strategic phase, from one year to one week before the operations, aggregated predictions of traffic flows are done in order to identify potential hotspots (i.e. where a demand/capacity imbalance is detected). The traffic prediction is done based on historical data, economic trends and considering seasonal effects, together with the available Flight Intentions (FIs) from the AUs.

The pre-tactical phase takes place from six to one day before operations, when the most of the Flight Plans (FPs) have not been filed yet (FPs are typically filled few hours before the departure time and could be updated by the AUs until the very last moment). In this situation, the FIs are still the most valuable traffic information and they include the flight callsign, the airline, the origin and destination airports, the estimated schedule time and the aircraft model. Yet, the actual trajectory is still not available because there is no information about the lateral route or the requested flight level (Mateos *et al.*, 2020). In Europe, the NM uses the PREDICT tool for trajectory prediction at this pre-tatical stage (EUROCONTROL, 2014). This information is used as well by the ANSPs, in order to facilitate the allocation of their capacity resources.

The tactical phase in ATFCM takes place at the day of operations. In this phase the traffic demand is evaluated through the FPs and the traffic predictions are done at short term using, in Europe, the Enhanced Tactical Flow Management System (ETFMS), which is the system that finally allocates delay by running the Computer-Assisted Slot Allocation (CASA) algorithm based on the Ration-by-Schedule (RBS) algorithm (first in first out strategy) (EUROCONTROL, 2017). With CASA, the demand is shifted in time in order to be below the declared capacity as shown in Figure I-1.

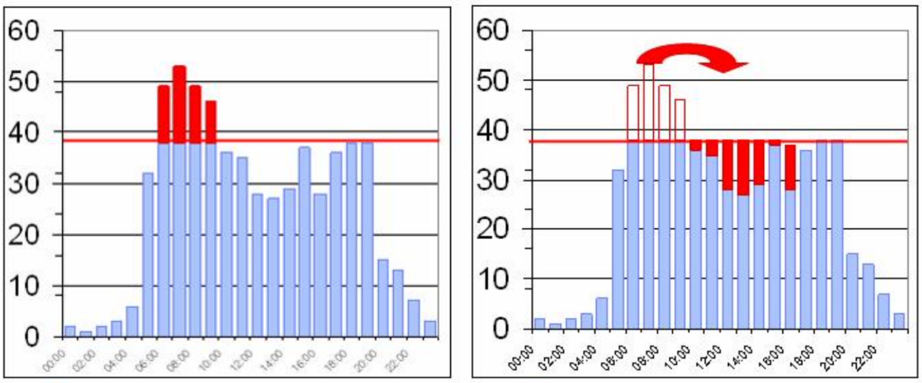

Figure I-1: *Illustrative example of delay allocation*

A part of delay allocation, other strategies like level capping or re-routing are currently used. Yet, these strategies are not integrated and automated in the DCB algorithms and are proposed ad hoc to certain flights. Both requires a FP re-submission indicating a change on the flight level (level capping) or a change in the lateral trajectory (re-routing).

Although the delay allocation based on RBS is accepted by the aviation community beacuse of its fairness criterion (Brinton *et al.*, 2010), it does not guaranty the optimality and it does not take into account the AU preferences. This PhD aims at overcoming the limitations of the current system by abandoning the first in first out strategy when the delay is allocated and considering the use of alternative trajectories (proposed by the AUs) into the same network optimisation problem.

I.1.2 Airspace management and capacity provision

The airspace under the responsibility of an Area Control Center (ACC) is divided in portions of airspace volumes, named elementary sectors, where ATC functions can be deployed efficiently and safely. These elementary sectors can be grouped together forming bigger airspace units called collapsed sectors. How the full airspace of an ACC is divided in operating sectors is called airspace configuration or sectorisation. The ACCs *open* different predefined configurations along the day in order to adapt the capacity profile to the expected demand. The list of used configurations with its opening/closing times is called the opening scheme.

Different capacity management decisions are taken depending on the ATFCM phase. The strategic phase contributes to the allocation of the fixed ATCOs resources for an upcoming season (summer or winter) and up to a year in advance. Note that this ATCO allocation restricts further capacity modifications at later stages. During the pre-tactical phase, the airspace sector opening scheme is defined considering the updated traffic demand and the ATCOs resources defined in the strategic phase. At the tactical phase, the information of traffic is constantly updated thought the flight plans and the opening scheme can be adjusted in order to deal with unexpected events (not predicted during the strategic and pre-tactical phase).

Thus, the capacity management nowadays is done by the definition of the opening scheme, based on the wise choice of predefined sector configurations along the day. This approach, however, is highly structured and fixed and it may not be flexible and responsive enough to face the increasing traffic demand (Treimuth, 2018). For this reason, this PhD proposes additional capacity management levels based on dynamic airspace configurations.

I.1.3 Demand and capacity balancing

In current operations, the NM applies regulations to the traffic, shifting the demand in order to accommodate it to the available capacity reported by the ANSPs.

Airspace and capacity management, in turn, are part of the ANSP functions. It is worth noting that the ANSPs are who decide whether an overloaded sector should be regulated or not, based on the type of overload (sustained or peak, for instance), the type of flows in the sector, and many other operational and expert judgement considerations. In Europe this is done in the Flow Management Positionss (FMPs) that are located at each ACC and which link, in fact, the NM with the different ANSPs.

Thus, the demand and capacity management in the current operations is still managed by two separated services with limited performance at system level. For this reason, this PhD proposes a new concept operation where the NM is the responsible for both demand and capacity management leading to a seamless integration.

I.1.4 Traffic Management Initiatives

ATFCM processes aim at maintaining the traffic demand below the capacity when the network is overloaded, situation that happens when the demand is too high and/or when capacity is reduced (as for example due to disruptive weather or staffing limitations) and leads to the application of Traffic Management Initiatives (TMIs) known as *regulations* in Europe.

In Europe, ATFCM is provided by the NM through the application of regulations consisting on the assignment of ground delay. The ATFCM slot allocation is done by the CASA algorithm (EUROCONTROL, 2017), based on rules agreed and accepted by relevant ATM stakeholders.

In the United States, Ground Delay Programs (GDPs) and Airspace Flow Programs (AFPs) are the most commonly used TMIs. GDPs assign departure delays in order to manage the demand at the arrival airport. On the other hand, AFPs focus on constrained en-route elements, i.e., Flow Constrained Areas (FCA) (FAA, 2009). The AFPs offer two different solutions to tackle the constrained area: delaying flights or specifying alternative routes that bypass the capacity-constrained area. Then, the aircraft operator concerned can choose either alternative (re-route or delay) (Pourtaklo & Ball, 2009).

The abovementioned regulations or TMIs use a RBS algorithm as basis for the flight scheduling, which is accepted by the aviation community due to its fairness (Brinton *et al.*, 2010). This methodology, however, has limited flexibility for taking into account the AUs preferences and could be improved to be better aligned with the new concept of operations proposed by SESAR[1] in Europe and NextGen[2] in the United States. In this context, Collaborative Decision Making (CDM) initiatives have already been introduced for enabling the airspace user involvement and to provide more flexibility in the route selection (EUROCONTROL, 2017). Under this scope, in the United States, the GDP concept with RBS was extended with flight substitutions and the cancellation-compression algorithm, allowing more flexibility to the airspace users for satisfying their own policies (Ball *et al.*, 2005). Regarding the AFPs, the CDM concept was introduced with the Collaborative Trajectory Options Program (CTOP), where the airspace users are able to communicate their preferences in terms of route selection using Trajectory Options Sets (TOSs) (FAA, 2014). The CDM philosophy was introduced in Europe through the User-Driven Prioritisation Process (UDPP), that allows the AUs to redistribute the delay across its fleet by granting more

[1] Single European Sky ATM Research
[2] Next Generation Air Transportation System

priority to flights with higher economic value over flights with lower economic value (Pilon *et al.*, 2016). Although the full UDPP concept is still under development, the Enhanced Slot Swapping feature was deployed to operations in May 2017 (Ruiz *et al.*, 2019).

All previous measures are applied at the pre-tactical and tactical phases of ATFCM. In Europe, some strategic actions are taken as well with the application of the Route Availability Document (RAD), which specifies a set of restrictions in some routes. For instance, cruise altitude constraints for specific routes or segments, route (and/or altitude) constraints for certain origin/destination airports, etc. The purpose of these RAD is to prevent (strategically) congestion in certain airspace imposing some restrictions beforehand, at the flight planning stage (EUROCONTROL, 2019). Therefore, the flight plans submitted by the AUs do not always reflect their real intentions since they are restricted by the RAD constraints, or the suggested re-routing and level capping indications. In this context, it has been reported that AUs fly longer routes in certain situations to avoid more expensive airspace (en-route charges) (Delgado, 2015), or to avoid possible congestion (Marcos *et al.*, 2018). This PhD aims at better considering the AU preferences maintaining as much as possible their real intentions.

I.1.5 Metrics for measuring demand and capacity

ATFCM processes, by definition, seek to keep traffic demand below capacity. As a result, both demand and capacity must be measured. The idea behind is to keep the ATC controller workload below a safety threshold so that ATC services are delivered with the appropriate level of safety.

Nowadays, the DCB methods in operations rely on the use of Traffic Monitoring Values (TMVs) such as entry counts (Figure I-1 is a example of regulation based on entry counts) and occupancy counts as a proxy for the ATC controller workload. The entry counts metric is defined as the number of aircraft that enter in a sector during a period of time, while the occupancy counts metric is defined as the number of aircraft that are inside a sector during a period of time. Entry/occupancy counts are just guidelines for the ATFCM actors to "monitor" the traffic loads but each individual ATFCM actor will apply different logic to each traffic situation being more subjective than objective. This difference in opinion of workload, in addition to the uncertainty of the trajectories, lead to the use of capacity buffers. This entails, in turn, a nominal capacity that is, in general, below the real capacity that could be offered (COTTON Consortium, 2018a,b; Gomez Comendador *et al.*, 2019).

Although entry and occupancy counts have been used as proxy of the ATC workload because of their simplicity, the harmonisation of the traffic or the difficulty required to control a given situation can not be evaluated through these simple metrics. For this reason, a large number of researchers have been focused on the development of complexity metrics able to measure more factors representative of the ATC workload. Although SESAR Joint Undertaking (2016) defines complexity as the *"...measure of the difficulty that a particular traffic situation will present to an air traffic controller..."*, none of the proposed metrics in the literature has been proven superior to all the others. This PhD aims to include complexity into the DCB methodolgies but it is not constrained to any particular complexity metric.

I.2 Motivation of this PhD

In the previous section, current ATFCM operations are outlined and some challenges have already been identified. This room for improvement, together with the new paradigm in ATM that is envisioned by initiatives like Single European Sky ATM Research (SESAR) in Europe, Next Generation Air Transportation System (NextGen) in the United States, ONESky in Australia and Collabora-

Table I-1: *Capacity elements given in each model (i.e., given inputs for the airspace capacity management optimisation)*

	Model 0	Model I	Model II	Model III	Model IV
Elementary sectors	✓	✓	✓	✓	✓
Collapsed sectors	✓	✓	✓	✓	
Configurations	✓	✓	✓		
Opening scheme	✓	✓			
	Entry counts		**Complexity**		

tive Actions for Renovation of Air Traffic Systems (CARATS) in Japan, drive the main motivation of this PhD thesis.

I.2.1 Holistic demand and capacity management

The demand management and the capacity management, are typically deployed independently, since the demand side is managed by the NM and the capacity side by the different air traffic control centers (which might be also managed by different ANSPs, as it happens in Europe). This leads to airspace sectorisations that are designed considering the initially planned demand, which may differ from the real traffic demand once the delay allocation and potential pre-tactical re-routings have been applied. In other words, the resulting sectorisation may not be optimal once the demand management initiatives have been deployed.

The integration of both demand and capacity management initiatives into a single optimisation problem was introduced by Xu *et al.* (2018b), where delay allocation and potential pre-tactical re-routing were considered at the same time that the sector opening scheme was chosen from a predefined set of configuration options. Xu *et al.* (2020b) extended this formulation in order to find the optimal sector opening scheme given a predefined set of operating sectors (i.e. sector configurations were not fixed beforehand).

Table I-1 depicts the airspace elements that are considered as known or given for the different DCB models presented in Chapters V and VI (i.e., that are not subject to optimisation).

I.2.2 Include AUs preferences into the DCB decision making

Although a first attempt for considering the AUs preferences is introduced through the CDM and UDPP initiatives, they are still not flexible enough, since they only offer to the AUs the possibility of prioritisation among their flights. It would be desirable, for instance, to allow the AUs the possibility to submit different options to avoid the same hotspot.

Current DCB methodologies consist of the delay allocation to the corresponding flights. A part of the delay allocation, the re-routing option can be considered as DCB mechanism by using trajectories that avoid hotspots (airspace sectors with more demand than capacity). Those hotspots (which are time-varying) can be anticipated in advance and this PhD assumes that this information is translated into lateral/vertical avoidance requirements that can be shared with the AUs in order to offer them the possibility of submitting new alternative trajectories. Although the FPs are typically submitted in the tactical phase, in this PhD it is assumed that AUs will be prompt to collaborate by submitting the FPs, along with the the alternative trajectories, during the pre-tactical phase.

This PhD considers the re-routing options given by the AUs together with the delay allocation. Hence, the DCB problem consists of choosing the best trajectory per each flight as well as the best option of delay allocation.

I.2.3 Use of complexity metrics

As previously explained, the current ATFCM processes rely on entry/occupancy counts as proxy of the controller's workload. Yet, the workload than one traffic situation creates does not depend only on the number of aircraft that enter to one sector or are simultaneously presented in the sector. How the traffic is distributed in a sector greatly affects the workload of the controller.

For example, in Figure I-2(a), there are three flights in a sector, but they are flying in parallel and no risk of loosing the separation is expected. Figure I-2(b) illustrates a different traffic scenario where the same number of flights generates a situation where the loose of separations is potentially high and the controller may need to monitor and give instructions to different flights. Hence, although they have the same number of aircraft (the same value in entry/occupancy counts), the complexity of controlling the traffic situation illustrated in Figure I-2(b) is much higher than the situation represented en Figure I-2(a). This example illustrates the limitation of the current metrics and motivates the introduction of complexity metrics in the DCB models presented in this Phd.

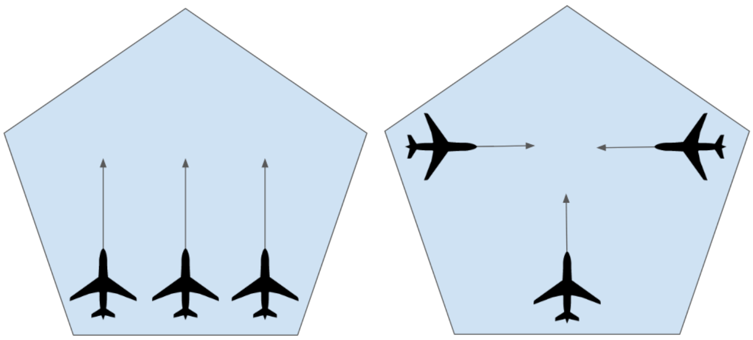

(a) Low complexity (b) High complexity

Figure I-2: *Illustrative example of traffic situations.*

I.2.4 Improvement on the capacity management initiatives

The main objective of the capacity management is the allocation of the available ATC resources in order to serve as much of the demand as possible. Two capacity solutions. i.e. Dynamic Airspace Configurations (DAC) and Flight Centric Air Traffic Control (FCA) are studied in this PhD.

The goal of the DAC solution is to dynamically redesign the airspace to accurately adjust its capacity to meet the foreseen demand. To create new operating sectors, pre-defined static airspace blocks are grouped together (SESAR PJ08 Consortium, 2019).

FCA is significantly distinct as it operates in a sectorless environment. Each new aircraft entering in the FCA area is assigned to an ATCO based on a specific set of FCA operational criteria (SESAR PJ10-01b Consortium, 2019).

These two capacity management solutions have been studied in two separate SESAR projects SESAR PJ08 Consortium (2019) and SESAR PJ10-01b Consortium (2019). This PhD explores the combination of DAC and FCA in the same airspace.

I.2.5 Alignment with SESAR concept of operations

In Europe, the SESAR program was established in 2004 with the goal of modernizing and harmonizing ATM systems by defining, developing, and deploying a new generation of innovative operational and technological solutions that are compliant with the Single European Sky (SES) objectives while also taking into account the human dimension (SESAR Joint Undertaking, 2020, 2015).

The SESAR programme aspires to improve in the following key performance areas: cost-efficiency, pacity, environment, safety and security (SESAR Joint Undertaking, 2020). In fact, SESAR visualises a future paradigm centered on trajectories, called Trajectory Based Operations (TBO), where the trajectory data is shared in four dimensions (4D trajectories), enabling a more efficient and predictable handling of flights. In addition, the future SESAR aspirations aim at considering the airspace users' preferences in the decision making processes, specially for the ATFCM measures. This can be achieved by increasing automation in the decision making and reducing the boundaries between the different ANSPs, enabling the management of a flight as a whole and not by segments as it is done today.

In order to progress towards the SESAR objectives a big number of solutions are defined. In fact, the concept of SESAR solution is defined in SESAR Joint Undertaking (2021) as:

SESAR solutions refer to new or improved operational procedures or technologies that are designed to meet the essential operational improvements outlined in the European ATM Master Plan. They are also developed in full accordance with the International Civil Aviation Organization (ICAO) and the Global Air Navigation Plan (GANP) and therefore applicable to ATM environments worldwide. Each solution is accompanied by a set of documents to support its implementation, including operational services and environment descriptions, safety, performance and interoperability requirements, technical specifications, regulatory recommendations, safety and security assessments, human and environmental performance reports, relevant ICAO and industry standards needed for implementation.

In particular, this PhD is linked with the following SESAR solutions:

- DAC, related with a more dynamic airspace management, where the sector design is based on the expected traffic demand, what can boost the capacity while decreasing delays and emissions.
- FCA, brings a paradigm shift from the current ATC sectors based on a geographical area to a flight centric structure without reference to geographical sectors.

Furthermore, this PhD addresses some of the significant operational changes identified in SESAR Joint Undertaking (2012, 2014):

- Moving from Airspace to 4D Trajectory Management.
- Network Collaborative Management and Dynamic Capacity Balancing. This point includes important topics addressed by this PhD:
  - The DCB process includes complexity management as a fundamental component.
  - The introduction of coordinated 4D constraints replaces the principle of first planned/first served currently used in the slot allocation process. These constraints are addressed using 4D measures (time, route, and level) aimed at maximising network capacity and allowing Airspace Users to constantly improve their operational business performance.
  - The DCB solution combines dynamic airspace configurations with 4D constraints aiming at optimally balancing the demand and the capacity, with minor demand changes.

I.3 Objectives of this PhD thesis

The main objective of this PhD is to improve the current state-of-the-art ATFCM models, aligning them to the TBO context and seeking a better integration between the different stakeholders involved when DCB measures have to be applied, while using complexity metrics to better estimate the demand and the capacity. Ultimately, the objective of this PhD is to decrease delay at Network level, while at the same time, improve AU and ANSP cost-efficiency when facing airspace or airport congestion.

Different sub-problems have been identified in order to address the overall purpose of this PhD. These more specific objectives are detailed as follows:

- Explore the limits of DAC and FCA solutions when using complexity metrics and address how they can be combined.
- Introduce a new concept of operations where the NM and ANSPs roles are more integrated and more flexibility to the AUs is given, allowing them with the possibility to provide alternative trajectories when facing with congested airspace.
- Use state-of-the-art trajectory optimisation to model the AUs behaviour when considering the generation of alternative trajectories.
- Formulate system-wide DCB holistic models that use complexity metrics and with different levels of capacity management.
- Propose an heuristic solution approach that could be scaled to solve realistic scenarios and compare it with an exact method.
- Address the performance of one of the proposed methods with a large-scale and realistic scenario and compare it with a baseline scenario that represents the best solution that could be achieved with the current system.

I.4 Scope and limitations of this PhD thesis

This section outlines the set of assumptions and simplifications considered in this PhD:

- All models and methods introduced in this PhD are scoped in the ATFCM pre-tactical phase.
- The AUs submit the FPs during the pre-tactical phase.
- All the demand is known during the pre-tactical phase, i.e. no unexpected flights are considered.
- The RAD constrains are disregarded when considering the alternative trajectory generation.
- The meteorological conditions at the departure time of each flight are considered static during the whole flight.
- The ATFCM stakeholders considered are the NM, the ANSPs and the AUs. Some airport constraints like the runway configuration are not considered.
- Airborne delay and linear holding are not considered.
- When complexity is used, a delayed trajectory is modelled as an alternate trajectory. Therefore, delay is taken from a discrete set of limited options.

- The cost of the delay is assumed based on the guidelines provided by Cook & Tanner (2015).
- The cost for open sectors is estimated with the criteria presented in PERFORMANCE REVIEW COMMISSION (2020).
- It is assumed that all stakeholders are willing to participate in the different decision making processes described in the new concept of operations introduced in this PhD.
- The AUs behaviour when dealing with competition is not modelled. It is assumed the AUs will choose the option that minimise the direct operating costs of that particular flight when computing trajectories.
- All elementary sectors considered in this PhD are operable by themselves.

I.5 Outline of this PhD thesis

The following is a summary of the contents of this dissertation, which is structured into eight Chapters and two Appendices:

- Chapter II contains some background and a review of the state of the art in demand and capacity methodologies, complexity metrics and resolution methods.
- Chapter III is focused on the capacity management. In particular, DAC and FCA solutions are considered together. A validation case study is also provided.
- Chapter IV presents the concept of operations proposed in this Phd. The roles and responsibilities of different stakeholders, as well as the relationship among them, are detailed in this Chapter. Moreover, this Chapter introduces the mathematical formulation necessary to define the DCB models presented in this PhD.
- Chapter V is dedicated to the demand management. Two models are introduced (Model 0 and Model I), using entry counts and complexity metrics respectively. This Chapter also includes a validation case study.
- Chapter VI presents three Mixed Integer Linear Programming (MILP) models for the holistic DCB, dealing with the demand and the capacity management at the same time (Models II, III and IV). The differences among the three holistic models is the level of capacity management offered.
- Chapter VII is focused on the resolution of the Model II. A new hybrid method based on the combination of Simulated Annealing and Dynamic programming is presented in this Chapter. Three validation case studies are provided. The first study compares the performances of the Hybrid method against the branch and bound algorithm. The second study consists of a sensitivity study of the parameter that models the penalty for different consecutive configurations. The third study is a big scale scenario which is compared with the current system in order to evaluate the advantages of the proposed concept of operations and the use of complexity metrics.
- Chapter VIII highlights the main contributions and observations of this PhD thesis, and outlines some paths for potential future research.

II

Background and literature review

This section contains the background and state of the art on Demand and Capacity Balancing (DCB) methodologies and metrics together with an introduction to mathematical optimisation.

II.1 Demand and capacity methodologies

As commented before, there are three different approaches to balance air traffic demand and capacity: a) demand management, b) capacity management, and c) both demand and capacity management (holistic management). In the next sections, the state-of-the-art of each of these approaches is given.

II.1.1 Demand management

The first option consists on applying regulations in order to shift the traffic demand and keep it below the available capacity. This is basically the main function of the Network Manager (NM) nowadays in Europe, which mainly allocates ground delay to the Airspace Users (AUs) using the Computer-Assisted Slot Allocation (CASA) methodology based on the Ration-by-Schedule (RBS) algorithm (EUROCONTROL, 2017). Although this methodology does not provide optimal solutions in terms of delay or cost, it is accepted by all the stakeholders because of its simplicity and fairness (Brinton *et al.*, 2010).

This RBS algorithm is complemented with Collaborative Decision Making (CDM) initiatives (in the United States) (Ball *et al.*, 2005) and the Enhanced Slot Swapping feature from the User-Driven Prioritisation Process (UDPP), as the first European approach for the inclusion of the AUs preferences (Pilon *et al.*, 2016; Ruiz *et al.*, 2019). However, the flexibility of these methods is still limited. For this reason, a lot of researchers have focused their activities to address the demand and capacity balancing problem as an optimisation problem in order to improve the limitations of the current RBS method.

A pioneer work was done by Odoni (1987) where the problem of scheduling flights in order to minimise congestion cost was defined and introduced, specifically focused on the response to the lack of airport capacity. After this work, several works proposed different formulations of the same problem. Terrab & Odoni (1993) formulates in a network flow problem the deterministic version of the problem where flights from many origins must be scheduled at a single and congested airport. This problem was known as Single-Airport Ground Holding Problem (SAGHP). The stochastic linear programming solution to the same problem was proposed by Richetta & Odoni (1993). In Andreatta *et al.* (1993), a review of optimisation models for the SAGHP was performed. After the research on SAGHP, the following works were focused on solving the Multi-Airport Ground-Holding Problem (MAGHP), where delays are assumed to propagate in the network of airports as aircraft perform consecutive flights. In Vranas *et al.* (1992) and Vranas *et al.* (1994), the MAGHP was formulated as an integer linear programming problem.

These works only tackled congestion in the airports, but they did not consider the en-route airspace. In Bertsimas & Patterson (1998), the authors presented a binary integer programming model for the deterministic, multiairport Air Traffic Flow and Capacity Management (ATFCM) problem that addressed capacity restrictions on the en-route airspace. Bertsimas & Patterson (2000) proposed how to introduce the reroute problem in the formulation since only ground delay before departure was considered in previous research. This formulation can be seen as an alternative to the current version of the Collaborative Trajectory Options Program (CTOP) (FAA, 2014), where the RBS allocations algorithm is substituted by a Mixed Integer Linear Programming (MILP) formulation that obtains a global optimal solution.

A similar approach was used in Lulli & Odoni (2007), where the complex nature of the European ATFCM solutions showed that, in certain circumstances, it is better, in terms of total delay and cost of delay, to assign to a flight more expensive airborne holding delay rather than a ground delay.

More recent research was done in Xu *et al.* (2018a, 2020a), where different delay initiatives and the consideration of alternative trajectories were considered in a MILP formulation in order to minimise the cost of the regulations.

II.1.2 Capacity management

The second option for balancing the demand and capacity consists on the capacity management applied by the Air Navigation Service Providers (ANSPs), which basically consists of a better allocation of the available Air Traffic Control (ATC) resources in order to meet as much of the demand as possible. Beside the current ATFCM approach (see Section I.1), new capacity solutions such Dynamic Airspace Sectorisation (DAS), Dynamic Airspace Configurations (DAC) and Flight Centric Air Traffic Control (FCA) have been introduced.

Both DAS and DAC aims at redesigning dynamically the airspace in order to provide an accurate adaptation of the capacity to the foreseen demand. The main difference between them lies in the way how they design the new sectors. While DAS provides airspace sectorisations adapted to the demand by designing new operating sectors (Chen *et al.*, 2013; Delahaye *et al.*, 1998; Martinez *et al.*, 2007; Tang *et al.*, 2012; Trandac & Vu Duong, 2002), DAC uses pre-defined static airspace blocks that are grouped in order to create new operating sectors (Kopardekar *et al.*, 2007; Delahaye *et al.*, 1995; Sergeeva *et al.*, 2017, 2015; Gianazza, 2019; Gianazza & Durand, 2020; Gianazza, 2010; Verlhac, C. and Manchon, S., 2005; Treimuth, 2018; Vidosavljevic & Delahaye, 2017).

Regarding the DAC solution, many different techniques have been used for tackling the problem, for instance, genetic algorithms (Delahaye *et al.*, 1995; Sergeeva *et al.*, 2017, 2015), ant colony systems (Gianazza & Durand, 2020), sequential A* algorithm (Gianazza, 2019), dynamical programming techniques (Vidosavljevic & Delahaye, 2017) or combinations of neural networks with tree search methods (Gianazza, 2010), among others.

Furthermore, different levels of DAC can be identified in the literature depending on the airspace unit which is used for the capacity management (this is also related with the different DCB models presented in this paper). In Verlhac, C. and Manchon, S. (2005); Vidosavljevic & Delahaye (2017), the DAC solutions consist in selecting which of the given configurations is used at each period of the day. Similarly, in Gianazza (2010, 2019); Gianazza & Durand (2020), although the problem is based on a given the set of elementary sectors, an initial preprocess is required in order to find out all feasible configurations. Instead, in Delahaye *et al.* (1995) the configurations used are based on a given set of operating sectors. In Sergeeva *et al.* (2017, 2015) the starting point were basic airspace blocks that can be collapsed in order to create new operating sectors. In Treimuth (2018) different models and approaches were introduced in order to find the sectorisation given a set of configurations, operating sectors or elementary sectors.

Finally, it is worth noting that in most of the DAC models, the aim is to balance the controller workload across all sectors. This is basically done by using complexity metrics (see Section II.2).

Radically different, FCA relies on a sectorless environment where each new aircraft entering in the FCA area is allocated to an Air Traffic Controller Officer (ATCO) based on a set of FCA operational criteria (Korn *et al.*, 2009).

These last two capacity management solutions have been studied in two separate SESAR projects SESAR PJ08 Consortium (2019) and SESAR PJ10-01b Consortium (2019). The combination of DAC and FCA was explored under the COTTON[1] SESAR project.

II.1.3 Holistic demand and capacity management

The integration of both options into a single optimisation problem (i.e. delay allocation and capacity management using DAC) was introduced by Xu *et al.* (2018b), through a formulation that includes the selection of the best ATC sector configuration opening scheme and the optimisation of the ATFCM resources at the same time. This work was extended in Xu *et al.* (2020b) allowing the creation of new sectorisations from existing operating sectors.

A similar approach was also explored in the COCTA[2] SESAR project (Ivanov *et al.*, 2019), where the authors introduced economic instruments and incentives in order to harmonise the traffic demand and coordinate the capacity and demand management decisions. This work was extended in the CADENZA[3] SESAR project (Künnen & Strauss, 2022), with the introduction of the concept of trajectory products (the AUs are rewarded with lower charges when giving more route flexibility to the NM). The consideration of the cross-border capacity was considered in Starita *et al.* (2021) in order to improve the performances of the capacity management.

[1] Capacity optimisation in trajectory-based operations
[2] Coordinated capacity ordering and trajectory pricing for better-performing ATM
[3] Advanced Capacity and Demand Management for European Network Performance Optimization

II.2 Demand and capacity metrics

All the existing Traffic Management Initiatives (TMIs) and the alternative methodologies are applied when the traffic demand is higher than the capacity available. Nowadays, the metric used to measure such demand and capacity is the sector entry counts, which is the number of aircraft entering in an ATC sector in a given period of time. Although this metric is very easy to compute, it does not consider how much time an aircraft is inside the sector or the difficulty (i.e. complexity) of the traffic to be controlled. For this reason, some Area Control Centers (ACCs) complement the previous metric with the occupancy counts, i.e. how many aircraft are inside the sector in a specific moment. Although entry and occupancy counts are used as proxys of the ATC workload, the harmonisation of the traffic or the difficulty required to control a given situation can not be estimated with these simple metrics.

For this reason, a large number of researchers have focused on the development of a complexity metric able to capture more factors representative of the ATC workload. This has lead to a large number of metrics and, although Single European Sky ATM Research (SESAR) defines complexity as *"...measure of the difficulty that a particular traffic situation will present to an air traffic controller..."* (SESAR Joint Undertaking, 2016), none of the proposed metrics in the literature has been proven superior to all the others. At the end, the "best" metric or set of metrics largely depends on the specific features of the problem to be solved, the particularities of the concerned airspace and/or traffic flows, particularities of the ANSPs and methods used for ATC, etc. Thus, different complexity metrics are found in the literature, capturing different causes for the complexity or Complexity Generators (CGs) and applying different rules for calculating a value.

Among the most significant metrics, the following ones will be explained because of their applicability under the Trajectory Based Operations (TBO) concept:

1. The Programme for Harmonised ATM Research in EUROCONTROL (PHARE) (EUROCONTROL, n.d.) was a collaborative research programme within Europe to investigate a future Air Traffic Management (ATM) concept. One of the new concepts addressed in the project was the redistribution of workload from single sector level to a wider multi-sector area controlled by a specialist controller known as multi-sector planner (Meckiff *et al.*, 1998). The Tactical Load Smoother is a tool that was developed to support the multi-sector planner. This tool provides three main outputs: 1) the Traffic Load Graph, that displays the expected number of aircraft in 10-40 minutes in the future; 2) the Problem Load Graph, which is based on the number of predicted conflicts and their degree of certainty; and 3) Complexity map, that shows, for a given time in the future, a heat contour map representing the complexity in the multi-sector area. This complexity map uses a metric that considers the probability and nature of conflicts between two or more aircraft, the equipment levels of the aircraft (3D Flight Management System (FMS), 4D FMS, datalink etc.), the aircraft's speed, the aircraft's vertical evolution (climbing, descending or stable), the aircraft's sector transit time, compatibility between an aircraft's route and it's flight level, the distance of the problem from the boundary of the sector.

2. The fractal dimension approach was proposed in Mondoloni & Liang (2001). The idea proposed is to use the fractal dimension of the traffic pattern as a metric for the traffic complexity. This methodology is useful for evaluating differences in traffic flows between alternative scenarios. In other words, the fractal dimension can be used as a metric to compare different concept of operations, i.e. current operations, free route, free flight or continuous climb. The metric considers the aircraft trajectories as well as the routes with altitude information and it is independent of the sectorisation.

3. The cognitive complexity can be understood as the difficulty of controlling an air traffic situation (Histon *et al.*, 2010; Cañas *et al.*, 2017; Ferreira *et al.*, 2017). As the cognitive complexity

of controllers is the functional limitation on the capacity of the ATC system, a controller mental model is required. This controller mental model must consider the situation awareness, decision-making and execution processes. The controller mental model introduced in Histon *et al.* (2010) is represented in Figure II-1.

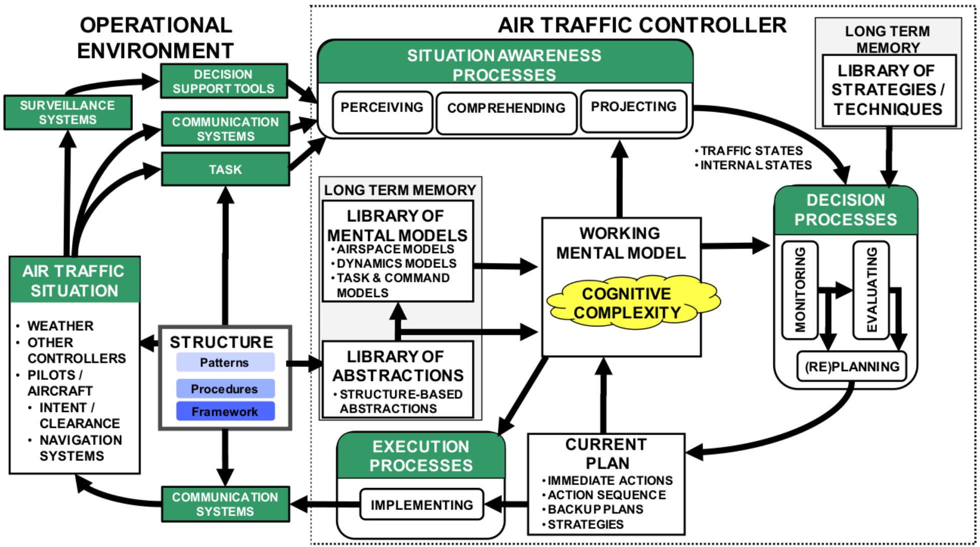

Figure II-1: *Model of air traffic control system. Source:* Histon et al. (*2010*)

4. Linked with the cognitive complexity there is the solution space metric (Abdul Rahman *et al.*, 2012; Hermes *et al.*, 2009; d'Engelbronner *et al.*, 2015) that aims at assessing the controller task demand load based on the geometric and kinematic properties of the traffic. This metric assumes that the controller workload is based on difficulty of the task to be conducted. In Hermes *et al.* (2009), the solution space is defined as "the subset of all possible vector (combined heading and velocity) commands that can be issued by an ATC controller that satisfy constraints of safety, productivity, and efficiency". In other words, it is related to the flexibility that the ATC has when it is needed to solve a conflict in terms of the airspace available to perform the resolution manoeuvrers.

5. Idris *et al.* (2007) defined the notion of trajectory flexibility as the ability of the trajectory (and hence the aircraft following the trajectory) to abide by all constraints imposed on it while mitigating its exposure to risks that cause violation of these constraints. The constraints intend to achieve ATM and aircraft objectives and include heading limits, required time of arrivals, and separation minima. To support the concept of trajectory flexibility, two trajectory characteristics are relevant, i.e. the robustness (ability of the aircraft to keep its planned trajectory unchanged in response to the occurrence of disturbances) and the adaptability (ability of the aircraft to change its planned trajectory in response to the occurrence of a disturbance that renders the current planned trajectory infeasible). Differently than other metrics, robustness and adaptability are trajectory-oriented since they are defined at trajectory level. The relationship with the complexity is based on the hypothesis that if each aircraft preserves its own trajectory flexibility, using an air-based or ground-based system, acceptable traffic complexity will naturally be achieved. The results of the analysis done in Idris *et al.* (2009) demonstrated that if adaptability and robust metrics are used during the trajectory planning phase, then the traffic complexity is mitigated naturally.

6. The trajectory based complexity (Prevot & Lee, 2011) is a modified aircraft count to predict sector complexity. Since the the currently used aircraft count is insufficient to predict controller workload under all conditions (specially in non-nominal conditions), this metrics

aims at modifying the aircraft count value considering dynamic factors such as weather, aircraft equipage or predicted separation violations, as well as static factors such as sector size.

7. The Input-Output approach (Lee *et al.*, 2007; Prandini *et al.*, 2009) evaluates the complexity in relationship to the control activity required to accept entering aircraft. The idea is similar to the solution-space approach because it also sees the complexity as "how difficult" a given traffic situation is. However, here the airspace is considered as closed loop input-output system. This metric has the input as a hypothetical aircraft entering the sector, and the output as the cost (defined as deviation from the original flight plans) of accepting this additional aircraft.

8. The dynamic density (Laudeman *et al.*, 1998; Sridhar *et al.*, 1998) is a complexity metric that includes the traffic density (or occupancy) and the traffic complexity in form of a weighted linear equation. The traffic complexity factors identified were heading change, speed change, altitude change, loss of separation and number of conflicts. This metric also combines occupancy with complexity as the trajectory based complexity, but, in this case, the result is a complexity value that cannot be compared directly with the aircraft count value.

9. The geometrical approach (Delahaye & Puechmorel, 2000) aims at considering the intrinsic traffic disorder as a complexity metric. This approach is based on the properties of the relative positions and the relative speeds of aircraft in a sector, so no human factors are involved in the process. The metric proposed considers the complexity due to the aircraft proximity (identifying spacial zones with high aircraft aggregation) and its divergence/convergence (how fast two aircraft move away from/get closer to each other).

10. The approach based on dynamical system modelling (Delahaye *et al.*, 2003; Puechmorel & Delahaye, 2009; Delahaye & Puechmorel, 2015) aims at identifying any trajectory organisation in the traffic pattern in order to quantify the associated control difficulty resulting in an air traffic complexity metric based on linear or non-linear dynamical system. The main idea is to find a dynamic system which modelises a vector field as close as possible to the observations given by the aircraft positions (and speeds). The trajectory disorder can be computed based on the dynamic system model.

11. A different approach is presented in Walter *et al.* (2010), where the complexity is related with the trajectory uncertainty. The strong correlation between trajectory uncertainty and controlled workload is considered by the introduction of a complexity component that quantifies the amount of uncertainty. This complexity component is based on sensitivity analysis, where the magnitude of uncertainty is obtained by directly investigating the impact of parameter variations to the aircraft's predicted position ahead in time.

12. Continuing with uncertainty consideration, in Prandini *et al.* (2012) describes the probabilistic approach. Here the complexity is evaluated in in terms of proximity in time and space of the aircraft present in the traffic as determined by their intent and current state while accounting for possible local deviations of the aircraft from their nominal trajectory. A probabilistic description of the uncertainty is adopted when the aircraft future position is considered. Thus, it is possible to attribute different likelihood to different trajectories, in particular, a lower likelihood to trajectories that are farther away from the nominal one.

In previous research papers on holistic DCB, both demand and capacity were measured using entry or occupancy counts. In fact, the introduction of complexity metrics in this holistic integration of the demand and capacity management increases the difficulty of the formulation of the models and, as a consequence, the difficulty to find a solution in a reasonable computational time.

This is related with the fact that slightly altering one single trajectory, may considerably change the complexity in a sector.

Furthermore, the introduction of alternative trajectories for the same flight may significantly change the traffic patterns, depending on which trajectory is finally selected. This is why previous works have used entry or occupancy counts, instead of a complexity metric, in order to evaluate demand and capacity.

This PhD aims at overcoming this issue by using complexity metrics in Holistic DCB models that allows the AUs to provide alternative trajectories.

II.3 Mathematical optimisation

A mathematical optimisation problem aims at minimising or maximising a function while satisfying some constraints. The generic definition of an optimisation problem can be formulated as follows:

$$\text{Minimise } f(x) \tag{II.1}$$

s.t.

$$g_j(x) \leq 0, \quad j = 1, ..., m \tag{II.2}$$

$$x \in X \tag{II.3}$$

where x is the vector of decision variables, X is the domain of the decision variables, f is the objective function and m is the total number of constraints. Equations (II.2) are the constraints of the optimisation problem.

Depending on the objective function, the constraints and the decision variables, a problem can be a classified as Linear Programming (LP), Integer Linear Programming (ILP), Mixed Integer Linear Programming (MILP), unconstrained continuous optimisation, Nonlinear Programming (NLP) or Mixed Integer Nonlinear Programming (MINLP). Table II-1 describes the conditions required to classify a problem in a specific category.

Table II-1: *Classification of optimisation problems*

Function f	**Constraints g_j**	**Domain X**	**Problem type**
linear	linear	continuous $\subseteq \mathbb{R}^n$	Linear programming (LP)
linear	linear	discrete $\subseteq \mathbb{Z}^n$	Integer linear programming (ILP)
linear	linear	cont./disc. $\subseteq \mathbb{R}^n \times \mathbb{Z}^n$	Mixed integer linear programming (MILP)
nonlinear	none	continuous $\subseteq \mathbb{R}^n$	Unconstrained continuous optimisation
nonlinear	(non)linear	continuous $\subseteq \mathbb{R}^n$	Nonlinear programming (NLP)
nonlinear	(non)linear	cont./disc. $\subseteq \mathbb{R}^n \times \mathbb{Z}^n$	Mixed integer nonlinear programming (MINLP)

II.3.1 Exact methods

An exact method is an optimisation method that guaranties to reach an optimal solution of a problem, if such a solution exists. Otherwise, it gives the proof of its infeasibility.

When a problem is linear (LP) it can be addressed with the Simplex algorithm, which was proposed by George Dantzig. The Simplex technique employs a highly efficient strategy: it progresses methodically from corner point to corner point, improving the value of the objective function at each stage; starting from the feasibility region where all the main variables are zero.

Other exact methods are required when the problem is ILP or MILP. The objective of these methods, such as Branch and Bound (B&B) (Fischetti *et al.*, 1994), cutting planes (Gomory, 1958), column generation (L.R. Ford, Jr. & D.R. Fulkerson, 1958), and dynamic programming (Bellman, 1957), among others, is to find the optimal solution of the problem.

Because of their relevance for this PhD, B&B and Dynamic programming are explained.

II.3.1.1 Branch and Bound

The B&B algorithm was introduced in Land & Doig (1960) aiming at solving programming problems where all or some variables can take discrete values (ILP or MILP).

The branching procedure creates new subproblems by recursively applying linear relaxation, which consists of the suppression of the constraints of integrity of the variables, so as to obtain a LP. If the solution of the linear relaxation satisfies the integrity constraints, then it is solution of the integer problem (feasible solution). The value of the best feasible solution found defines the upper bound of the solution of the minimisation problem. If the solution of the linear relaxation does not complain the integrity constraints, it is used to establish the lower bound of the minimisation problem. The difference between the upper and the lower bound is a measure of the proximity of the actual point and the optimum solution, if this exists. Hence, in a minimisation problem, the branching procedure increase progressively the lower bound and decrease progressively the upper bound. When the upper and lower bounds are coincident the optimum solution is found.

The purpose of the bounding procedure is to reduce the size of the search tree by eliminating subproblems that do not contain the optimal solution. At each iteration of the branching procedure, the following option are addressed:

- If the solution of the linear relaxation fulfils the integrity conditions, it has no sense to continue branching the current subproblem.
- If the solution of the linear relaxation does not satisfy the integrity conditions and exceeds the best current know feasible solution (upper bound), the current subproblem certainly does not contain the optimum, so it can be eliminated.
- If the subproblem is infeasible, the current subproblem is closed.

II.3.1.2 Dynamic programming

The Dynamic programming was introduced by Richard Bellman (Bellman, 1957) and it is based on the decomposition of a complex problem into simpler subproblems in a recursive way. A recursion is a rule for calculating a value based on previously calculated values (Bertsekas, 1995). When a subproblem is solved the information is stored avoiding the need of re-computing when required later. Typically, dynamic programming simplifies a choice by decomposing it into series of decision stages. The sequence of decisions that results into the optimal solution is called optimal policy. The Dynamical programming is based on the Bellman's Principle of Optimality stated as:

An optimal policy has the property that whatever the initial state and the initial decisions are, the remaining decisions must continue an optimal policy with regard to the state resulting from the first decision (Bellman & Dreyfus, 1962).

This principle can be recursively used in order to obtain the subproblems expressed in recursive expressions.

II.3.2 Heuristic techniques

Differently than exact methods that aim at finding the optimal solution, the objective of the heuristic techniques is to rapidly get one or several solutions of a problem, with no guaranty to get an optimal solution, or to get any proof of infeasibility

Greedy, one of the simplest algorithms, executes a greedy search beginning at a random point. Then, it makes small changes to the position and keep only improving movements. Yet, this method has the disadvantage of often stacking at local optima. This algorithm can be summarised as follows:

$x \leftarrow$Initial solution
$N \leftarrow$Number of iterations
while $n \leq$N **do**
  $x' \leftarrow$solution in the neighbourhood of x
  if $f(x') \leq f(x)$ **then**
    $x \leftarrow x'$

Other evolutionary-based techniques mimic and emulate natural processes of the real world, like genetic algorithms, particle swarm or simulated annealing, among others.

II.3.2.1 Genetic algorithms

Genetic algorithms emulate the laws of natural selection described by Charles Darwin: survival of the fittest by mutation, crossover and selection (Holland, 1992).

The basic concept is to produce a population of individuals and store the information about them in the form of chromosomes (typically an array of character strings). The chromosomes evolves using mutation and crossover and the best individuals are finally selected. The pseudo-code is as follows (Weise, 2009):

Initial population of random individuals
$N \leftarrow$Number of iterations
while $n \leq$N **do**
  Evaluation. Compute the objective values of the solution candidates
  Fitness assignment. Use the objective values to determine fitness values
  Selection. Select the fittest individuals for reproduction
  Reproduction. Create new individuals by crossover and mutation

II.3.2.2 Particle swarm

The swarm behaviour of animals like fish and birds inspired the trajectory-based approach known as particle swarm (Kennedy & Eberhart, 1995). Adjusting the trajectory of individual solutions known as particles, the algorithm searches the space of the objective function. A particle's trajectory evolves by adding a velocity vector ($\overrightarrow{v}_i$) to the position vector ($\overrightarrow{x}_i$) of the particle. At every iteration two solutions are updated and saved:

- $\overrightarrow{x}^*_i$ is the best historical solution of each particle i
- $\overrightarrow{g}^*$ is the best historical solution for the entire swarm

There are three potential drivers that guide the evolution of every particle. A particle can be attracted to $g*$ and attracted to x_i^* together with some random movements. This is reflected in the way how the velocity vector is updated at every iteration:

$$\vec{v}_i \leftarrow \vec{v}_i + \alpha\epsilon_1(\vec{g}^* - \vec{x}_i) + \beta\epsilon_2(\vec{x}_i^* - \vec{x}_i), \tag{II.4}$$

where ϵ_1 and ϵ_2 are random values, and α and β are weighting factors that indicate the magnitude of the acceleration towards the global best ($\vec{g}^*$) or the current own personal best ($\vec{x}_i^*$), respectively.

The particle swarm algorithm can be summarised as:

Define the number of particles, I, in the swarm
Initialise the position $\vec{x}_i$ and velocity $\vec{v}_i$ of each particle in the swarm ($\forall i \in I$)
Initialise $\vec{x}_i^* \leftarrow \vec{x}_i$
Initialise $\vec{g}^* \leftarrow \vec{x}_i$
$N \leftarrow$Number of iterations
while $n \leq$N **do**
    while $i \leq I$ **do**
        Calculate new velocity $\vec{v}_i$
        Calculate new position $\vec{x}_i \leftarrow \vec{x}_i + \vec{v}_i$
        Evaluate the cost of the particle $f(\vec{x}_i)$ at the new position
        if $f(\vec{x}_i) \leq f(\vec{x}_i^*)$ **then**
            $\vec{x}_i^* \leftarrow \vec{x}_i$
        if $f(\vec{x}_i) \leq f(\vec{g}^*)$ **then**
            $\vec{g}^* \leftarrow \vec{x}_i$

II.3.2.3 Simulated annealing

The simulated annealing method is inspired by the metal's annealing process during which it cools and crystallises with low energy and big crystals Kirkpatrick *et al.* (1983). The molecular structure of a material becomes weaker when the material is heated and is more prone to change. When a substance cools down, its molecular structure becomes rigid and less prone to transformation. The fundamental concept is to employ a random search technique that not only selects better solutions but also retains worse ones within an arbitrary probability p. This probability or Boltzmann probability factor is defined as:

$$p = \exp\left[-\frac{\Delta_E}{k_B T}\right], \tag{II.5}$$

where T is the temperature of the system, k_B is the Boltzmann's constant and Δ_E is the change in the energy of the system. The change of energy Δ_E can be interpreted as function of the change in the objective function between two solutions, x and x^*, as follows:

$$\Delta_E = \gamma(f(x^*) - f(x)), \tag{II.6}$$

where γ is a constant that typically can be set equal to k_B. Hence, the probability factor of the simulated annealing method is:

$$p = \exp\left[-\frac{f(x^*) - f(x)}{T}\right]. \tag{II.7}$$

The pseudo-code for the simulated annealing method is described in detail below:

$T \leftarrow$ Initial temperature

$T_{min} \leftarrow$ Final temperature
$\alpha \leftarrow$ Cooling rate
$x \leftarrow$ Initial random solution
while $T > T_{min}$ **do**
    $f(x) \leftarrow$ Objective function of solution x
    $x^* \leftarrow x + \epsilon$ (random change)
    $f(x^*) \leftarrow$ Objective function of solution x^*
    if $f(x^*) < f(x)$ **then**
        $x \leftarrow x^*$
    else
        if $p > rand()$ **then**
            $x \leftarrow x^*$
    $T \leftarrow \alpha T$

III

Capacity management

This chapter is focused on the management of the airspace capacity. The capacity resources are deployed and adapted to the expected demand aiming at minimising the impact on the demand side (in terms of delay allocation). In this context, two SESAR solutions have been studied in the literature, i.e. Dynamic Airspace Configurations (DAC) and Flight Centric Air Traffic Control (FCA), but not the integration of both concepts. Hence, the main objective of this chapter is to present the validation of the holistic integration of the DAC and FCA capacity management solutions proposed in the SESAR exploratory research project COTTON[1], to derive potential benefits in terms of capacity and cost-efficiency improvements in comparison with the deployment of only one capacity management solution separately. A novel delineation method for dividing the airspace in DAC and FCA aereas is presented and the current DAC and FCA models are improved with the introduction of complexity (instead of entry counts or occupancy) as a metric for measuring the traffic load.

Summarising, the contributions of this chapter are: 1) a novel delineation method to identify when/where DAC and FCA shall be applied; 2) the introduction of complexity in the DAC and FCA processess; and 3) a validation assessment of the benefits of the integration of DAC/FCA solutions.

Note that this chapter deals only with the capacity management and the demand is regulated through the allocation of delays (after the capacity decisions are taken). Thus, no alternative trajectories neither holistic integration between demand and capacity are taken into account.

[1]Capacity optimisation in trajectory-based operations

III.1 Integration of DAC and FCA

The main motivation for integrating DAC/FCA is that both DAC and FCA operations deployed separately are better adapted to different operational environments. Therefore, the ideal way to achieve high performance and continuous optimal use of the resources (airspace and Air Traffic Controller Officers (ATCOs)) is to combine, harmonise and eventually fully integrate them.

The initial trigger for this approach is the fact that FCA operations are proven to provide high performance until a certain level of demand complexity in a subject airspace is reached (Martins *et al.*, 2019). Beyond this level, FCA mode of operations becomes impracticable. The main reason lies in the way the Air Traffic Control (ATC) service is provided in FCA (i.e. sectorless Controller Working Positions (CWPs)). When the complexity is high, some situation awareness limitations and a high increment in the number of internal coordination arise, which leads to a potential decrease of safety and an exponential increment of workload.

On top of that, a DAC/FCA integrated environment would require design criteria based on complexity assessment to decide, monitor and refine the airspace boundaries delineating DAC and FCA areas. The design of such boundaries is based on DAC airspace design components, which can be building blocks or shareable blocks. The main difference between them is that a shareable block cannot be operated as an ATC sector by itself and needs to be collapsed with one or more building blocks. Building blocks can also be collapsed in order to create bigger collapsed sectors. As illustrated in Figure III-1(a), vertical delineation of DAC and FCA boundaries can be assessed through the analysis of complexity of the 5 vertical layers and then through the complexity assessment of individual building and shareable blocks. The resulting delineation is then illustrated in Figure III-1(b).

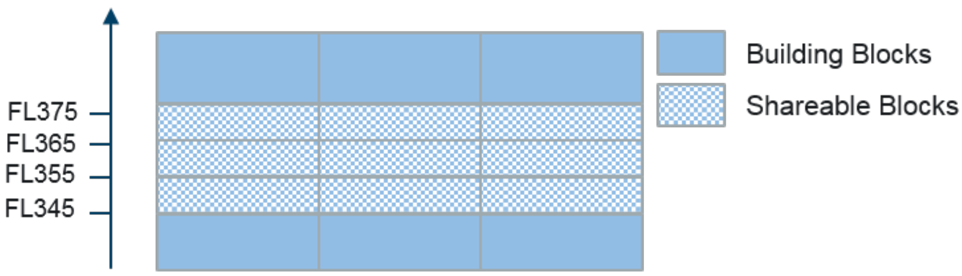

(a) Design principles of airspace components in DAC concept

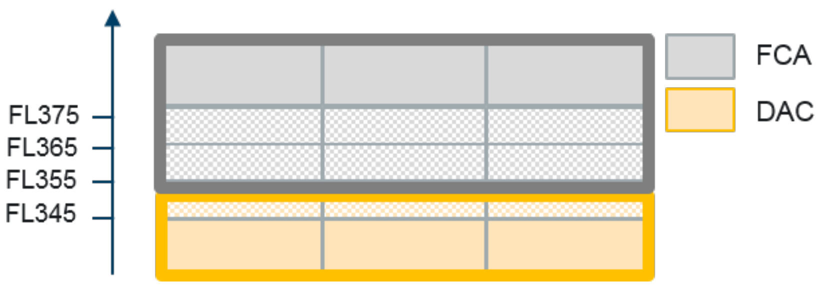

(b) DAC/FCA modes delineation based on complexity assessment of DAC airspace components

Figure III-1: *Delineation process example*

Two delineation modes supported by complexity assessment are proposed:

- Static DAC/FCA. It consists in the identification of one single altitude boundary above which FCA can be applied along the day such that the demand complexity in the FCA area remains lower than a maximum acceptable value. Static DAC/FCA boundary is identified through the analysis of complexity generated at each vertical layer of the airspace. The highest layer with complexity higher than the limit defines the boundary between FCA and DAC.

- Dynamic DAC/FCA. It consists in identifying variable DAC/FCA altitude boundaries per time period depending on the complexity of altitude layers along the day.

Although the application of the presented study is illustrated on the pre-tactical phase, the proposed methodology is applicable in all the ATM layered planning.

III.2 Methodology

This section aims at presenting the used methodology for the DAC/FCA integration.

III.2.1 Use of expert advise

In this study, some decisions are taken and many parameters are calibrated by the assignment of specific values which are justified with expert judgement. During the COTTON project, several workshop sessions were conducted with ATC controllers and people experienced in the Network Manager (NM) operations. Questions and results were presented to the experts and the collected feedback was used for the calibration of the different parameters related with the complexity metric, the different defined thresholds and the setup of the algorithms.

III.2.2 Introduction of complexity

An adaptation of the existing Geometrical complexity metric is used in this study. The Geometrical complexity metric proposed in Delahaye & Puechmorel (2000); Vidosavljevic *et al.* (2017) provides 'null' complexity in traffic situations diverging and widely distributed regardless of the number of flights involved. Based on expert judgment and simulation tests, even in such 'simple' situations there is ATCO workload linked to the monitoring task, that is a linear function of the number of flights in the controlled area. The mathematical model used to calculate the complexity in a CWP is given by the following expression:

$$C = mN + \sum_{i=1}^{N}(1+\delta_i)(1+\lambda_i)\sum_{j=1\setminus\{i\}}^{N} Cv_{ij}e^{-\alpha d_{ij}^2}, \tag{III.1}$$

where N is the number of flights in the sector and Cv_{ij} is the geometrical complexity that aircraft j produces on aircraft i, which is modulated in order to consider the vertical evolution of flights with λ_i, the proximity with the sector boundary using δ_i and the aircraft proximity with α. Finally, the monitoring load is added trough m .This complexity metric provides only a numeric value and no unit is considered.

The parameter values (i.e. m, δ, λ, α) could only be determined with an extensive study , that is beyond the scope of this PhD. The calibration parameters are selected based on expert judgment and small real-time simulation tests.

III.2.3 Complexity threshold identification

Since the complexity metric used in the analysis is a new metric, no threshold had been previously defined. The approach used to find out this threshold was focused on the the analysis of historical regulations, where the reason was the lack of ATC capacity. For this analysis, the Aeronautical Information Regulation and Control (AIRAC) 1808 was used containing 48 regulations of this type over the Hungarian airspace, and 34 of them were used in this study. The remaining ones were excluded because they started the day before or ended the day after, or because they were applied in more than one period of time.

The hypothesis in this analysis was that whenever a regulation is triggered there is necessarily a capacity issue, i.e. the traffic complexity should be greater than the capacity threshold. After the regulation is applied, the complexity value should be under the threshold.

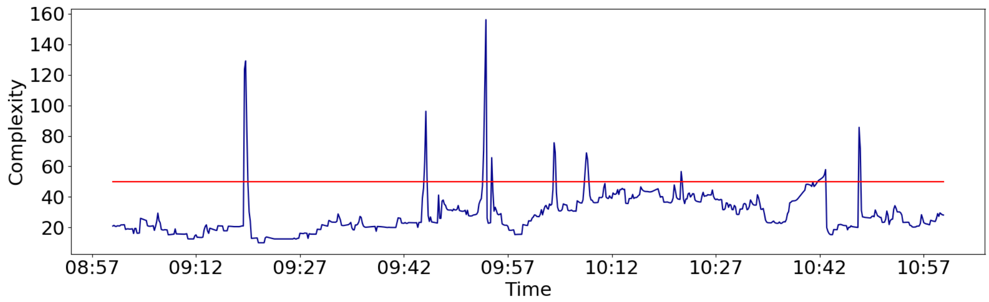

(a) Complexity before the regulation

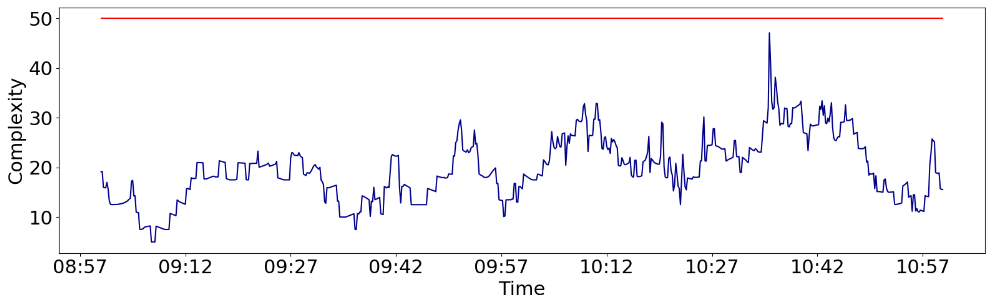

(b) Complexity after the regulation

Figure III-2: *Empirical assessment to identify complexity threshold for sustained overload, example for LHCCENH*

Figure III-2(a) shows the complexity of the sector LHCCENH before the regulation where some peaks can be seen above the red line representing the threhold. After applying the regulation, that is Figure III-2(b), the complexity during the regulation period is always below the threshold (red line). Based on this assessment on all workable sectors, the threshold was computed to be 50 for sustained overloads, and 80 for peak overloads.

FCA is not applied in real operation, so the same approach could not be performed. Thus, based on the experience and knowledge obtained in SESAR PJ10-01b Consortium (2019), it is assumed that the threshold for FCA will be a little bit lower than for DAC, because of the nature of the concept. Firstly, because in FCA there is only 1 controller per CWP whereas in DAC there are 2 per CWP. Secondly, due to the higher coordination required between different CWP sharing the same airspace. According to these reasons, and based on operational expert judgement, the complexity threshold for overloads in FCA has been established at 40, which is 20% less than in DAC.

III.2.4 Overload and underload detection process

For DAC operations two different types of overload have been considered:

- Sustained overload: the complexity is above the sustained overload threshold during a sustained period of time longer than the sustained duration threshold.
- Peak overload: the complexity is above the peak overload threshold during a short period of time, but longer than the peak duration threshold.

It is important to note that if the demand is above the capacity but that lasts less than the duration threshold, the overload is not considered. Hence, there is a threshold for the capacity value and another for the duration. A similar approach is followed for detecting underloads. Nevertheless, only sustained underloads are considered.

For FCA, the process considers only sustained overloads and sustained underloads.

III.2.5 Airspace delineation process

The DAC/FCA airspace delineation aims at defining the boundary between the DAC and FCA ares and it is based on a complexity assessment following a top-down approach from the highest level point of view showing the total complexity of the ACC compared to occupancy to the elementary sector level to show which portions of the airspace and time periods are more critical. The aim is to foster a global understanding of the complexity metric, assess how it resembles and/or differs from occupancy, identify what regions of the airspace contribute more to the complexity and what times of the day are more critical. The methodology of such delineation process can be summarised in four steps:

- Step 1: assessment of instantaneous complexity at Area Control Center (ACC) level. It allows to identify the preliminary time periods when the workload will be high. In addition, the comparison of the complexity values with occupancy allows to identify if the workload is generated due to the high number of flights or due to the geometric issues consequence of the traffic flows.
- Step 2: assessment of aggregated complexity per vertical layer. The airspace can be divided vertically in different layers in order to identify vertical portions of airspace where the complexity is higher. The comparison between entry counts and complexity is always recommended since it provides added information about the major source of complexity.
- Step 3: assessment of instantaneous complexity per vertical layer. This step allows to identify the temporal evolution of the complexity per vertical layer and offers a better view to define a dynamic boundary between the DAC and FCA areas.
- Step 4: assessment of instantaneous complexity at elementary sector. The study of the complexity at a lower level allows to refine the outputs of previous steps and clearly identify the portions of airspace where the complexity is high.

Following this top-down approach together with the support of expert judgement allows to identify when and where DAC and FCA could be deployed respectively.

III.2.6 DAC algorithm

The sector configuration optimisation algorithm aims at balancing demand and capacity dynamically inside the DAC area and it is based on the Improved Configuration Optimizer (ICO) developed and refined by the EUROCONTROL Experimental Centre (Verlhac, C. and Manchon, S., 2005). It internally runs a branch and bound algorithm aiming at finding the best sector opening scheme that satisfies the following multiobjetive criteria:

1. Minimises the overloads and underloads.
2. Minimises the number of controllers.
3. Maximises the overload and underload balance between sectors.
4. Minimises the number of sector changes.

This algorithm evaluates the demand and the capacity using the complexity metric introduced in Section III.2.2, while the overload and underload detection is done using the approach explained in Section III.2.4. The optimisation process is also dependant on the following set up parameters: 1) minimum opening duration of a configuration; 2) minimum opening duration of a sector; 3) maximum difference in number of sectors between consecutive configurations; and 4) minimum opening duration of a dynamic airspace configuration.

This last point requires an explanation in order to clarify the concept of dynamic airspace configuration. There may be some configurations where the only difference among them is where the shareable blocks are located. In this situation, a change of configuration is less intrusive for the controllers and more flexibility can be given to the optimisation process.

III.2.7 FCA algorithm

In order to determine the number of CWPs required for the FCA area in the pre-tactical phase, the FCA algorithm allocates trajectories entering the FCA area to the CWPs with the support of the complexity metric presented in Section III.2.2. First, complexity is assessed for each trajectory crossing the FCA airspace. Complexity at CWP level is computed by the sum of the complexity that the controller already has when the flight enters the FCA area plus what this particular flight would add to it. Then, based on this complexity assessment principle, the algorithm allocates the trajectories to the controllers so that complexity is evenly distributed among the CWPs along the day of operations.

Although the flight allocation algorithm does not provide a global optimal solution, it aims at:

- Minimising the overloads and underloads.
- Minimising the number of CWPs.
- Balancing the workload of the CWPs.

In the proposed approach, flight reallocation is not considered. Hence, once a trajectory is allocated, it will be controlled by the same CWP before leaving the FCA area. In addition, when a CWP is identified to be closed (because of low traffic demand), it remains open until all flights controlled have left the FCA area.

III.3 Validation case study

In order to analyse the performance of integrated DAC/FCA and compare it with DAC and FCA implemented separately, a case study of 24 hours of traffic over the Hungarian airspace (LHCC-CTA) is proposed because it is representative of any airspace with high complexity values. The day of the study is the 29th of July of 2018 and the traffic sample obtained from the EUROCONTROL's Demand Data Repository 2 (DDR2) database contains 3,046 flights crossing the considered

Table III-1: *Parameters for the DAC and FCA optimisation strategies*

DAC mode	
Minimum opening duration of a configuration	30 minutes
Minimum opening duration of sectors	30 minutes
Limit steps of the number of sectors when there is a configuration change	2 sectors
Minimum duration for dynamic airspace configuration	15 minutes
FCA mode	
Minimum opening duration of a CWP	30 minutes
Flight reallocation between openened CWPs	NO

ACC. Both DAC and FCA algorithms are simulated using the the R-NEST suite EUROCONTROL (2020b) from EUROCONTROL. This validation exercise was done in the scope of the Capacity optimisation in trajectory-based operations (COTTON) project and more detailed information can be found in COTTON Consortium (2019).

III.3.1 DAC and FCA setup

The DAC process requires to be calibrated fixing some operating values agreed and validated together with EUROCONTROL and Hungarocontrol experts. In this sense, the minimum operating duration of a configuration is limited to 30 minutes. However, a smaller duration of 15 minutes is allowed when the change from one configuration to the next one is affecting only to the shareable blocks. In other words, the exchange of shareable blocks between different building blocks is allowed every 15 minutes. In addition, another limitation related with consecutive configurations is the difference in the number of sectors. This value is fixed to 2 sectors, avoiding big configuration changes ensuring the traffic situation awareness and safety from the controller point of view. Moreover, the minimum operating duration of a sector is limited to 30 minutes.

Regarding the FCA algorithm, it also requires some operational constraints. Since there are no configurations neither sectors in FCA, the minimum operating duration is applied directly to the CWPs, limited to 30 minutes. All these constraints for the DAC and FCA algorithms are summarised in Table III-1.

Focusing on the complexity, the equation (III.1) has been calibrated using the following parameters:

- Monitoring complexity is m = 0.5.
- $\lambda = 0.25$ for climb and $\lambda = 0.15$ for descent.
- $\gamma = 0.3$ at the border (distance = 0 NM) linearly decreasing to 0 at the distance = 10 NM.
- $\alpha = 1.7$.

The DAC and FCA overload and underload thresholds are summarised in Table III-2.

III.3.2 Definition of scenarios

Three scenarios are defined:

- Scenario 1: full DAC. All the Hungarian airspace is operated under DAC ATC rules.

Table III-2: *Parameters for overloads and underloads*

Variable	DAC mode	FCA mode
Complexity sustained overload threshold	50	40
Complexity sustained overload duration	7 minutes	4 minutes
Complexity peak overload threshold	80	N/A
Complexity peak overload duration	3 minutes	N/A
Complexity underload threshold	15	15
Minimum complexity underload duration	7 minutes	4 minutes

- Scenario 2: FCA/DAC static. The Hungarian airspace is statically divided in one part operated with DAC rules and another under the FCA paradigm. This scenario is designated as "static" because the boundary between the DAC and FCA airspace does not change during the day. This is equivalent to consider that FCA is deployed alone since it is impossible to use FCA in the full airspace.
- Scenario 3: FCA/DAC dynamic. The boundary between the DAC and FCA areas is dynamically adapted accordingly with the characteristics of the traffic demand.

It is worth noting that the definition of the DAC/FCA boundaries in scenarios 2 and 3 is result of the delineation process introduced in section III.2.5. Next section is devoted to deeply explain this process for the day of simulation.

III.3.3 Delineation of DAC and FCA areas

The delineation process for identifying when and where DAC and FCA can be applied introduced in section III.2.5 is divided in several steps. For this case study the steps are:

- Step 1: assessment of instantaneous daily complexity at ACC level. In this case the ACC is the Hungarian airspace denoted by LHCCCTA and the instantaneous complexity registered along the day can be showed in Figure III-3(a). One can identify periods with low complexity at the early morning and late evening periods, as well as high complexity values in the middle of the day. By comparing the complexity with the occupancy showed in Figure III-3(b), a similar envelope between them is identified because the monitoring complexity has a big contribution. However, there are mismatches in some moments reflecting that the geometry of the traffic demand is so complex in these situations, what may create high workload periods to the controllers.
- Step 2: assessment of aggregated complexity per vertical layer. From Figure III-4(a) it can be observed that [FL365 to FL375], [FL345 to FL355] and [FL305 to FL345] are the most complex layers, with nearly 20% of the total each. For FL305 to FL345, this could be explained with a high percentage of evolving flights that climb or descend to their corresponding en-route flight levels because they are in a transition zone between the Lower Airspace and the Upper (see Figure III-4(b)). Yet, it stands out that FL365 to FL375 is so complex, when most of the traffic is en-route and flights are in cruise. This demonstrates why in the Hungarian Airspace these flight levels are crucial and deserve special attention in terms of ATC. As a result of this assessment, the study considers that FL375 is a good flight level to divide airspace in static DAC/FCA. FCA will handle 9%+14% = 23% of the total complexity, while DAC takes airspace below FL375 which accounts for 77% of the total complexity, as it is more adequate to this kind of traffic, with more complex trajectories, flight level changes, etc.
- Step 3: assessment of instantaneous complexity per vertical layer. Figure III-5 shows how the vertical layers are contributing in terms of complexity during the day. The dark blue

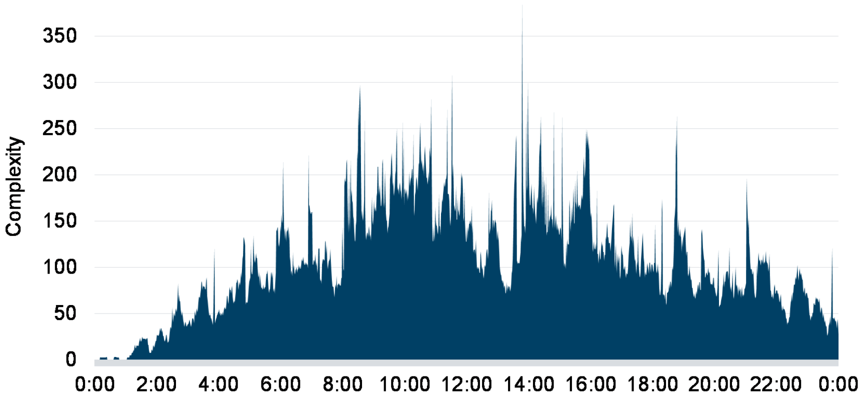

(a) Complexity

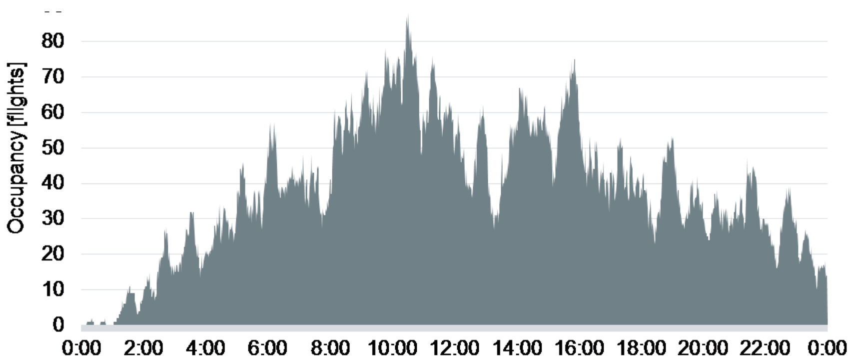

(b) Occupancy

Figure III-3: *Demand of the ACC LHCCCTA*

strip corresponding to Flight Levels FL365 to FL375 has a big contribution (as seen in Figure III-4(a)), also containing the most of the peaks. The valuable information to derive from this graph are the allocation periods for DAC or FCA areas in the integrated and dynamic DAC/FCA concept based on operational expert judgement from EUROCONTROL and Hungarian Airspace (HungaroControl). The following delineation according to complexity evolution and peaks is proposed:

– From 0:00h to 3.00h: Only FCA in the airspace, since complexity is low (lower than 40 which is the complexity threshold for FCA).

– At 3.00h: following the first peak greater than 40 and 50 which are the complexity thresholds for FCA and DAC respectively, open DAC from FL095 to FL305.

– At 5.00h: There is a peak above 100 and in general complexity is growing, so to extend DAC to FL345.

– At 8.00h: there are peaks of 200-250 in order of magnitude, and complexity brought by FL365 and FL375 is already important, so DAC is extended to FL375. There is a complexity drop between 12.00h and 14.00h, but it was decided to maintain the airspace allocation because later the traffic is again intense until 16.00h.

– At 16.00h: After 16.00h the average complexity is dropping, although at 19.00h there is a great peak, so DAC is lowered to FL345.

– At 19.00h: After the peak at 19.00h, complexity is always below 200 and thus, DAC is lowered to FL305.

– At 23.00h: Complexity will decrease to 50 and below until midnight, so again full FCA is applied.

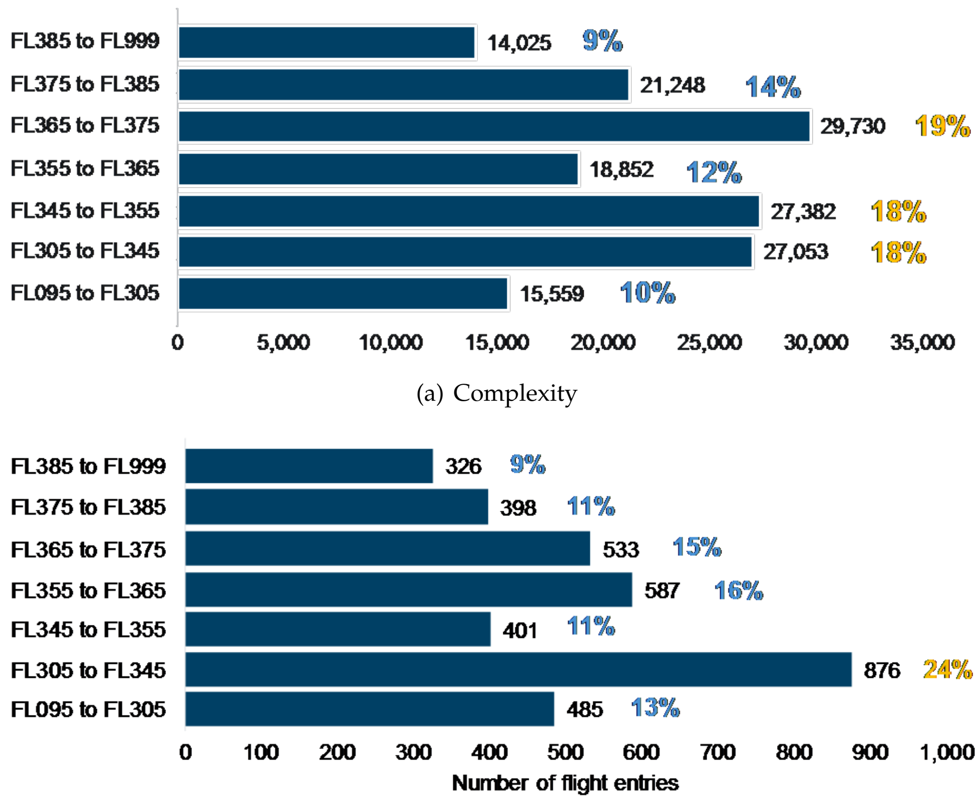

Figure III-4: *Demand per vertical layers*

- Step 4: assessment of instantaneous complexity at elementary sectors. Complementing the high-level assessment, the analysis of data at elementary sector level was performed, for the 15 elementary sectors of the LHCCCTA airspace, confirming the decisions taken in the previous step. For example, Figure III-6 shows the instantaneous complexity of the elementary sector LHCCWESTH (FL365 to FL385).

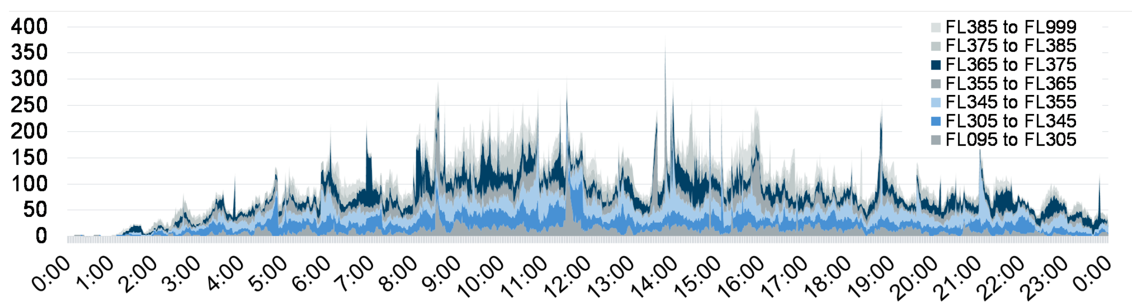

Figure III-5: *Instantaneous complexity per flight level division*

The result of applying this delineation process is presented in Figure III-7.

III.3.4 Results: Capacity analysis

In this study, the total overload and underload sums are used as capacity Performance Indicators (PIs). On the one hand, the overloads are the periods where the demand is above the capacity threshold of a sector, while the underloads, represent periods where more aircraft could be handled. The overload and underload sums are, respectively, the aggregation of all overloads and

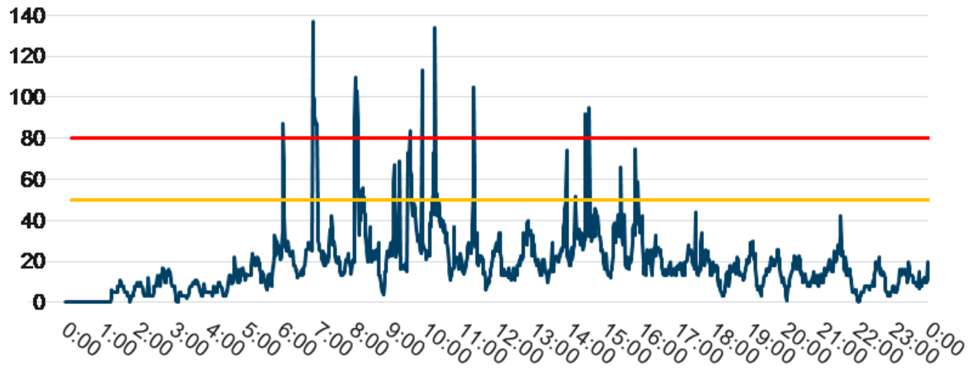

Figure III-6: *Example of instantaneous complexity in the elementary sector LHCCWESTH*

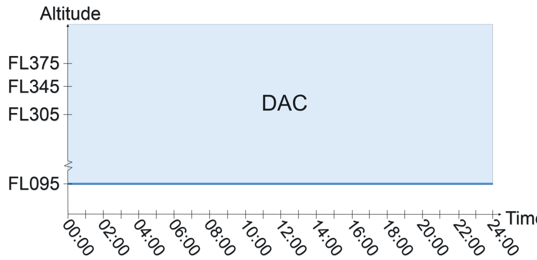

(a) Scenario 1: DAC

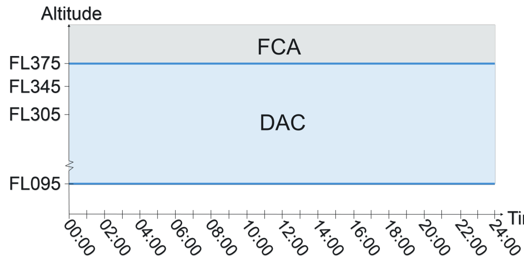

(b) Scenario 2: static DAC/FCA

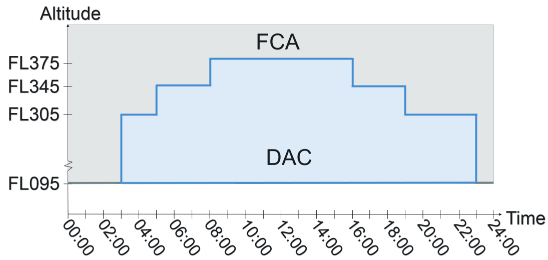

(c) Scenario 3: dynamic DAC/FCA

Figure III-7: *Resulting airspace delineation for the three scenarios assessed*

underloads among all open sectors and periods.

The overload sum observed in Figure III-8(a) shows that DAC/FCA both static and dynamic processes outperform DAC alone, reducing the overloads significantly, 33% and 47% respectively. These reductions are significant and demonstrate that capacity planning can be improved with the use of integrated DAC/FCA mode. A possible explanation is that since FCA does not make use of the trajectory reallocation, the algorithm opens a new CWP when foresees an increased complexity period (and new trajectories are arriving). This reasoning is also consistent with the fact that there is a big number of underloads (see Figure III-8(b)) for FCA in Scenario 2 DAC/FCA static, since it takes some time to close the active CWPs that were decided to be closed but still have few aircraft in the area and, thus, are really underloaded. In other words, instead of reallocating those few flights to other CWPs, there is a lapse of time where too many CWPs are opened and many underloads are accounted.

The integrated and dynamic DAC/FCA offers even more flexibility, hence, results are even better in terms of overloads (there are less overall although more in FCA region, obviously because it is taking more airspace along the day) and underloads (there are less overall) meaning that the capacity is better balanced.

III.3.5 Results: Cost-effectiveness analysis

The cost-effectiveness indicators compared are Control Working Position Hours, as a measure of what are the resources needed to handle the demand with the particular airspace configuration. If more CWPs hours are needed, this implies the Air Navigation Service Provider (ANSP) would need more ATCOs on duty, thus increasing costs associated to ATCO salaries. A reduction of CWPs would mean that scenario is more efficiently prepared and ANSP can control the same flight hours with less cost.

Figure III-8(c) depicts the comparison of the CWP hours for the three scenarios. Results show an increment of controlling hours when the static DAC/FCA is applied. It can be explained due to the static FL of the DAC/FCA boundary. If complexity is concentrated in the FCA area, additional controllers would be needed to manage the complexity which may have been better dealt with in a DAC scenario whereby 2 controllers could have opened a sector to manage this complex area which would be more efficient than FCA. In addition, because of the FCA trajectory allocation algorithm does not include a reallocation mechanism of trajectories, some CWPs are underloaded during some periods of the day. Looking at the dynamic DAC/FCA scenario a reduction of the controlling hours is obtained, even with lack of reallocation in the FCA algorithm which confirms that the use of DAC mode in some complex areas/periods would be more efficient than FCA mode.

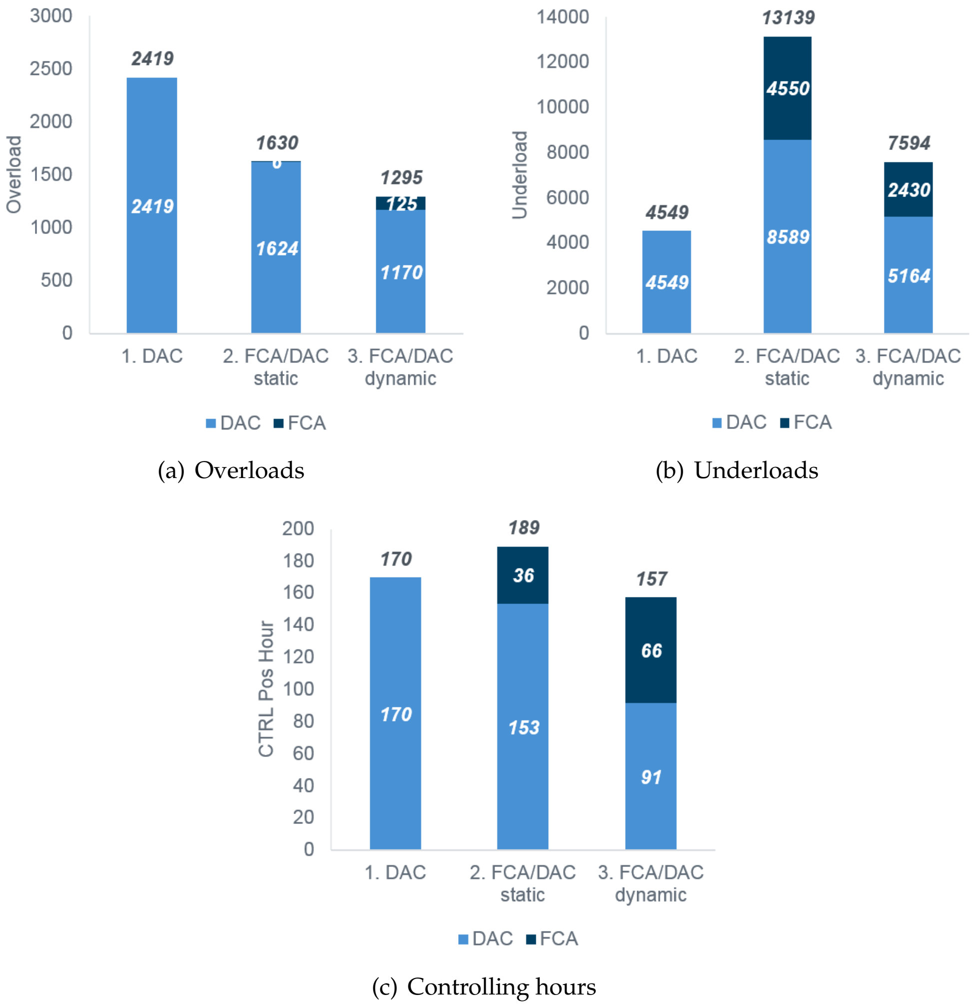

(a) Overloads

(b) Underloads

(c) Controlling hours

Figure III-8: *Capacity and cost-effectiveness indicators for all the scenarios*

III.4 Discussion on holistic DAC/FCA

Although the combination of DAC/FCA looks like very promising with some benefits in terms of capacity and cost-effectiveness, some operational consideration must be taken into account:

- The cost of changing the DAC/FCA airspace delineation has not been considered in this study and it may have an impact in the cost-effectiveness analysis.
- These results shows that the dynamic DAC/FCA scenario is very promising from the cost-effectiveness point of view. However, to achieve the potential benefit especially in longer term, it is very important to introduce more sophisticated Human Resource Planning tools (adapted to this new concept) in order translate the reduction in controlling hours in economic savings.
- The FCA allocation algorithms are very simple nowadays and must be improved in the future. Since the situation awareness of the FCA controlling working position is limited, the flight allocation algorithm shall group the flights involved in potential separation issues into the same CWP.
- The FCA concept by itself was criticised by controllers when the study exposed in this chapter was presented in a workshop during the 9th Single European Sky ATM Research (SESAR) Innovation Days hosted in Athens. Again the FCA situation awareness was questioned.
- A more recent study Capiot *et al.* (2022) analysed the FCA concept on non-nominal condition (emergency decompression, radio failure and thunderstorms). Regarding the situation awareness, controllers reported that in some situations they were overwhelmed and further improvements were identified in this domain.

For all these reasons, the FCA solution is not longer explored in this PhD since it is not considered to be mature enough at the moment this dissertation is written. Hence, DAC will be considered as main capacity management initiative when deployed together with demand management initiatives in the holistic Demand and Capacity Balancing (DCB) models that are proposed in this PhD.

IV

ATFCM concept of operations and general mathematical formulation for holistic DCB

As stated before, one of the main objectives of this thesis is to improve the state-of-the-art Air Traffic Flow and Capacity Management (ATFCM) models, in order to better integrate the functions of the Network Manager (NM) and Air Navigation Service Providers (ANSPs) when dealing with demand and capacity imbalances, while considering (to some extent) the preferences of the AUs by means of alternative trajectories. This approach requires to introduce some changes in the concept of operations currently implemented by the Network Manager. Hence, this chapter is devoted to explain this new (or modified) concept of operations for ATFCM, including the new roles proposed for the involved stakeholders, along with the different interactions and processes needed to solve the Demand and Capacity Balancing (DCB) problem. Furthermore, this chapter introduces the mathematical formulation that will be required to formalise the different DCB Models presented in the following chapters.

IV.1 Proposed demand and capacity balancing concept

The concept of operations proposed in this PhD represents a significant paradigm shift since the NM will also decide which sectorisations shall be used in the airspace under its responsibility. Thus, demand *and* capacity are both responsibility of the NM and considered in a single mathematical optimisation problem (i.e., holistic DCB).

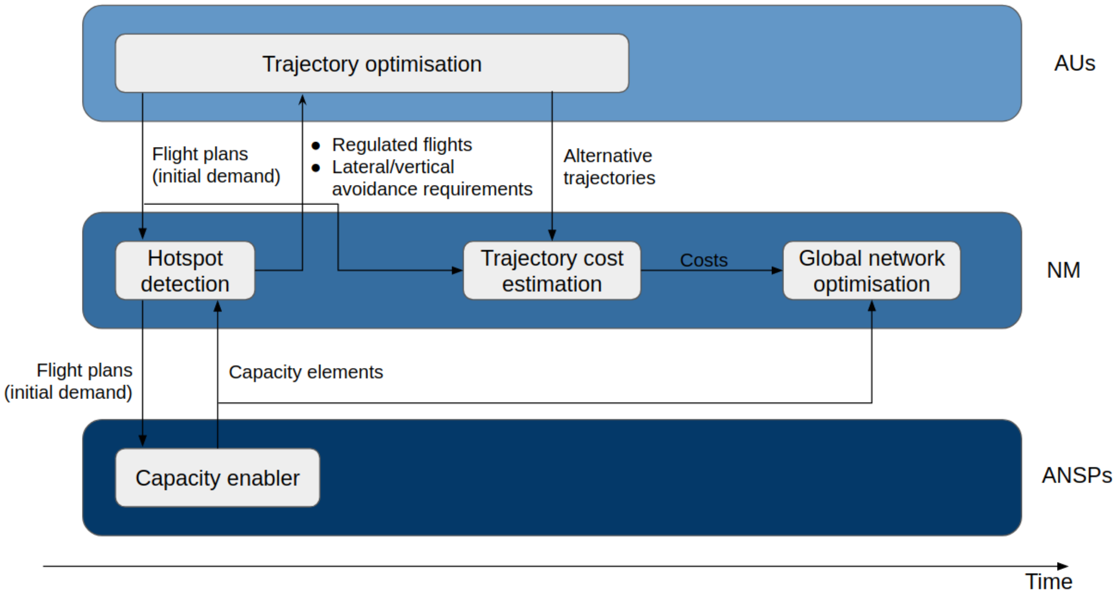

Figure IV-1: *Framework of the proposed concept of operations.*

Figure IV-1 presents the framework proposed, identifying the 3 main stakeholders and the interactions among them. The process starts when the Airspace Users (AUs) share their initial flight plans, which basically represent their original preferences. This initial demand is collected by the NM, as in current operations. At the same time, this initial demand information is shared with the ANSPs, who act as capacity enablers. Note that in this framework "capacity enablers" is used instead of "capacity providers", since in the proposed concept of operations the contribution of the ANSPs in capacity management is to provide the capacity elements options in terms of airspace configurations, operating sectors or elementary sectors, but not deciding which operating sectors should be implemented.

With the initial demand and capacity elements options, the NM can preliminary identify where and when the demand may be above the capacity (i.e. hotspots). Then, the NM identifies which flights are crossing a hotspot and provides geographical and temporal information of the hotspot to the concerned AUs. This information is then used by the AUs to provide (if they want) new trajectories avoiding the hotspots for the concerned flights. Note that in case the AUs reject the possibility of providing alternative trajectories, they are restricting the NM to allocate them only delay what may lead to an unfavorable solutions for the AUs. These new trajectories are added as alternatives to the trajectory initially submitted by the AUs, which is still considered by the NM. At the end of the process, the AUs will have disposed the initial trajectories as well as different alternative trajectories for all (or some) concerned flights.

The ANSPs will provide the capacity elements together with the costs incurred when providing Air Traffic Services (ATS) for the different airspace configurations. The same assumption does not hold for the AUs, which are typically very reluctant to disclose their cost models due to business privacy. For this reason, in this proposed concept of operations it is assumed that the NM estimates the cost of the initial, as well as the alternative trajectories. This fact would also avoid some "cheating" mechanism that airlines may use if they would report the costs of their flights (for example, they could report more expensive costs in order be prioritised). It is worth noting, however, that all models presented in this PhD are still valid (and would be even more precise) if the AUs would provide their real costs rather than being estimated by the NM.

All models presented in this PhD aim at providing the system-wide optimum solution in terms of cost, considering both the AUs and the ANSPs associated costs. With all the available trajectories (and their estimated costs) and all the capacity options (and their reported costs), the NM solves a global optimisation problem to decide which trajectory will finally be used for each flight; how much delay will be allocated (if any); and which operating sectors will be used by the ANSPs at every period of time. As explained above, this decision is taken considering a minimisation of a network-wide cost function.

This mechanism is fully aligned with the latest SESAR concept of operations (SESAR PJ19 Consortium, 2019), which aims at restricting AUs demand as less as possible, shifting capacity where demand is needed (instead of restricting demand when capacity is scarce). In particular, the Dynamic Airspace Configurations (DAC) and the advanced DCB solutions (studied in projects PJ08 (SESAR PJ08 Consortium, 2019) and PJ09 (SESAR PJ09 Consortium, 2019), respectively) are considered integrated into a single optimisation problem.

It is expected that the concept of operations provided in this PhD will provide more flexibility to the AUs through the possibility to submit alternative trajectories, and the role of "capacity provider" is shared between the different ANSPs under the umbrella of the same NM. While the ANSP provide the capacity options and ATS, is the NM who finally decides how the capacity will be provided considering the global picture of the network as a whole.

IV.2 Problem definition

The DCB problem addressed in this PhD consists of finding an optimal combination of airspace sectorisations and trajectory/delay allocation that minimises the total cost of the system as a whole (considering the cost of the different sectorisations and the cost of the flights), while keeping demand below the capacity.

One of the contributions of this PhD is the introduction of complexity as metric for demand and capacity together with the use of different levels of DAC for the capacity management. The choice of the airspace sectorisation (capacity management) depends on the level at which capacity management is performed. In this PhD, four different levels are considered and outlined in Table I-1. Along with a reference model that is not using complexity but entry counts, this leads to the five different DCB models considered in this PhD:

- Demand management only

  Model 0: fixed opening schemes with entry counts at Traffic Volume (TV) level.

  Model I: fixed opening schemes with complexity metric.

- Holistic demand and capacity management with complexity metric

  Model II: with a given set of configurations among which the active one should be chosen for each time period.

  Model III: with a given set of operating sectors. Flexible configurations can be done combining the existing operating sectors.

  Model IV: with a fixed set of elementary sectors. The elementary sectors can be collapsed in order to create new collapsed sectors. Then, the elementary and collapsed sectors are grouped in sectorisations for each time period.

IV.3 DCB mathematical formulation

Firstly, the mathematical sets that will be used across all proposed the models of this PhD are defined:

$\mathcal{F}$	Set of flights
$\mathcal{T}$	Set of instants of time
$\mathcal{P}$	Set of periods of time
$\mathcal{T}^p \subset \mathcal{T}$	Set of instants of times in the period $p, \forall p \in \mathcal{P}$
$\mathcal{T}_k^v \subset \mathcal{T}$	Set of instants of times when trajectory k can potentially arrive at the traffic volume v, $\forall k \in \mathcal{K}, \forall v \in \mathcal{V}$
$\mathcal{K}$	Set of all trajectories
$\mathcal{K}_f \subset \mathcal{K}$	Set of trajectories for flight $f, \forall f \in \mathcal{F}$
$\mathcal{V}$	Set of traffic volumes
$\mathcal{V}_k$	Set of traffic volumes that the trajectory k crosses
$\mathcal{S}_{\text{E}}$	Set of elementary sectors
$\mathcal{S}_{\text{C}}$	Set of collapsed sectors
$\mathcal{S} = \mathcal{S}_{\text{E}} \cup \mathcal{S}_{\text{C}}$	Set of operating sectors
Λ	Set of configurations
Λ^s	Set of configurations that contain the operating sector $s, \forall s \in \mathcal{S}$
$\mathcal{E}^s$	Set of elementary sectors in operating sector $s, \forall s \in \mathcal{S}$
$\mathcal{S}^{s_{\text{E}}}$	Set of operating sectors that contains the elementary sector $s_{\text{E}}, \forall s_{\text{E}} \in \mathcal{S}_{\text{E}}$
$\mathcal{S}_a^p$	Set of active operating sectors during the period $p, \forall p \in \mathcal{P}$

It should be noted that not all sets are used in all models since some of them are applicable depending on the capacity management level. The different particularities will be given in the specific sections defining each model.

Besides sets, the following parameters are also defined:

$\underline{\mathcal{T}}_k^v$	First instant of time when the trajectory k can arrive at traffic volume v
$\overline{\mathcal{T}}_k^v$	Last instant of time when the trajectory k can arrive at traffic volume v
J_k	Total cost of trajectory $k, \forall k \in \mathcal{K}$
J_{F_k}	Cost of fuel of trajectory $k, \forall k \in \mathcal{K}$
J_{D_k}	Cost of arrival delay of trajectory $k, \forall k \in \mathcal{K}$
J_{T_k}	Cost of trip time of trajectory $k, \forall k \in \mathcal{K}$
R_k	Cost of route charges for trajectory k, $\forall k \in \mathcal{K}$
$\bar{J}_k$	Cost of the initial submitted trajectory of the flight associated with trajectory $k, \forall k \in \mathcal{K}$
$\bar{J}_{\text{F}_k}$	Cost of fuel of the initial submitted trajectory of the flight associated with trajectory $k, \forall k \in \mathcal{K}$
$\bar{J}_{\text{D}_k}$	Cost of arrival delay of the initial submitted trajectory of the flight associated with trajectory $k, \forall k \in \mathcal{K}$
$\bar{J}_{\text{T}_k}$	Cost of time of the initial submitted trajectory of the flight associated with trajectory $k, \forall k \in \mathcal{K}$
$\bar{R}_k$	Cost of route charges of the initial submitted trajectory of the flight associated with trajectory k, $\forall k \in \mathcal{K}$
r_k^v	Estimated time of arrival of trajectory k at traffic volume v, $\forall k \in \mathcal{K}, \forall v \in \mathcal{V}$
v_k^*	The next traffic volume that the trajectory k crosses after v
$\underline{\mathcal{V}}_k$	First traffic volume that the trajectory k crosses
$\overline{\mathcal{V}}_k$	Last traffic volume that the trajectory k crosses

α_k	Arrival delay unit cost for trajectory k, $\forall k \in \mathcal{K}$
β_k	Fuel unit cost for trajectory k, $\forall k \in \mathcal{K}$
F_k	Trip fuel used in trajectory k, $\forall k \in \mathcal{K}$
T_k	Trip time of trajectory k, $\forall k \in \mathcal{K}$
D_k	Ground delay of trajectory k, $\forall k \in \mathcal{K}$
$\bar{T}_k$	Trip time of the initial submitted trajectory of the flight associated with trajectory k, $\forall k \in \mathcal{K}$
$\bar{J}_k$	Cost of operating the initial submitted trajectory of the flight associated with trajectory k, $\forall k \in \mathcal{K}$
$H^{t,s}$	Complexity threshold of sector s at time t, $\forall t \in \mathcal{T}$, $\forall s \in \mathcal{S}$
$H^{p,v}$	Entry count threshold of traffic volume v during the period p, $\forall v \in \mathcal{V}$, $\forall p \in \mathcal{P}$
$\theta^{p,s}$	Cost of opening sector s during the period p, $\forall p \in \mathcal{P}$, $\forall s \in \mathcal{S}$
ρ	Penalty cost of allocating one elementary sector to a different operating sector

As for sets, not all parameters are required in all models. In fact, some of them are decision variables in some models. The particular details will be given in the specific section for each model.

When using complexity metrics, choosing one alternative trajectory or just allocating delay to some flights changes the traffic patterns and, consequently, the complexity of controlling the traffic situation. Hence, the delay options for a trajectory are modelled as new alternative trajectories.

Thus, the demand management is reduced to the selection of a single trajectory among a set of available options for each concerned flight. This is considered though the decision variable z_k defined as follows:

$$z_k = \begin{cases} 1, & \text{if trajectory } k \text{ is chosen} \\ 0, & \text{otherwise} \end{cases}, \quad \forall k \in \mathcal{K}. \tag{IV.1}$$

Aside from z_k, more decision variables might be needed depending on the chosen model. These will be introduced and described in the corresponding sections for each model separately.

IV.3.1 Time considerations

An important remark is required to clarify the difference between the sets $\mathcal{T}$ and $\mathcal{P}$. The set $\mathcal{T}$ contains instants of time and the set $\mathcal{P}$ contains periods of time. One period $p \in \mathcal{P}$ contains one or more instants of times defined in $\mathcal{T}^p$.

During a period, the opening scheme does not change, so it can be understood as the minimum amount of time that one configuration is open. Moreover, in Model 0, where traffic load is evaluated in entry counts, the demand and capacity is balanced during the periods $p \in \mathcal{P}$. In the models with complexity metric (i.e. Models I, II, III and IV) the demand and capacity in the open sectors is balanced at every instant of time $t \in \mathcal{T}$.

IV.3.2 Cost function

All the models have the same cost function, which accounts, on the one hand, for the extra cost for the AU when comparing the cost of the selected trajectory with the cost of the trajectory initially planned ($J_{\Delta A}$). On the other hand, the cost function also considers the capacity provision cost for the ANSPs, based on the activation of certain sectors (J_O). Additionally, differences in sector configurations are penalised with an extra term J_S, being represented as function of the number of elementary sectors that change the operating sector in consecutive periods of time. This is done in order to obtain smoother sector transitions. Mathematically, this cost function is expressed as follows:

$$J = J_{\Delta A} + J_O + J_S, \tag{IV.2}$$

where the extra cost for the AUs, $J_{\Delta A}$, is:

$$J_{\Delta A} = \sum_{k \in \mathcal{K}} (J_k - \bar{J}_k) z_k, \tag{IV.3}$$

being J_k the cost of trajectory k and $\bar{J}_k$ the cost of the initial submitted trajectory of the flight associated with trajectory k.

The cost for the ANSP due to the active sectors (J_O) and the penalty cost explained above (J_S) have different definitions depending on the specific DCB model. Hence, they will be defined in the dedicated section to each model.

It is worth noting that the cost of the trajectories (J_k and $\bar{J}_k$) is estimated by the NM (see Section IV.1). In this PhD, this cost is estimated as follows: the cost of the trajectory k, J_k, could be modelled taking into account the cost of fuel (J_{F_k}), the extra cost due to arrival delay (J_{D_k}), the cost of the trip time (J_{T_k}) and (if applicable) the route charges (R_k):

$$J_k = J_{\mathrm{F}_k} + J_{\mathrm{D}_k} + J_{\mathrm{T}_k} + R_k, \quad \forall k \in \mathcal{K}. \tag{IV.4}$$

with,

$$J_{\mathrm{F}_k} = \beta_k F_k, \quad \forall k \in \mathcal{K}, \tag{IV.5}$$

$$J_{\mathrm{D}_k} = \alpha_k (T_k - \bar{T}_k + D_k), \quad \forall k \in \mathcal{K}, \tag{IV.6}$$

$$J_{\mathrm{T}_k} = \beta_k \mathrm{CI}_k T_k, \quad \forall k \in \mathcal{K}, \tag{IV.7}$$

where α_k is the arrival delay unit cost for trajectory k, β_k is the fuel unit cost for trajectory k, CI_k is the cost index for trajectory k, F_k is the trip fuel used in trajectory k, T_k is the trip time of trajectory k, $\bar{T}_k$ is the trip time of the initial submitted trajectory of the flight associated with trajectory k and D_k is the ground delay of trajectory k.

It is acknowledged that a network-wide cost minimisation does not guarantee a fair distribution of the total cost on the individual airspace users in the obtained solution. Fairness aspects for these type of problems have been widely studied in the literature (see for instance Barnhart *et al.* (2012) and Bertsimas & Gupta (2016). Some ways to take into account fairness can be found in Tosic & Babic (1995). The fairness, however, is out of the scope of the formulation presented in this PhD.

IV.3.3 Complexity modeling

One of the contributions of this PhD is the introduction of complexity in the concept of operations for ATFCM proposed in Section IV.1. Since in this work the choice of the particular trajectory a flight will operate is part of the decision process, the sector complexity is not known in advance. For this reason, the complexity has to be computed initially for all pairs of trajectories (independently of whether they are finally selected in the solution or not). It is worth noting that this is not a significant drawback since, even in the worst case, the complexity has to be computed $|\mathcal{K}|^2$ times (being $\mathcal{K}$ the set of trajectories), due to the assumptions listed below.

The models introduced in this thesis are not restricted to any particular complexity metric and are valid for any complexity metric that satisfies the following conditions:

- The complexity induced by a pair of aircraft is independent for any surrounding traffic, meaning that the complexity contribution of flight j to the flight i does not depend on other flights.

- The complexity metric at trajectory level is additive, hence, the complexity of one trajectory is the addition of the contributions of all other trajectories to that one.

Note that these assumptions are not introduced in order to simplify the mathematical formulation presented in this PhD. In fact, a large number of state-of-the-art complexity metrics (e.g. cognitive complexity, trajectory based complexity, dynamic density or geometrical complexity, among others) satisfy these conditions, as well as the current metrics used in operations (entry or occupancy counts). For this reason, these assumptions allow to present formulations with the highest level of granularity (from pairwise trajectory level to sector level), but without restricting them to any particular complexity metric.

Moreover, the majority of those complexity metrics do not have a closed analytical formulation. Due to this fact, in this PhD the complexity induced by any pair of aircraft is computed in advance, and it is considered as an input data for the DCB models. This last premise requires that delays are considered as new trajectories. This significantly increases the number of alternative trajectories and hence the problem size (dependant on the discretisation step of the delay).

Since the DCB models presented in this PhD aim at balancing demand and capacity at the different Air Traffic Control (ATC) sectors, this pre-computed complexity given per pairs of trajectories needs to be aggregated at sector level. The following subsection describes in detail this process.

IV.3.3.1 Complexity aggregation

As commented above, it is assumed that the complexity is given per pairs of trajectories. Let $C^t_{k,k'}$ be the complexity that trajectory k' generates on trajectory k at time t. Since we assume that the complexity is additive, the total complexity that all trajectories generate on trajectory k at time t in sector s can be computed as:

$$C^{t,s}_{\mathrm{T}_k} = \sum_{s_\mathrm{E} \in \mathcal{E}^s} B^{t,s_\mathrm{E}}_k \sum_{k' \in \mathcal{K} \setminus \{k\}} C^t_{k,k'} z_{k'} z_k, \quad \forall k \in \mathcal{K}, \forall t \in \mathcal{T}, \forall s \in \mathcal{S}, \tag{IV.8}$$

where B^{t,s_E}_k is a binary incidence parameter that indicates whether the aircraft of trajectory k is located in the elementary sector s_E at the instant of time t:

$$B^{t,s_\mathrm{E}}_k = \begin{cases} 1, & \text{if trajectory } k \text{ is in the elementary} \\ & \text{sector } s_\mathrm{E} \text{ at the instant of time } t \\ 0, & \text{otherwise} \end{cases} \quad \forall k \in \mathcal{K}, \forall t \in \mathcal{T}, \forall s_\mathrm{E} \in \mathcal{S}_\mathrm{E}. \tag{IV.9}$$

Note that $C^{t,s}_{\mathrm{T}_k}$ will be zero when the aircraft that follows trajectory k is not in sector s at the instant of time t. Yet, the complexity contribution of other trajectories k' will be considered regardless of whether they are crossing sector s or not at the instant of time t. This is especially important when aircraft are close to the sector boundary, where potential interactions with aircraft in adjacent sectors are more likely.

Furthermore, the contribution of z_k in equation (IV.8) is to ensure that $C^{t,s}_{\mathrm{T}_k}$ is null when the trajectory k is not selected, while z'_k avoids the addition of complexity contributions from trajectories that are finally not selected either.

Finally, the complexity at sector s at time t is computed by the addition of the complexity associated to all trajectories within it at that instant of time:

$$C^{t,s}_{\mathrm{S}} = \sum_{k \in \mathcal{K}} C^{t,s}_{\mathrm{T}_k}, \quad \forall t \in \mathcal{T}, \forall s \in \mathcal{S}. \tag{IV.10}$$

A simple illustrative example showing the computation of the complexity at sector level from the complexity at trajectory level is provided in Annex A.

As stated before, the principal constraint in a DCB problem is to ensure that the traffic demand is kept below the available capacity, $H^{t,s}$. Since this PhD considers complexity as main capacity indicator, this is ensured by the following constraint:

$$C_{\mathrm{S}}^{t,s} = \sum_{k \in \mathcal{K}} C_{\mathrm{T}_k}^{t,s} \leq H^{t,s}, \quad \forall s \in \mathcal{S}_a^p, \forall p \in \mathcal{P}, \forall t \in \mathcal{T}^p, \tag{IV.11}$$

where $H^{t,s}$ is the complexity threshold of sector s at the instant of time t. $\mathcal{S}_a^p$ is the set of active sectors during the period p, $\mathcal{P}$ is the set of periods and $\mathcal{T}^p$ is the set of instants of time in the period p.

Note that the previous constraint is only applied to the sectors that are activated at each instant of time t. This is considered through the set $\mathcal{S}_a^p$ when the sector opening scheme is fixed and known (i.e. in Model I), but it is treated differently in the remaining models, where choice of active sector is part of decision process. These differences are properly explained in the corresponding DCB model sections.

IV.3.3.2 Linearisation

Equation (IV.8) and, as a consequence, the equations (IV.10) and (IV.11) are clearly non-linear, but they can be reformulated in order to obtain linear expressions. The complexity contribution of trajectory k to the sector s at time t, introduced in Equation (IV.8), takes the following values depending on the z_k:

$$C_{\mathrm{T}_k}^{t,s} = \begin{cases} \sum_{s_{\mathrm{E}} \in \mathcal{E}^s} B_k^{t,s_{\mathrm{E}}} \sum_{k' \in \mathcal{K} \setminus \{k\}} C_{k,k'}^t z_{k'}, & \text{if } z_k = 1 \\ 0, \quad \text{if } z_k = 0 \end{cases}, \quad \forall k \in \mathcal{K}, \forall t \in \mathcal{T}, \forall s \in \mathcal{S}. \tag{IV.12}$$

Hence, it is modeled with new auxiliary decision variable, $C_{\mathrm{T}_k}^{*t,s}$, which represents a chosen value of complexity for the trajectory k in sector s at time instant t, whose value is bounded with the following two constraints :

$$C_{\mathrm{T}_k}^{*t,s} \geq 0\,, \quad \forall k \in \mathcal{K}, \forall t \in \mathcal{T}, \forall s \in \mathcal{S}, \tag{IV.13}$$

$$C_{\mathrm{T}_k}^{*t,s} \geq \sum_{s_{\mathrm{E}} \in \mathcal{E}^s} B_k^{t,s_{\mathrm{E}}} \sum_{k' \in \mathcal{K} \setminus \{k\}} C_{k,k'}^t z_{k'} + M(z_k - 1), \quad \forall k \in \mathcal{K}, \forall t \in \mathcal{T}, \forall s \in \mathcal{S}, \tag{IV.14}$$

where M is a new parameter that is greater than any possible value of $C_{\mathrm{T}_k}^{t,s}$. Therefore, depending on the value of z_k there are two options:

- Trajectory k is selected (z_k = 1). The constraint defined in Equation (IV.14) is active and leads to:

$$C_{\mathrm{T}_k}^{*t,s} \geq \sum_{s_{\mathrm{E}} \in \mathcal{E}^s} B_k^{t,s_{\mathrm{E}}} \sum_{k' \in \mathcal{K} \setminus \{k\}} C_{k,k'}^t z_{k'}, \quad \forall k \in \mathcal{K}, \forall t \in \mathcal{T}, \forall s \in \mathcal{S}. \tag{IV.15}$$

- Trajectory k is not selected (z_k = 0). Now, the constraint defined in Equation (IV.14) results in:

$$C_{\mathrm{T}_k}^{*t,s} \geq \sum_{s_{\mathrm{E}} \in \mathcal{E}^s} B_k^{t,s_{\mathrm{E}}} \sum_{k' \in \mathcal{K} \setminus \{k\}} C_{k,k'}^t z_{k'} - M, \quad \forall k \in \mathcal{K}, \forall t \in \mathcal{T}, \forall s \in \mathcal{S}, \tag{IV.16}$$

making it non-active since its right hand side takes zero or negative value due to the parameter M. Thus, only the non-negativity constraint defined in Equation (IV.13) is active.

Then, the constraint defined in Equation (IV.11) can be rewritten as:

$$\sum_{k \in \mathcal{K}} C^{*t,s}_{\mathrm{T}_k} \leq H^{t,s}, \quad \forall s \in \mathcal{S}^p_a, \forall p \in \mathcal{P}, \forall t \in \mathcal{T}^p. \tag{IV.17}$$

Note that ${C_{\mathrm{T}}}^{*t,s}_k$ represents an upper bound of ${C_{\mathrm{T}}}^{t,s}_k$, hence could take greater values than the actual load. This does not, anyhow, affect the actual value of ${C_{\mathrm{T}}}^{t,s}_k$ (neither optimal number of active sectors), but guarantees that it will always be below the capacity threshold, as it can be seen in the next expression:

$$C^{t,s}_{\mathrm{S}} = \sum_{k \in \mathcal{K}} {C_{\mathrm{T}}}^{t,s}_k \leq \sum_{k \in \mathcal{K}} {C_{\mathrm{T}}}^{*t,s}_k \leq H^{t,s}, \quad \forall s \in \mathcal{S}^p_a, \forall p \in \mathcal{P}, \forall t \in \mathcal{T}^p. \tag{IV.18}$$

After solving the DCB problem, the actual values of ${C_{\mathrm{T}}}^{t,s}_k$ can be easily computed through the application of Equation (IV.8).

The following chapters explain the different DCB problems and their Mixed Integer Linear Programming (MILP) formulations identifying all required decision variables, the particularities of the objective function and the constraints. A simple example, which aims to verify the models and their formulations is reported in Annex B. Chapter V introduces the demand management models, i.e. Model 0 and Model I; and Chapter VI presents Models II, III and IV where the holistic integration between demand and capacity management initiatives is deployed.

V

Demand management

This chapter aims at introducing the Demand and Capacity Balancing (DCB) models focused only on the demand side. The sector opening scheme is fixed and the models presented lead at choosing which trajectory will be flown per flight and how much delay is allocated.

Two subproblems have been investigated: Model 0, that uses entry counts on traffic volumes, and Model I, that uses complexity in order to evaluate the demand and the capacity. Model 0 is introduced as an intermediate step towards the use of complexity metrics in DCB.

V.1 Model 0: traffic volume approach

In current operations, a certain amount of capacity overloads are usually allowed for certain sectors. Several reasons could explain this phenomenon: the lack of initial schedules for non-planed flights, the use of entry rate for assessing the demand without considering the occupancy, a conservative way for estimating the capacity and the complexity of traffic patterns, etc. Although some of the previous limitations can be solved by the introduction of complexity metrics, an intermediate step consists on changing the airspace unit used in the hotspot detection from sector to Traffic Volume (TV).

A TV is related with a reference location, that can be a sector, a collapsed sector or an airport. In addition, one TV is defined by a set of included and excluded flows, what can be understood as a directional filter. For example, Fig. V-1 shows a sector with three major flows, A-E, B-D, and C-F. It seems logical that the intersection between the flows A-E and B-D can create some capacity constraint. Thus, a regulation over a TV related with this sector and including the flows A-E and B-D and excluding C-F may be applied. Currently, the regulations in Europe are applied to TVs.

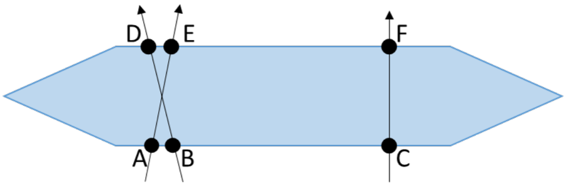

Figure V-1: *Illustrative example of traffic volume*

Hence, the Model 0 evaluates the demand and capacity using entry counts on TVs (and not at sector level) as directional traffic filters and not entry counts in the sector. This offers an intermediate step towards the full usage of complexity metrics since the regulations can be deployed only affecting the traffic flows that arguably create more traffic complexity.

This model disregards the capacity management since the opening scheme is given and the only decision is on the demand side by choosing the trajectory and the amount of delay for each flight. Note that in this case, since no complexity metric is used, trajectory and ground delay are decoupled (meaning that the ground delay is not considered as new alternative trajectories).

The decision variables, objective function, and restrictions are all explained in the sections that follow.

V.1.1 Decision variables

There are two decisions to be taken: 1) Which trajectory is used per each flight? 2) How much delay is applied? These decisions are modelled with the following decision variables:

$$z_k = \begin{cases} 1, & \text{if trajectory } k \text{ is chosen} \\ 0, & \text{otherwise} \end{cases} \quad , \forall k \in \mathcal{K}, \tag{V.1}$$

$$b_k^{t,v} = \begin{cases} 1, & \text{if trajectory } k \text{ arrives at traffic volume } v \text{ by time } t \\ 0, & \text{otherwise} \end{cases} \quad , \forall k \in \mathcal{K}, \forall t \in \mathcal{T} \cup \{0\}, \forall v \in \mathcal{V}, \tag{V.2}$$

where $\mathcal{K}$ is the set of trajectories, $\mathcal{T}$ is the set of instants of time and $\mathcal{V}$ is the set of traffic volumes. Note that, according to Bertsimas & Patterson (1998), the use of "by" time provides faster solution time than "at" time. However, the "at" time expressions can be easily found by $(b_k^{t,v} - b_k^{t-1,v})$, for all k, v and t in their respective sets.

The set of instants of time is defined as $\mathcal{T} = \{1, ..., t_{max}\}$ and t_{max} is the latest arrival time r_k^v over all trajectories and traffic volumes plus de maximum amount of delay allowed ϕ:

$$t_{max} = \max(r_k^v) + \phi, \quad \forall k \in \mathcal{K}, \forall v \in \mathcal{V}. \tag{V.3}$$

The decision variable $b_k^{t,v}$ is defined $\forall t \in \mathcal{T} \cup \{0\}$, which include one instant of time before the first instant of $\mathcal{T}$. The value of $b_k^{t,v}$ at this time is always null:

$$b_k^{0,v} = 0, \quad \forall k \in \mathcal{K}, \forall v \in \mathcal{V}. \tag{V.4}$$

V.1.2 Objective function

Equation (IV.2) gives a general definition of the objective function used in this dissertation. Yet, the capacity related costs, i.e. J_O and J_S, are not considered since the opening scheme is given, so they are constant for every feasible solution. Thus, this model aims to minimise the total additional trajectory cost for the airspace users:

$$J = J_{\Delta A}, \tag{V.5}$$

where $J_{\Delta A}$ is defined by equation IV.3, together with the expressions IV.4, IV.5, IV.6 and IV.7. Since the ground delay in this model is not addressed with new alternative trajectories defined in advance, the ground delay (D_k) in Equation (IV.6) is defined as:

$$D_k = \sum_{t \in \mathcal{T}_k^{\underline{\mathcal{V}_k}}} (t - r_k^{\underline{\mathcal{V}_k}})(b_k^{t,\underline{\mathcal{V}_k}} - b_k^{t-1,\underline{\mathcal{V}_k}}), \quad \forall k \in \mathcal{K}, \tag{V.6}$$

where $\underline{\mathcal{V}_k}$ is the first traffic volume that the trajectory k crosses. Note that the consideration of the ground delay costs as well as the extra cost due to longer trip times means that this models is evaluating the cost of the arrival delays.

V.1.3 Constraints

This section lists and describes all the constraints applied to Model 0:

- One trajectory, i.e. the initial or one of the alternatives must be selected:

$$\sum_{k \in \mathcal{K}_f} z_k = 1, \quad \forall f \in \mathcal{F}. \tag{V.7}$$

- Constraints for applying the "by" time technique (Bertsimas & Patterson, 1998):

$$b_k^{\underline{\mathcal{T}}_k^v - 1, v} = 0, \quad \forall k \in \mathcal{K}, \forall v \in \mathcal{V}_k, \tag{V.8}$$

$$b_k^{\overline{\mathcal{T}}_k^v, v} = z_k, \quad \forall k \in \mathcal{K}, \forall v \in \mathcal{V}_k, \tag{V.9}$$

$$b_k^{t,v} - b_k^{t-1,v} \geq 0, \quad \forall k \in \mathcal{K}, \forall v \in \mathcal{V}_k, \forall t \in \mathcal{T}_k^v. \tag{V.10}$$

  Constraint V.9 forces that all the decision variables are equal to zero when the trajectory is not selected.

- Only ground holding is allowed:

$$b_k^{t + r_k^{v_k^*} - r_k^v, v_k^*} - b_k^{t,v} = 0, \quad \forall k \in \mathcal{K}, \forall v \in \mathcal{V}_k \setminus \{\overline{\mathcal{V}_k}\}, \forall t \in \mathcal{T}_k^v. \tag{V.11}$$

  where v_k^* is the next traffic volume that the trajectory k crosses after v and $\overline{\mathcal{V}_k}$ is the last traffic volume that the trajectory k crosses and it is excluded from the set $\mathcal{V}_k$.

- The demand can not exceed the capacity of any traffic volume:

$$\sum_{k \in \mathcal{K}} \sum_{t \in \mathcal{T}_k^v \cap \mathcal{T}^p} (b_k^{t,v} - b_k^{t-1,v}) \leq H^{p,v}, \quad \forall v \in \mathcal{V}, \forall p \in \mathcal{P}, \tag{V.12}$$

  being $H^{p,v}$ the entry counts threshold of TV v during the period of time p.

V.1.4 MILP formulation for Model 0

Wrapping up, and for the sake of completeness, this section summarises the full Mixed Integer Linear Programming (MILP) formulation for this model.

$$\min J_{\Delta A} = \sum_{k\in\mathcal{K}} \Big[(J_{\mathrm{F}_k} - \bar{J}_{\mathrm{F}_k}) + (J_{\mathrm{T}_k} - \bar{J}_{\mathrm{T}_k}) + (R_k - \bar{R}_k) + \alpha_k \Big[(T_k - \bar{T}_k) + \sum_{t\in\mathcal{T}_k^{\underline{\mathcal{V}_k}}} (t - r_k^{\underline{\mathcal{V}_k}})(b_k^{t,\underline{\mathcal{V}_k}} - b_k^{t-1,\underline{\mathcal{V}_k}})\Big]\Big] z_k \tag{V.13}$$

s.t.

$$\sum_{k\in\mathcal{K}_f} z_k = 1, \quad \forall f \in \mathcal{F} \tag{V.14}$$

$$b_k^{\underline{\mathcal{T}_k^v}-1,v} = 0, \quad \forall k \in \mathcal{K}, \forall v \in \mathcal{V}_k \tag{V.15}$$

$$b_k^{\overline{\mathcal{T}_k^v},v} = z_k, \quad \forall k \in \mathcal{K}, \forall v \in \mathcal{V}_k \tag{V.16}$$

$$b_k^{t,v} - b_k^{t-1,v} \geq 0, \quad \forall k \in \mathcal{K}, \forall v \in \mathcal{V}_k, \forall t \in \mathcal{T}_k^v \tag{V.17}$$

$$b_k^{t+r_k^{v_k^*}-r_k^v, v_k^*} - b_k^{t,v} = 0, \quad \forall k \in \mathcal{K}, \forall v \in \mathcal{V}_k \setminus \{\overline{\mathcal{V}_k}\}, \forall t \in \mathcal{T}_k^v \tag{V.18}$$

$$\sum_{k\in\mathcal{K}} \sum_{t\in\mathcal{T}_k^v\cap\mathcal{T}^p} (b_k^{t,v} - b_k^{t-1,v}) \leq H^{p,v}, \quad \forall v \in \mathcal{V}, \forall p \in \mathcal{P} \tag{V.19}$$

V.2 Model I: complexity approach

This model uses complexity metrics for measuring the traffic load and considers a given opening scheme (i.e. which operating sectors are open and when in time). This information is provided in this model through the set $\mathcal{S}_a^p$ containing the active sectors during every period of time p.

The following subsections explain in detail the decision variables, the objective function and the constraints of this model.

V.2.1 Decision variables

Since this model only affects to the demand side, the decision of the alternative trajectories that would be selected is modelled as:

$$z_k = \begin{cases} 1, & \text{if trajectory } k \text{ is chosen} \\ 0, & \text{otherwise} \end{cases}, \quad \forall k \in \mathcal{K}. \tag{V.20}$$

The real valued auxiliary variable $C_{\mathrm{T}_k}^{*t,s}$ is introduced in order to deal with the linearisation of the capacity limitation constraint as it explained in section IV.3.3.2:

$$C_{\mathrm{T}_k}^{*t,s} \geq 0, \quad \forall k \in \mathcal{K}, \forall t \in \mathcal{T}, \forall s \in \mathcal{S}. \tag{V.21}$$

V.2.2 Objective function

The general definition of the objective function (J) is given in Equation (IV.2). Yet, since the airspace capacity is given in this model, the cost of operation of the sectors, J_O, and the cost of having different configurations, J_S, are fixed and do not affect the optimisation. Thus, this model aims to minimise the total additional trajectory cost:

$$J = J_{\Delta A}. \tag{V.22}$$

V.2.3 Constraints

Two main constraints are identified for the problem:

- From all trajectory options $k \in \mathcal{K}_f$ of flight f, one and only one must be selected:

$$\sum_{k \in \mathcal{K}_f} z_k = 1, \quad \forall f \in \mathcal{F}. \tag{V.23}$$

- The demand can not exceed the capacity (in terms of complexity) in any active sector s and in any instant of time t. As explained in Section IV.3.3.2, equation (IV.11) is not linear, but it is linearised by the introduction of the auxiliary decision variable ${C_{\mathrm{T}}}_k^{*t,s}$ and the constraints (IV.13), (IV.14) and (IV.17).

V.2.4 MILP formulation for Model I

Wrapping up, and for the sake of completeness, this section summarises the full MILP formulation for this model.

$$\min J_{\Delta A} = \sum_{k \in \mathcal{K}} (J_k - \bar{J}_k) z_k \tag{V.24}$$

s.t.

$$\sum_{k \in \mathcal{K}_f} z_k = 1, \quad \forall f \in \mathcal{F} \tag{V.25}$$

$$\sum_{k \in \mathcal{K}} {C_{\mathrm{T}}}_k^{*t,s} \leq H^{t,s}, \quad \forall p \in \mathcal{P}, \forall t \in \mathcal{T}^p, \forall s \in \mathcal{S}_a^p \tag{V.26}$$

$${C_{\mathrm{T}}}_k^{*t,s} \geq \sum_{s_{\mathrm{E}} \in \mathcal{E}^s} B_k^{t,s_{\mathrm{E}}} \sum_{k' \in \mathcal{K} \setminus \{k\}} C_{k,k'}^t z_{k'} + M(z_k - 1), \quad \forall k \in \mathcal{K}, \forall t \in \mathcal{T}, \forall s \in \mathcal{S} \tag{V.27}$$

$${C_{\mathrm{T}}}_k^{*t,s} \geq 0\,, \quad \forall k \in \mathcal{K}, \forall t \in \mathcal{T}, \forall s \in \mathcal{S} \tag{V.28}$$

$$z_k \in \{0, 1\}, \quad \forall k \in \mathcal{K} \tag{V.29}$$

A verification example of this formulation is presented in Annex B.

V.3 Relation with previous research

This chapter presents two models that take decision only on the demand side. The current role of the NM is maintained, which is nowadays the delay allocation using the Computer-Assisted Slot Allocation (CASA) tool EUROCONTROL (2017).

Different works found in the literature only considered the demand side (i.e. fixed capacity). Firstly, researchers tried to solve the Single-Airport Ground Holding Problem (SAGHP) (Odoni, 1987; Terrab & Odoni, 1993; Richetta & Odoni, 1993; Andreatta *et al.*, 1993). Later, the Multi-Airport Ground-Holding Problem (MAGHP) was introduced (Vranas *et al.*, 1992, 1994). These efforts focused solely on the problem in airports, ignoring the en-route airspace. For this reason, Bertsimas & Patterson (1998) proposed a binary integer programming model for the deterministic and multiairport Air Traffic Flow and Capacity Management (ATFCM) problem, which addressed capacity constraints in the en-route airspace. This approach is also used by Xu & Prats (2017), where ground, airborne and linear holding were considered as options for the delay.

The introduction of the alternative trajectories in the DCB formulation was introduced by Bertsimas & Patterson (2000), where the authors tried to minimise the delay costs. A similar approach was considered in Xu *et al.* (2018a, 2020a) but, in this case, the objective was to minimise the total deviation with regard to airspace users' preferences, considering the fuel consumption, the route charges and the cost of delay. Note that the problem addressed by these last works (i.e. fixed sectorisation and alternative trajectories) is similar to the Models 0 and I of this paper. Yet, the demand and the capacity were measured using occupancy or entry counts at sector level.

The Model 0 is one of the first works of DCB that consider the traffic interaction in the traffic load by using traffic volumes instead of sectors. This enables the possibility to define regulations to specific traffic flows instead of applying restrictions to all aircraft in a sector. The model I is a step forward in the DCB formulations. In fact, this model: a) uses alternative trajectories, b) minimises the deviations with respect to the airspace users' preferences, and c) uses a generic complexity metric defined at trajectory level in order to measure the demand and the capacity.

V.4 Validation case study

The study analyses a 24 hour scenario based on the European Civil Aviation Conference (ECAC) area. The day of study is the 28th July of 2016 representing one of the busiest summer days and the traffic sample contains 32,960 flights crossing the ECAC zone. During this day, there were 179 regulations but, only the regulations starting and ending in the same day are considered. It means that the scenario takes into consideration 175 regulations affecting a total of 144 traffic volumes, meaning that some traffic volumes were affected with more than one regulation. Figure V-2 shows the regulated traffic volumes on 28th July of 2016.

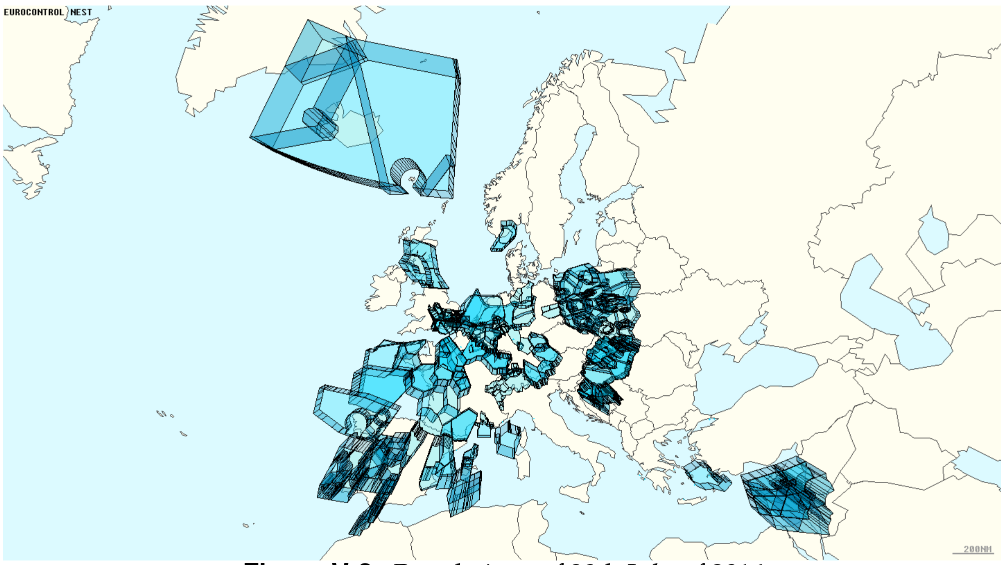

Figure V-2: *Regulations of 28th July of 2016*

V.4.1 Data sources

The initial traffic, the regulation list and the traffic volume definition are obtained from the Demand Data Repository 2 (DDR2) database. The identification of regulated flights in a TV is done using NEST v1.6.6, which allows to get the entry list for every traffic volume (containing the flight identification code together with the entry time to the traffic volumes).

The trajectory optimisation is done by DYNAMO, that needs the mass at the arrival airport and the Cost Index (CI) [1] of the aircraft as inputs for the trajectory optimisation. Not having access to passenger data and load factor, for this study, the final mass is assumed to be the 90% of the Maximum Payload (MPL). With respect to the CI, it is set with the information found in the TOGA report (TOGA projects, 2018) which aims at simulating flights as closely as possible to the real-world operating environment. To the best of the author's knowledge, it is the only source of CI information that is currently available. Still, the information for specific carriers might be missing in the TOGA report leading to some assumptions for those airlines. Hence, the CI allocation method adopted in this PhD (and similar to the method adopted by CADENZA Consortium (2021), can be summarised as follows:

1. Take the value of CI from the TOGA database when the information of the airline is available.
2. For the majority of the remaining airlines, clustering techniques are applied in order to use the most similar airline from those available in the TOGA database.
3. For the remaining unclassified airlines, the CI used is a random number between 10 and 25 Kg/min.

The alternative trajectories are generated using the same mass and cost index assigned for the nominal trajectories but avoiding certain traffic volumes (provided by the network manager).

In line with the ATFCM costs in Europe proposed in Cook & Tanner (2015), the cost assumed for the ground delay is 81€/min. The cost of fuel is assumed to be 0.4 €/kg (2016 average into-plane fuel cost adapted from published fuel spot prices Airline Business (2016)). For this experiment, cost of the delay and the cost of fuel is also assumed the same for all flights.

V.4.2 Alternative trajectories generation

A total of 7,168 flights crossed at least one traffic volume during the time they were under a regulation. Nevertheless, only the flights departing from airports inside the network manager area are subject to regulations, so the DCB problem is applied to only 6,386 flights. The rest of the flights (exempted of regulations) follow their initial flight plan with no regulation applied.

Note that if the regulated traffic volume is linked with the origin and/or destination airport, these can not be avoided with alternative trajectories. Thus, from the 6,386 regulated flights, only 4,931 could submit alternative trajectories to avoid the regulated airspace. In this experiment, two alternative trajectories are requested per flight, avoiding the regulated traffic volumes (non related with any airport) vertically and horizontally. Some of these alternative trajectories, however, are not feasible. There could be different reasons, such as the regulated traffic volume is very close to the origin or destination airport and can not be avoided; or the current route structure do not allow to connect the origin and destination with the avoidance restrictions.

The lateral trajectories have been simulated by minimising as much as possible the lateral deviation with respect to the initial trajectories. The vertical alternatives maintain the same lateral route but change the vertical profile in order to avoid the constrained TVs. In both cases (lateral

[1] The cost index is a number representing the ratio of the time-related cost of an aircraft operation and the cost of fuel (Airbus, 1998).

Table V-1: *Summary of the experiment data of Model 0*

Traffic data	
Flights crossing ECAC	32,960
Flights crossing a regulated TV	7,168
Regulated flights	6,386
Lateral trajectories	3,140
Vertical trajectories	2,084
Constrained airspace	
Number of regulations	175
Regulated TVs	144

and vertical), the trajectories are 4D optimised resulting in different flight levels with respect to the nominal trajectory although they are constrained to not flying higher than the initial trajectory. Figure V-3 shows an example of lateral and vertical alternative trajectories for one flight.

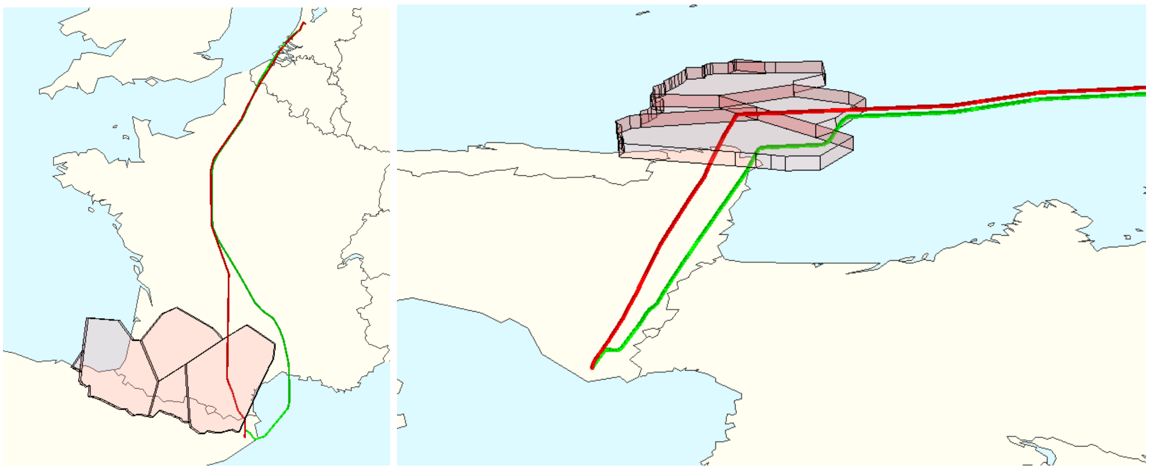

(a) Lateral alternative (green) vs initial trajectory (red)

(b) Vertical alternative (green) vs initial trajectory (red)

Figure V-3: *Example of alternative trajectories for a BCN-AMS flight*

The final number of alternative trajectories is 3,140 (49.17% of the regulated flights) and 2,084 (32.63% of the regulated flights), avoiding the regulated traffic volumes laterally and vertically, respectively. This data is summarized in Table V-1.

The comparison between the lateral alternative trajectories and the nominal trajectories in terms of flight distance, time or fuel, as well as costs, is shown in Figure V-4. All lateral re-routed trajectories are longer in trip time. With respect to the fuel consumption, the majority of the lateral re-routed trajectories need more fuel but in some occasions they are more fuel efficient. In terms of distance flown, the majority of the lateral re-routed trajectories also fly more distance but in very few occasions they fly shorter distances. The conversion of these magnitudes to costs, however, leads always to more expensive trajectories in comparison with the nominal ones.

The same analysis for vertical re-routed trajectories is provided in Figure V-5. Again the vertical re-routed trajectories are longer in time and the majority of the trajectories need more fuel. However, note that the difference in distance is null since the only differences between the vertical re-routed and the nominal trajectories is in the vertical profile. In the same way as the lateral options, all vertical re-routed trajectories are more expensive than the nominal ones.

The shorter and/or more fuel efficient alternative trajectories could be explained because of the optimisation of the vertical profile of the alternative trajectories or the lack of RAD constraints.

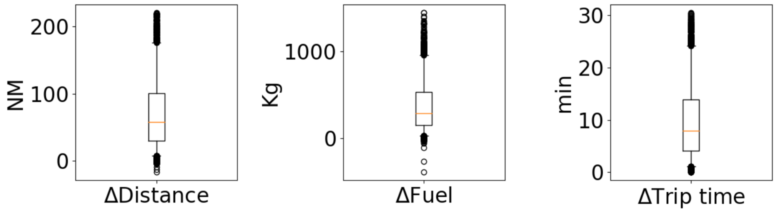

(a) Lateral vs. nominal magnitudes

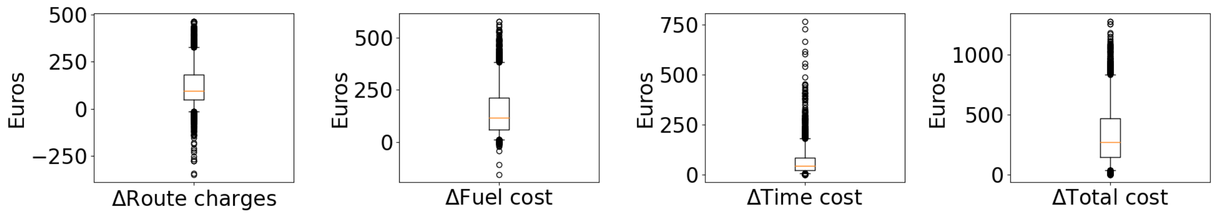

(b) Lateral vs. nominal costs

Figure V-4: *Comparison between lateral and nominal trajectories*

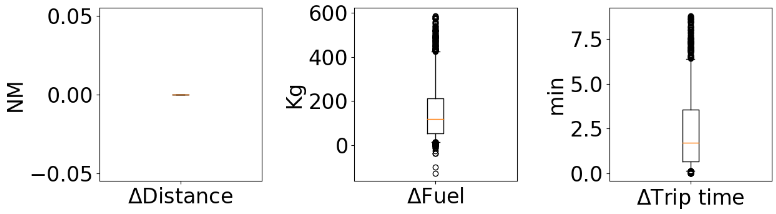

(a) Vertical vs. nominal magnitudes

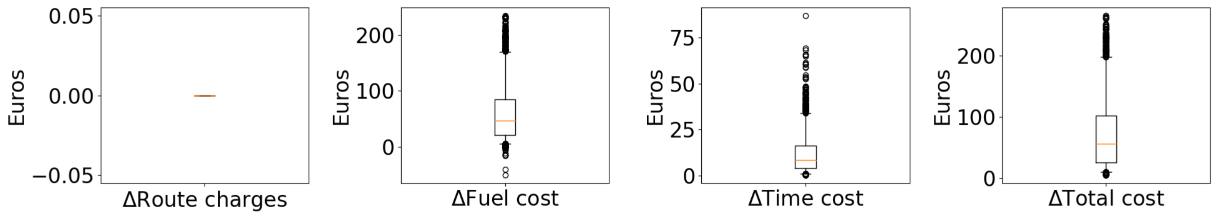

(b) Vertical vs. nominal costs

Figure V-5: *Comparison between vertical and nominal trajectories*

V.4.3 Baseline scenario

A baseline scenario is considered in order to compare the results. In this study, the baseline scenario is obtained from historical data from the DDR2 database, where the DCB problem is solved using the CASA delay algorithm (based on RBS). A total of 3,518 flights were delayed, accumulating a delay of 58,622 minutes. Considering only the delayed flights, the average delay is 16.66 minutes, with maximum delay of 139 minutes. The median of 14 minutes indicates that the half of the delayed flights have 14 minutes of delay or less. The standard deviation of the delay is 11.50 minutes (see Table V-2).

Table V-2: *Summary of the results*

		CASA	Model 0	Δ
Cost	Total regulation cost [€]	4,748,382	1,129,978	-76.20%
	Arrival delay cost [€]	4,748,382	1,099,768	-76.84%
	ΔFuel cost [€]	0	18,736	-
	ΔRoute Charges [€]	0	6,762	-
	ΔTrip time cost [€]	0	4,712	-
Delay	Total ground delay [min]	58,622	12,785	-78.19%
	Delayed flights (ground)	3,518	751	-78.65%
	Total arrival delay [min]	58,622	13,577	-76.84%
	Delayed flights (arrival)	3,518	1,129	-67.91%
	Max. arrival delay [min]	139	355	155.40%
	Average arrival delay [min]	16.66	12	-27.85%
	Median arrival delay [min]	14	5	-64.29%
	Std. Dev. arrival delay [min]	11.5	21.69	88.61%
Trip data	ΔFuel [Tn]	0	47	-
	ΔTrip time [min]	0	792	-
	ΔDistance [NM]	0	3,359	-
Traj. options	Nominal	6,389	5,980	-
	Lateral	0	133	-
	Vertical	0	273	-

V.4.4 DCB with Model 0

The main results of solving Model 0 for this case study are summarised in the following lines.

V.4.4.1 Time setup

The time resolution is set to five minutes in $\mathcal{T}_k^v$. This set indicates the instants of times when the trajectory k can potentially arrive at the traffic volume b.

The load of TVs, measured in entry counts, is counted in periods of 20 minutes. As the experiment is applied to 24 hours, the experiment is divided in 72 periods.

V.4.4.2 Traffic volume capacities

The traffic volume capacity threshold is set based on the information of DDR2 data. Some regulations are applied to traffic volumes that are not active. It means, that the regulated traffic volume is related to a sector that is not used. This situation can happen, for example, to avoid an airspace zone due to bad weather conditions or to force an Air Traffic Control (ATC) routing deviation. For the non-active traffic volumes there are not declared capacities available. In this work, a minimum of 20 operations per hour is assumed in these situations.

V.4.4.3 Results

The solution of the presented case study with Model 0 shows 12,785 minutes of ground delay applied to 751 flights. Looking at the arrival delay, a total of 1129 flights arrive later than planed accumulating 13,577 minutes of delay. The differences between ground and arrival delay are due to the use of alternative trajectories, which may have longer trip times. The average arrival delay per delayed flights is 12 minutes what is a 27.85% lower than using CASA. The median is 5 minutes, what means that the half of the delayed flights are delayed 5 minutes or less (64.29% less than using CASA). These values of arrival delay are illustated in Figure V-7.

These improvements contrast with the value of the maximum value of arrival delay, i.e. 355 minutes, which is much higher than the value of 139 minutes obtained with CASA (155.40% more). Such big value of maximum delay matches with the big standard deviation (21.69 minutes) obtained with Model 0. Thus, the model allows to reduce the total delay, but a few number of flights can accumulate a big amount of delay. It means that, with this model, the system-wide delay can be reduced but the fairness is decreased. This can be seen in Figure V-6 where some flights (the upper outliers) of Model 0 solution have significantly more delay than in the CASA scenario. The same data is showed in Figure V-7 by filtering the outliers.

One can note that Model 0 performs better in terms of arrival delay in the majority of the cases, what means that this fairness issue is only experienced by a minority of the flights. This could be partially mitigated by including in the objective function a fairness factor (i.e., a super-linear coefficient for the cost of delay imposed to the flight) as done in Xu *et al.* (2018a), but it is not considered in this study.

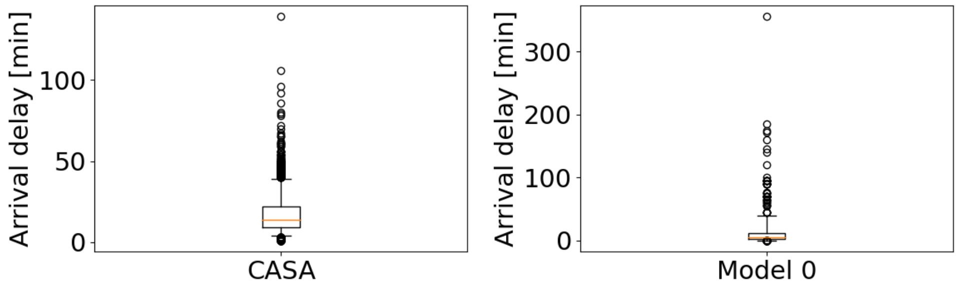

Figure V-6: *Arrival delay boxplot with outliers*

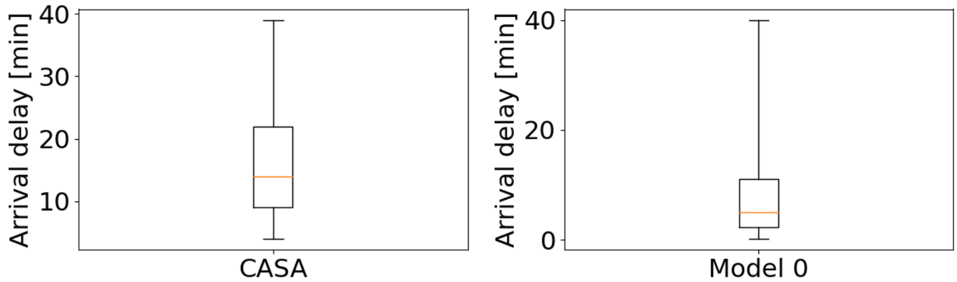

Figure V-7: *Arrival delay boxplot without outliers*

The flights with arrival delay in Model 0 represents only the 32.09% of the delayed flights obtained with the CASA algorithm. Besides, the Model 0 uses alternative trajectories. From the 6,386 regulated flights, 5,982 flights used the nominal trajectory, 133 flights preferred to use the lateral re-route trajectory and 273 used vertical re-routed trajectories. Note than the solution contains very few alternative trajectories (only 6.36% of the 6,386 regulated flights). This is because the alternative trajectories entail extra direct operating costs, but also additional arrival delay due to the longer trip times (see Figures V-4 and V-5). Table V-2 shows the summary of the results in comparison with the baseline scenario.

It is important to recall that the Model 0 is solved minimising the cost of the arrival delay and the difference in terms of direct operating costs between the alternative trajectories and the original trajectory (see Equation V.13). In fact, although Model 0 decreases the regulation cost due to arrival delay, it adds additional costs due to the extra fuel burned, the extra trip time and the extra route charges. The Model 0 solution needs 47 additional tons of fuel at system level, what is translated to an extra cost of 18,736€. Moreover, the route charges increase by 6,762€. This is because the alternative trajectories overfly regions with more expensive unit rates and because they fly longer (in particular 3,359 NM more). Finally, the use of alternative trajectories represents an extra trip time of 792 minutes, what represents an extra cost of 4,712€. Although Model 0 introduces extra operating costs, the total regulation cost is reduced by a 76.20% due to the huge reduction in the arrival delays.

V.4.4.4 Impact on the network

The Model 0, as well as the current model based on the CASA algorithm, only considers the regulated traffic volumes. It means that the solution obtained may create a negative impact on the surrounding traffic volumes (or even in the regulated traffic volumes but in periods when the regulation is not activated). In order to analyse this phenomenon, the overloads are calculated in all active TV crossed by any of the initial or alternative trajectories numbering a total of 1,240. In addition, the overloads are only considered during the periods where the corresponding sector is open according to the sector opening scheme.

Figure V-8 shows the aggregated value of overloads (over all traffic volumes and over all periods of time) for the initial traffic demand, the regulated demand with CASA and the regulated demand based Model 0. As expected, the initial traffic demand is the one which creates a greater value of overloads since no regulation is applied. With CASA, the aggregated overloads is reduced slightly but the model 0 reduces the aggregated overloads even more. It is surprising to find such big overload values in the CASA and Model 0 solution since it is the resulting traffic demand after the regulations. Although it was expected to experience overloads (because capacity is only considered in the regulated TVs) the values are unexpectedly very comparable to the initial traffic demand (see also Figure V-9):

- Total number of aggregated overloads of the initial scenario: 11,212
- Total number of aggregated overloads after CASA: 10,543
- Total number of aggregated overloads after Model 0: 10,300

The remaining overloads that have not result in new regulations, as well as the regulations defined when the traffic load is lower that the capacity, are a good indicator that the simple number of flights, like the entry counts, is not a good proxy for the ATC workload.

This study of the overloads is extended analysing the distribution of overloads per TV. In Figure V-9 the outliers representing the 10% of the TVs are removed in order to compare the most representative TV. The overload distributions are similar among the three scenarios meaning that the network impact of both solutions is limited.

V.4.5 Potential comparison with Model I

The results obtained in the previous section reinforces the idea that the DCB based on complexity metrics may improve the DCB performance. Such hypothesis could be tested with the comparison between Model 0 and Model I since both models only have demand management (fixed sectorisation). However, their direct comparison is not possible due to the following reasons. In the scenario of Model 0 the historical regulation list has been used as a first attempt to disregard the entry counts overloads that do not represent a big deal in terms of complexity. Nevertheless, the reasons of those regulations are diverse. The regulations due to ATC capacity are clearly candidates to be analysed in terms of complexity metrics. Other reasons like ATC equipment, weather

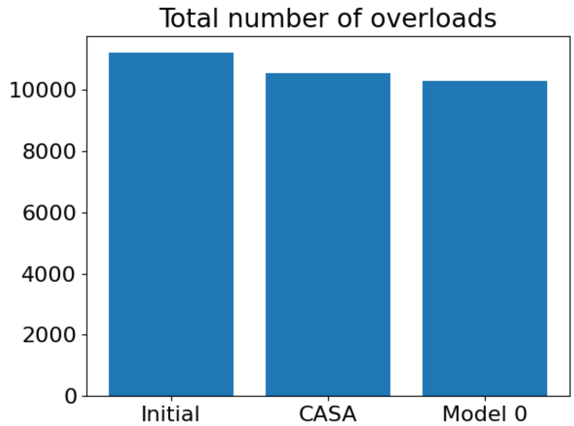

Figure V-8: *Aggregated overloads for all TV and periods for the three scenarios of demand management*

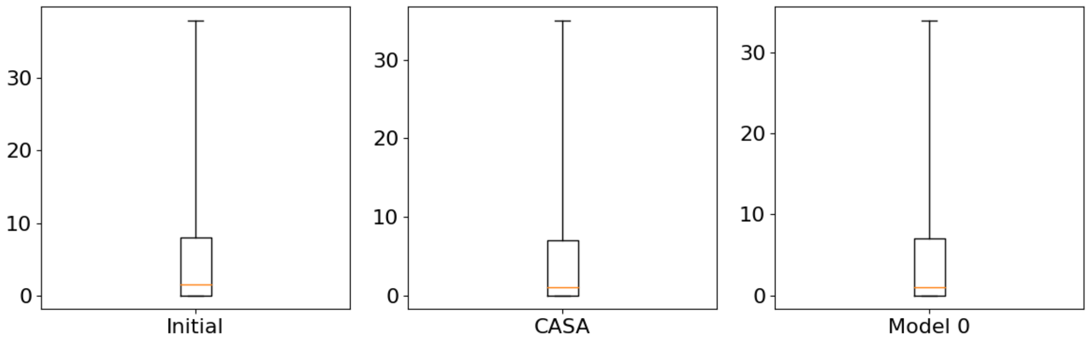

Figure V-9: *Distribution of overloads per TV (excluding outliers)*

or environmental issues, among others, are not related with the harmonisation of the traffic demand and, therefore, are not linked with the complexity.

As a consequence, with Model I not all regulations can be analysed using complexity metrics and a different number regulations should be considered (i.e. only those related with ATC capacity), making impossible the direct comparison between Model 0 and Model I. Nevertheless, the formulation of the Model I is verified with a simple example in Appendix B.

VI

Holistic Demand and Capacity management

This chapter introduces three models that consider the capacity management together with the demand management in the same optimisation problem, i.e., the holistic Demand and Capacity Balancing (DCB) problem. The differences between the models is the level of capacity management that is provided. The details and particularities of the models are explained in the following sections.

VI.1 Model II: selection of the sector configurations

The problem consists of selecting one trajectory for every flight and on choosing the sectorisation opening scheme. Nowadays, the sector opening scheme is defined at Area Control Center (ACC) level. Then, the problem aims at choosing one configuration per period ($p \in \mathcal{P}$) and per ACC ($\gamma \in \Gamma$). Note that the duration of all period does not need to be the same. The set $\mathcal{T}^p$ contains the instants of time in the period p and can be used to define periods with different time duration. Hence, the presented formulation is valid for both synchronised and non-synchronised period steps.

All decision variables, the objective function and all constraints are fully described in the following subsections.

VI.1.1 Decision variables

This model aims at choosing one trajectory for each flight, at the same time it selects the best configuration opening scheme. Thus, there are two decision variables for this problem:

$$z_k = \begin{cases} 1, & \text{if trajectory } k \text{ is chosen} \\ 0, & \text{otherwise} \end{cases} \quad , \quad \forall k \in \mathcal{K}, \tag{VI.1}$$

$$x^{p,\lambda} = \begin{cases} 1, & \text{if configuration } \lambda \text{ is chosen during the period } p \\ 0, & \text{otherwise} \end{cases} \quad , \quad \forall p \in \mathcal{P}, \forall \lambda \in \Lambda. \tag{VI.2}$$

Let $y^{t,s}$ be an auxiliary variable directly related to the sectors instead of the configurations:

$$y^{p,s} = \begin{cases} 1, & \text{if sector } s \text{ is active during period } p \\ 0, & \text{otherwise} \end{cases} \quad , \quad \forall p \in \mathcal{P}, \forall s \in \mathcal{S}. \tag{VI.3}$$

The relationship between $x^{p,\lambda}$ and $y^{p,s}$ is then given as follows with the consideration that only one configuration can be selected during a period p:

$$y^{p,s} = \sum_{\lambda \in \Lambda^s} x^{p,\lambda}, \quad \forall p \in \mathcal{P}, \forall s \in \mathcal{S}. \tag{VI.4}$$

In addition, we define another auxiliary variable (q^{p,s_E}) that indicates if the elementary sector s_E belongs to a different collapsed sector s between the periods p and $p-1$:

$$q^{p,s_\mathrm{E}} = \begin{cases} 1, & \text{if elementary sector } s_\mathrm{E} \text{ belongs to a different} \\ & \text{collapsed sector between } p \text{ and } p-1 \\ 0, & \text{otherwise} \end{cases} \quad , \quad \forall p \in \mathcal{P} \backslash \{1\}, \forall s_\mathrm{E} \in \mathcal{S}_\mathrm{E}. \tag{VI.5}$$

q^{p,s_E} is linked with other variables through:

$$q^{p,s_\mathrm{E}} \geq y^{p,s} - y^{p-1,s}, \quad \forall p \in \mathcal{P} \setminus \{1\}, \forall s \in \mathcal{S}, \forall s_\mathrm{E} \in \mathcal{E}^s. \tag{VI.6}$$

Finally, and for linearisation purposes, the real valued auxiliary variable $C_{\mathrm{T}_k}^{*t,s}$ is introduced as in the Model I, representing the chosen value of complexity contribution of trajectory k to the sector s at instant of time t:

$$C_{\mathrm{T}_k}^{*t,s} \geq 0, \quad \forall k \in \mathcal{K}, \forall t \in \mathcal{T}, \forall s \in \mathcal{S}. \tag{VI.7}$$

VI.1.2 Objective function

The objective function (J) of this model is given by Equation (IV.2), with the capacity provision cost during all periods, J_O, defined as follows:

$$J_O = \sum_{s \in \mathcal{S}} \sum_{p \in \mathcal{P}} \theta^{p,s} y^{p,s}, \tag{VI.8}$$

where $\theta^{p,s}$ is the cost of opening the sector s during the period p.

J_S in Equation (IV.2) is the penalty cost of having differences in consecutive sector configurations and, for this model, it is calculated as:

$$J_S = \rho \sum_{p \in \mathcal{P} \setminus \{1\}} \sum_{s_\mathrm{E} \in \mathcal{S}_\mathrm{E}} q^{p,s_\mathrm{E}}, \tag{VI.9}$$

where ρ is the penalty cost of allocating one elementary sector to a different operating sector in consecutive periods.

VI.1.3 Constraints

In this model, three constraints are identified as follows:

- From all trajectory options of flight f, one and only one must be selected:

$$\sum_{k \in \mathcal{K}_f} z_k = 1, \quad \forall f \in \mathcal{F}. \tag{VI.10}$$

- For all periods, one and only one configuration must be selected in every ACC:

$$\sum_{\lambda \in \Lambda^\gamma} x^{p,\lambda} = 1, \quad \forall p \in \mathcal{P}, \forall \gamma \in \Gamma. \tag{VI.11}$$

- The demand can not exceed the capacity (in terms of complexity) in any active sector s and at any instant of time t. After applying the linearsiation process described in Section IV.3.3.2, the constraint (IV.17) from Model I takes the following form since the active sectors are not known in advance ($\mathcal{S}_a^p$ not available) in Model II:

$$\sum_{k \in \mathcal{K}} C_{\mathrm{T}_k}^{*t,s} \leq H^{t,s} + M_H(1 - y^{p,s}), \quad \forall p \in \mathcal{P}, \forall t \in \mathcal{T}^p, \forall s \in \mathcal{S} \tag{VI.12}$$

  where $C_{\mathrm{T}_k}^{*t,s}$ satisfies the additional constraints (IV.13) and (IV.14), and M_H is a positive value bigger than any possible value of complexity in a sector, $C_\mathrm{S}^{t,s}$.

VI.1.4 MILP formulation for Model II

Wrapping up, and for the sake of completeness, this section summarises the full Mixed Integer Linear Programming (MILP) formulation for this model.

$$\min J = J_{\Delta A} + J_O + J_S = \sum_{k \in \mathcal{K}} (J_k - \bar{J}_k) z_k + \sum_{s \in \mathcal{S}} \sum_{p \in \mathcal{P}} \theta^{p,s} y^{p,s} + \rho \sum_{p \in \mathcal{P} \setminus \{1\}} \sum_{s_\mathrm{E} \in \mathcal{S}_\mathrm{E}} q^{p,s_\mathrm{E}} \tag{VI.13}$$

s.t.

$$\sum_{k \in \mathcal{K}_f} z_k = 1, \quad \forall f \in \mathcal{F} \tag{VI.14}$$

$$\sum_{\lambda \in \Lambda^\gamma} x^{p,\lambda} = 1, \quad \forall p \in \mathcal{P}, \forall \gamma \in \Gamma \tag{VI.15}$$

$$\sum_{k \in \mathcal{K}} C_{\mathrm{T}_k}^{*t,s} \leq H^{t,s} + M_H(1 - y^{p,s}), \quad \forall p \in \mathcal{P}, \forall t \in \mathcal{T}^p, \forall s \in \mathcal{S} \tag{VI.16}$$

$$y^{p,s} \geq \sum_{\lambda \in \Lambda^s} x^{p,\lambda}, \quad \forall p \in \mathcal{P}, \forall s \in \mathcal{S} \tag{VI.17}$$

$$q^{p,s_{\mathrm{E}}} \geq y^{p,s} - y^{p-1,s}, \quad \forall p \in \mathcal{P} \setminus \{1\}, \forall s \in \mathcal{S}, \forall s_{\mathrm{E}} \in \mathcal{E}^s \tag{VI.18}$$

$$C_{\mathrm{T}_k}^{*t,s} \geq \sum_{s_{\mathrm{E}} \in \mathcal{E}^s} B_k^{t,s_{\mathrm{E}}} \sum_{k' \in \mathcal{K} \setminus \{k\}} C_{k,k'}^t z_{k'} + M(z_k - 1), \quad \forall k \in \mathcal{K}, \forall t \in \mathcal{T}, \forall s \in \mathcal{S} \tag{VI.19}$$

$$C_{\mathrm{T}_k}^{*t,s} \geq 0\,, \quad \forall k \in \mathcal{K}, \forall t \in \mathcal{T}, \forall s \in \mathcal{S} \tag{VI.20}$$

$$z_k \in \{0,1\}, \quad \forall k \in \mathcal{K} \tag{VI.21}$$

$$x^{p,\gamma} \in \{0,1\}, \quad \forall p \in \mathcal{P}, \forall \lambda \in \Lambda \tag{VI.22}$$

$$y^{p,s} \in \{0,1\}, \quad \forall p \in \mathcal{P}, \forall s \in \mathcal{S} \tag{VI.23}$$

$$q^{p,s_{\mathrm{E}}} \in \{0,1\}, \quad \forall p \in \mathcal{P} \setminus \{1\}, \forall s_{\mathrm{E}} \in \mathcal{S}_{\mathrm{E}} \tag{VI.24}$$

A verification example of this formulation is presented in Annex B.

VI.1.5 Relation with previous research

Differently than Model I, now the sectorisation is not given and the capacity management is part of the optimisation problem. Thus, this model uses alternative trajectories to manage the demand side and the selection of active configuration at each period of time, i.e. the first level Dynamic Airspace Configurations (DAC) concept, to deal with the capacity side.

This level of capacity management is not new. In fact, it is proposed in Verlhac, C. and Manchon, S. (2005); Vidosavljevic & Delahaye (2017); Gianazza (2010, 2019); Gianazza & Durand (2020); Treimuth (2018) and some of them consider complexity metrics as main capacity indicator as well. These works, however, do not take the demand management into account (i.e. the nominal flight plan is considered when applying capacity management measures).

Similar holistic approaches to this Model II can be found in Xu *et al.* (2018b), Xu *et al.* (2020b), Starita *et al.* (2021) and Künnen & Strauss (2022) where the problem formulation includes the selection of the best configuration opening scheme and the selection of the best trajectory for each flight. In the previous papers, the demand and the capacity are measured using entry counts and the problem minimises the total deviation with regard to airspace users' preferences.

The Model II presented in this paper represents an evolution with respect to the previous research by considering a generic generic complexity metric as measure of the traffic load. In addition, the problem minimises the costs for the airspace users as well as the costs for the Air Navigation Service Providers (ANSPs).

VI.2 Model III: selection of the operating sectors

Similarly to Model II, this model considers the capacity management as part of the optimisation problem. Yet, the sector configuration set is not known here. Thus, the problem consists of selecting one trajectory for every flight and the active sectors at every time instant, from a given set of operating sectors. This Model III gives additional flexibility compared with Model II because it is not restricted to use a given set of sector configurations.

The following subsections are focused on describing the decision variables, the objective function and constraints of this third model.

VI.2.1 Decision variables

This model aims at choosing the trajectory for every flight at the same time it selects the combination of active operating sectors for every instant of time. This leads to the use of following decision variables:

$$z_k = \begin{cases} 1, & \text{if trajectory } k \text{ is chosen} \\ 0, & \text{otherwise} \end{cases}, \quad \forall k \in \mathcal{K}, \tag{VI.25}$$

$$y^{p,s} = \begin{cases} 1, & \text{if sector } s \text{ is active during period } p \\ 0, & \text{otherwise} \end{cases}, \quad \forall p \in \mathcal{P}, \forall s \in \mathcal{S}. \tag{VI.26}$$

Similarly to Model II, the auxiliary variable q^{p,s_E} indicates if the element sector s_E belongs to a different collapsed sector s between the periods p and $p-1$:

$$q^{p,s_\mathrm{E}} = \begin{cases} 1, & \text{if elementary sector } s_\mathrm{E} \text{ belongs to a different} \\ & \text{collapsed sector between } p \text{ and } p-1 \\ 0, & \text{otherwise} \end{cases}, \quad \forall p \in \mathcal{P} \setminus \{1\}, \forall s_\mathrm{E} \in \mathcal{S}_\mathrm{E}. \tag{VI.27}$$

As in the previous model, q^{p,s_E} is linked with other variables through Equation (VI.6).

In order to provide a linear formulation, the real valued auxiliary variable $C_{\mathrm{T}_k}^{*t,s}$ is also introduced here, representing the chosen value of complexity contribution of trajectory k to the sector s at instant of time t:

$$C_{\mathrm{T}_k}^{*t,s} \geq 0\,, \quad \forall k \in \mathcal{K}, \forall t \in \mathcal{T}, \forall s \in \mathcal{S}. \tag{VI.28}$$

VI.2.2 Objective function

This model uses the same objective function (J) as in the previous model (see Section VI.1.2).

VI.2.3 Constraints

Three main constraints are identified and considered in this model:

- From all trajectory options of flight f, one and only one must be selected:

$$\sum_{k \in \mathcal{K}_f} z_k = 1, \quad \forall f \in \mathcal{F}. \tag{VI.29}$$

- The demand can not exceed the capacity (in terms of complexity) in any active sector s and in any instant of time t. This constraint leads to the same formulation obtained in Model II and expressed in Equation (VI.12), where $C_{\mathrm{T}_k}^{*t,s}$ is constrained by equations (IV.13) and (IV.14).

- For all periods, every elementary sector must be selected once and only once. This constraint also ensures that all elementary sectors are chosen at every time instant, meaning that the whole airspace is controlled:

$$\sum_{s \in \mathcal{S}^{s_\mathrm{E}}} y^{p,s} = 1, \quad \forall s_\mathrm{E} \in \mathcal{S}_\mathrm{E}, \forall p \in \mathcal{P}. \tag{VI.30}$$

VI.2.4 MILP formulation for Model III

Wrapping up, and for the sake of completeness, this section summarises the full MILP formulation for this model.

$$\min J = J_{\Delta A} + J_O + J_S = \sum_{k \in \mathcal{K}} (J_k - \bar{J}_k) z_k + \sum_{s \in \mathcal{S}} \sum_{p \in \mathcal{P}} \theta^{p,s} y^{p,s} + \rho \sum_{p \in \mathcal{P} \setminus \{1\}} \sum_{s_{\mathrm{E}} \in \mathcal{S}_{\mathrm{E}}} q^{p,s_{\mathrm{E}}} \tag{VI.31}$$

s.t.

$$\sum_{k \in \mathcal{K}_f} z_k = 1, \quad \forall f \in \mathcal{F} \tag{VI.32}$$

$$\sum_{s \in \mathcal{S}^{s_{\mathrm{E}}}} y^{p,s} = 1, \quad \forall s_{\mathrm{E}} \in \mathcal{S}_{\mathrm{E}}, \forall p \in \mathcal{P} \tag{VI.33}$$

$$\sum_{k \in \mathcal{K}} C_{\mathrm{T}_k}^{*t,s} \leq H^{t,s} + M_H (1 - y^{p,s}), \quad \forall p \in \mathcal{P}, \forall t \in \mathcal{T}^p, \forall s \in \mathcal{S} \tag{VI.34}$$

$$q^{p,s_{\mathrm{E}}} \geq y^{p,s} - y^{p-1,s}, \quad \forall p \in \mathcal{P} \setminus \{1\}, \forall s \in \mathcal{S}, \forall s_{\mathrm{E}} \in \mathcal{E}^s \tag{VI.35}$$

$$C_{\mathrm{T}_k}^{*t,s} \geq \sum_{s_{\mathrm{E}} \in \mathcal{E}^s} B_k^{t,s_{\mathrm{E}}} \sum_{k' \in \mathcal{K} \setminus \{k\}} C_{k,k'}^t z_{k'} + M(z_k - 1), \quad \forall k \in \mathcal{K}, \forall t \in \mathcal{T}, \forall s \in \mathcal{S} \tag{VI.36}$$

$$C_{\mathrm{T}_k}^{*t,s} \geq 0\,, \quad \forall k \in \mathcal{K}, \forall t \in \mathcal{T}, \forall s \in \mathcal{S} \tag{VI.37}$$

$$z_k \in \{0,1\}, \quad \forall k \in \mathcal{K} \tag{VI.38}$$

$$y^{p,s} \in \{0,1\}, \quad \forall p \in \mathcal{P}, \forall s \in \mathcal{S} \tag{VI.39}$$

$$q^{p,s_{\mathrm{E}}} \in \{0,1\}, \quad \forall p \in \mathcal{P} \setminus \{1\}, \forall s_{\mathrm{E}} \in \mathcal{S}_{\mathrm{E}} \tag{VI.40}$$

A verification example of this formulation is presented in Annex B.

VI.2.5 Relation with previous research

This model, like Model II, considers the capacity management as part of the optimisation problem. It adds an additional level of flexibility to the DAC concept since the capacity management consists in the selection of the active sector at every period of time from a given set of sectors (instead of choosing configuration from a limited set). Furthermore, the use of alternative trajectories is still the way to deal with the demand side.

This level of capacity management together with the use of complexity metrics can be found in the literature when no demand management is considered. Some referent works are Delahaye *et al.* (1995) and Treimuth (2018).

The same level of holistic demand and capacity management was introduced in Xu *et al.* (2020b) where new configurations were created from a given set of operating sectors at the same time that one trajectory was chosen for each flight. The problem formulation was defined using entry counts and the objective function minimised the airspace users' costs.

This model III represents a step beyond the state of the art by the introduction of the generic complexity metric at trajectory level and the consideration of the ANSPs cost. Furthermore, this formulation enforces the operational feasibility from the Air Traffic Control (ATC) point of view of the solution by penalising differences in consecutive sector configurations.

VI.3 Model IV: dynamic creation of operating sectors

Similarly to Models II and III, this model also considers the capacity management as part of the optimisation problem. The main difference with respect to previous models is that only the elementary sectors definition is available as input. It means that there are not predefined collapsed sectors nor configurations, so elementary sectors can be dynamically collapsed to create active sectors at every period of time. Thus, the problem consists of selecting one trajectory for every flight and dynamically collapsing the available elementary sectors for each period of time.

The author acknowledges that with this model formulation, one does not have the direct control of the resulting shape of the sectors (convexity, vertical alienation). Yet, this model may be used for exploring the theoretical limits of the capacity management. Further, what it is nowadays operationally not recommended from the sector shape point of view may change in a future concept of operations.

The decision variables, objective function and constraints of this model are fully explained in the following subsections. However, due to the particularities of this model, how the airspace structure is modelled is firstly explained.

VI.3.1 Airspace sectorisation

The airspace is modelled as an undirected graph G($\mathcal{S}_{\mathrm{E}}$,E) with the set of vertices $\mathcal{S}_{\mathrm{E}}$ and the set of edges E, where the vertices are the elementary sectors and the edges connect the elementary sectors that are direct geographical neighbours. Each edge $e \in E$ is defined by two elementary sectors s_{E} and s'_{E}, i.e. $e = (s_{\mathrm{E}}, s'_{\mathrm{E}})$.

With this graph representation, it is possible to introduce an adjacency matrix $A^{s_{\mathrm{E}},s'_{\mathrm{E}}}$ indicating, in a binary way, if the elementary sectors s_{E} and s'_{E} are direct neighbours or not:

$$A^{s_{\mathrm{E}},s'_{\mathrm{E}}} = \begin{cases} 1, & \text{if elementary sectors } s'_{\mathrm{E}} \text{ and } s_{\mathrm{E}} \text{ are} \\ & \text{direct geographical neighbours} \\ 0, & \text{otherwise} \end{cases}, \quad \forall s_{\mathrm{E}}, s'_{\mathrm{E}} \in \mathcal{S}_{\mathrm{E}} | s_{\mathrm{E}} < s'_{\mathrm{E}}. \tag{VI.41}$$

It's worth noting that the adjacency matrix $A^{s_{\mathrm{E}},s'_{\mathrm{E}}}$ is controlling which elementary sectors could be collapesed together. Hence, the independence of different ANSPs could be easily preserved.

Each operating sector is modelled as a imaginary path (called "sector path" in this paper) that joins in sequence all the elementary sectors that belong to it, as illustrated in Figure VI-1. Although one may imagine that knowing which elementary sectors belong to each collapsed sectors would be enough and precedence is not needed, it would be explained that this formulation is needed in order to ensure the connectivity of all the elementary sectors in a collapsed sector.

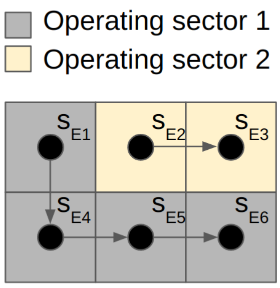

Figure VI-1: *Illustrative example of a sectorisation, with two hypothetical operating sectors and their corresponding* sector paths*.*

VI.3.2 Decision variables

This model aims at choosing the optimal trajectory and the best combination of elementary sectors. This leads to the definition of the following decision variables:

$$z_k = \begin{cases} 1, & \text{if trajectory } k \text{ is chosen} \\ 0, & \text{otherwise} \end{cases} \quad , \forall k \in \mathcal{K}, \tag{VI.42}$$

$$w^{p,s_{\mathrm{E}},s'_{\mathrm{E}}} = \begin{cases} 1, & \text{if elementary sector } s'_{\mathrm{E}} \text{ is after } s_{\mathrm{E}} \text{ in the} \\ & \text{sector path which defines an operating} \\ & \text{sector during the period } p \\ 0, & \text{otherwise} \end{cases} \quad , \quad \forall p \in \mathcal{P}, \forall s_{\mathrm{E}}, s'_{\mathrm{E}} \in \mathcal{S}_{\mathrm{E}} | s_{\mathrm{E}} < s'_{\mathrm{E}}. \tag{VI.43}$$

In addition, $d^{p,s_{\mathrm{E}}}$ is introduced in order to identify the first elementary sector of a sector path (which is required to count the number of active sectors):

$$d^{p,s_{\mathrm{E}}} = \begin{cases} 1, & \text{if the elementary sector } s_{\mathrm{E}} \text{ is the first} \\ & \text{elementary sector of a sector path during period } p \\ 0, & \text{otherwise} \end{cases} \quad , \quad \forall p \in \mathcal{P}, \forall s_{\mathrm{E}} \in \mathcal{S}_{\mathrm{E}}. \tag{VI.44}$$

Furthermore, the auxiliary variable $l^{t,s_{\mathrm{E}},s'_{\mathrm{E}}}$ is defined in this model and it indicates if the element sectors s_{E} and s'_{E} are collapsed differently in periods p and $p-1$:

$$l^{p,s_{\mathrm{E}},s'_{\mathrm{E}}} = \begin{cases} 1, & \text{if elementary sector } s_{\mathrm{E}} \text{ and } s'_{\mathrm{E}} \text{ where} \\ & \text{collapsed in } p-1 \text{ but not in } p\text{; or if} \\ & \text{elementary sector } s_{\mathrm{E}} \text{ and } s'_{\mathrm{E}} \text{ are collapsed} \\ & \text{in } p \text{ but they were not collapsed in } p-1 \\ 0, & \text{otherwise} \end{cases} \quad , \quad \forall p \in \mathcal{P} \setminus \{1\}, \forall s_{\mathrm{E}}, s'_{\mathrm{E}} \in \mathcal{S}_{\mathrm{E}} | s_{\mathrm{E}} < s'_{\mathrm{E}}. \tag{VI.45}$$

Links between $l^{t,s_{\mathrm{E}},s'_{\mathrm{E}}}$ and other variables are given by:

$$l^{p,s_{\mathrm{E}},s'_{\mathrm{E}}} \geq w^{p,s_{\mathrm{E}},s'_{\mathrm{E}}} + w^{p,s'_{\mathrm{E}},s_{\mathrm{E}}}, \quad \forall p \in \mathcal{P} \setminus \{1\}, \forall s_{\mathrm{E}}, s'_{\mathrm{E}} \in \mathcal{S}_{\mathrm{E}} | s_{\mathrm{E}} < s'_{\mathrm{E}}, \tag{VI.46}$$

$$l^{p,s_{\mathrm{E}},s'_{\mathrm{E}}} \geq w^{p-1,s_{\mathrm{E}},s'_{\mathrm{E}}} + w^{p-1,s'_{\mathrm{E}},s_{\mathrm{E}}}, \quad \forall p \in \mathcal{P} \setminus \{1\}, \forall s_{\mathrm{E}}, s'_{\mathrm{E}} \in \mathcal{S}_{\mathrm{E}} | s_{\mathrm{E}} < s'_{\mathrm{E}}. \tag{VI.47}$$

In order to provide a linear formulation, the real valued auxiliary variable $C_{\mathrm{P}_{k,k'}}^{t,s_{\mathrm{E}}}$ is introduced as the chosen pairwise complexity that the trajectory k' induces on the trajectory k at time instant t when the trajectory k is in the elementary sector s_{E} or in one of its successors:

$$C_{\mathrm{P}_{k,k'}}^{t,s_{\mathrm{E}}} \geq 0, \quad \forall k \in \mathcal{K}, \forall k' \in \mathcal{K} \setminus \{k\}, \forall t \in \mathcal{T}, \forall s_{\mathrm{E}} \in \mathcal{S}_{\mathrm{E}}. \tag{VI.48}$$

The auxiliary variable $C_{\mathrm{A}_k}^{*t,s_{\mathrm{E}}}$ is introduced for linearisation purposes, which represents a chosen value of complexity for the trajectory k at time instant t considering the elementary sector s_{E} and its successors:

$$C_{\mathrm{A}_k}^{*t,s_{\mathrm{E}}} \geq 0, \quad \forall k \in \mathcal{K}, \forall t \in \mathcal{T}, \forall s_{\mathrm{E}} \in \mathcal{S}_{\mathrm{E}}. \tag{VI.49}$$

The detailed linearisation process is explained in Section VI.3.6.

VI.3.3 Illustrative example of airspace organisation

In order to complement the previous definitions, the modelisation of the airspace organisation for the example of Figure VI-1 is explained.

The decision variable $w^{p,s_{\mathrm{E}},s'_{\mathrm{E}}}$ indicates if the elementary sector s'_{E} is after the elementary sector s_{E} in the sector path that defines an operating sector during period p. In other words, $w^{p,s_{\mathrm{E}},s'_{\mathrm{E}}} = 1$ if s_{E} and s'_{E} are part of the same sector path being s'_{E} successor of s_{E} and, consequently, being s_{E} predecessor of s'_{E}. In this example, there are six elementary sectors collapsed in two operating sectors (identified in grey and yellow in Figure VI-1) at the period p. The two sector paths are defined with the variable $w^{p,s_{\mathrm{E}},s'_{\mathrm{E}}}$ as follows:

- Operating sector 1: $w^{p,s_{\mathrm{E1}},s_{\mathrm{E4}}} = w^{p,s_{\mathrm{E1}},s_{\mathrm{E5}}} = w^{p,s_{\mathrm{E1}},s_{\mathrm{E6}}} = 1$, $w^{p,s_{\mathrm{E4}},s_{\mathrm{E5}}} = w^{p,s_{\mathrm{E4}},s_{\mathrm{E6}}} = 1$, $w^{p,s_{\mathrm{E5}},s_{\mathrm{E6}}} = 1$.
- Operating sector 2: $w^{p,s_{\mathrm{E2}},s_{\mathrm{E3}}} = 1$.
- Other w variables are all equal to zero.

Furthermore, the decision variable $d^{p,s_{\mathrm{E}}}$ indicates whether the elementary sector s_{E} is the first one of the sector path defining the collapsed sector it belongs at period p. In this particular example, $d^{p,s_{\mathrm{E}}}$ values are:

- Operating sector 1: $d^{p,s_{\mathrm{E1}}} = 1$.
- Operating sector 2: $d^{p,s_{\mathrm{E2}}} = 1$.
- Other d variables are all equal to zero.

Please remark that sectorisation is not a simple partitioning problem due to required connectivity of the elementary sectors collapsed together. This justifies the use of the sector path as a modelisation artefact.

VI.3.4 Objective function

The objective function for this model is equivalent to the previous models and can be seen in Equation (IV.2). Yet, a special insight has to be done with the capacity provision cost (J_O) and the penalty cost of having differences in consecutive sector configurations (J_S).

The cost of using sector s during the period p ($\theta^{p,s}$) that is used to calculate the capacity provision cost (C_O) in Equation (VI.8) is not known a priori since the regrouping of the elementary sectors is now part of the decision process. Thus, the cost of opening a generic sector during period p (ψ^p) is defined. Then, J_O can be expressed as:

$$J_O = \sum_{p \in \mathcal{P}} \psi^p \sum_{s_{\mathrm{E}} \in \mathcal{S}_{\mathrm{E}}} d^{p,s_{\mathrm{E}}}. \tag{VI.50}$$

Note than the sum of all $d^{p,s_{\mathrm{E}}}$ over all elementary sectors gives the number of open sectors at period p.

Regarding the penalty cost of consecutive sector regrouping that are very different (J_S), it is calculated through the auxiliary variable $l^{p,s_{\mathrm{E}},s'_{\mathrm{E}}}$ as follows:

$$J_S = \rho \sum_{p \in \mathcal{P} \setminus \{1\}} \sum_{s_{\mathrm{E}} \in \mathcal{S}_{\mathrm{E}}} \sum_{s'_{\mathrm{E}} \in \mathcal{S}_{\mathrm{E}} | s_{\mathrm{E}} < s'_{\mathrm{E}}} l^{p,s_{\mathrm{E}},s'_{\mathrm{E}}}. \tag{VI.51}$$

VI.3.5 Constraints

The constrains for this model are:

- From all trajectory options of flight f, one and only one must be selected:

$$\sum_{k\in\mathcal{K}_f} z_k = 1, \quad \forall f \in \mathcal{F}. \tag{VI.52}$$

- Each elementary sector (except the first one in a given sector path) must have at least one predecessor which is a direct neighbour:

$$\sum_{s'_{\mathrm{E}}\in\mathcal{S}_{\mathrm{E}}|s_{\mathrm{E}}>s'_{\mathrm{E}}} w^{p,s'_{\mathrm{E}},s_{\mathrm{E}}} A^{s'_{\mathrm{E}},s_{\mathrm{E}}} \geq 1 - d^{p,s_{\mathrm{E}}}, \quad \forall p \in \mathcal{P}, \forall s_{\mathrm{E}} \in \mathcal{S}_{\mathrm{E}}. \tag{VI.53}$$

This constraint also ensures that every elementary sector is included in an operating sector.

- The decision variable $d^{p,s_{\mathrm{E}}}$ must be 1 for the first elementary sector of each sector path (i.e. each collapsed sector) and 0 in all other cases:

$$(1 - d^{p,s_{\mathrm{E}}})|\mathcal{S}_{\mathrm{E}}| \geq \sum_{s'_{\mathrm{E}}\in\mathcal{S}_{\mathrm{E}}|s_{\mathrm{E}}>s'_{\mathrm{E}}} w^{p,s'_{\mathrm{E}},s_{\mathrm{E}}}, \quad \forall p \in \mathcal{P}, \forall s_{\mathrm{E}} \in \mathcal{S}_{\mathrm{E}}, \tag{VI.54}$$

where $|\mathcal{S}_{\mathrm{E}}|$ is the cardinality of set $\mathcal{S}_{\mathrm{E}}$. Note that $\sum_{s'_{\mathrm{E}}\in\mathcal{S}_{\mathrm{E}}|s_{\mathrm{E}}>s'_{\mathrm{E}}} w^{p,s'_{\mathrm{E}},s_{\mathrm{E}}}$ is equal to 0 in the first elementary sector of the sector path because it has no predecessors and it is greater than 0 in all other cases. Thus, Equation (VI.54) ensures that $d^{p,s_{\mathrm{E}}} = 0$ when the elementary sector s_{E} is not the first one in the sector path, but it is not sufficient to ensure $d^{p,s_{\mathrm{E}}} = 1$ when s_{E} is the first elementary sector of the sector path. Nevertheless, equation (VI.53) is ensuring that $d^{p,s_{\mathrm{E}}} = 1$ in this particular situation.

- If s'_{E} is after s_{E} in the sector path, and s''_{E} is after s'_{E}, then s''_{E} is after s_{E}:

$$w^{p,s_{\mathrm{E}},s'_{\mathrm{E}}} + w^{p,s'_{\mathrm{E}},s''_{\mathrm{E}}} - 1 \leq w^{p,s_{\mathrm{E}},s''_{\mathrm{E}}}, \quad \forall p \in \mathcal{T}, \forall s_{\mathrm{E}}, s'_{\mathrm{E}}, s''_{\mathrm{E}} \in \mathcal{S}_{\mathrm{E}}|s_{\mathrm{E}} < s'_{\mathrm{E}}, s'_{\mathrm{E}} < s''_{\mathrm{E}}. \tag{VI.55}$$

- If two elementary sectors s_{E} and s'_{E} have the same successor s''_{E} in the sector path, then s'_{E} is after s_{E} or s_{E} is after s'_{E}:

$$w^{p,s_{\mathrm{E}},s''_{\mathrm{E}}} + w^{p,s'_{\mathrm{E}},s''_{\mathrm{E}}} - 1 \leq w^{p,s_{\mathrm{E}},s'_{\mathrm{E}}}, \quad \forall p \in \mathcal{P}, \forall s_{\mathrm{E}}, s'_{\mathrm{E}}, s''_{\mathrm{E}} \in \mathcal{S}_{\mathrm{E}}|s_{\mathrm{E}} < s'_{\mathrm{E}}, s'_{\mathrm{E}} < s''_{\mathrm{E}}. \tag{VI.56}$$

- The demand can not exceed the capacity (in terms of complexity) in any active operating sector at any instant of time t. Differently from previous models, the set $\mathcal{S}$ is no longer available. For this reason, let us define $C_{\mathrm{A}_k}^{t,s_{\mathrm{E}}}$ as the complexity that all trajectories generate on trajectory k at time t in the collapsed sector formed by s_{E} and all its successors as follows:

$$C_{\mathrm{A}_k}^{t,s_{\mathrm{E}}} = \sum_{k'\in\mathcal{K}\setminus\{k\}} [C^t_{k,k'} B_k^{t,s_{\mathrm{E}}} + \sum_{s'_{\mathrm{E}}\in\mathcal{S}_{\mathrm{E}}|s_{\mathrm{E}}<s'_{\mathrm{E}}} C^t_{k,k'} B_k^{t,s'_{\mathrm{E}}} w^{p,s_{\mathrm{E}},s'_{\mathrm{E}}}] z_{k'} z_k \tag{VI.57}$$
$$\forall k \in \mathcal{K}, \forall p \in \mathcal{P}, \forall t \in \mathcal{T}^p, \forall s_{\mathrm{E}} \in \mathcal{S}_{\mathrm{E}}.$$

Then, the demand could be maintained below the capacity threshold through the following expression:

$$C_{\mathrm{A}_k}^{t,s_{\mathrm{E}}} \leq H^t, \quad \forall t \in \mathcal{T}, \forall s_{\mathrm{E}} \in \mathcal{S}_{\mathrm{E}}, \tag{VI.58}$$

where, H^t is the complexity threshold of an operating sector for an instant of time t. Note that the previous constraint is evaluated over all elementary sectors, but the ones related with the first elementary sector of each sector path ($d^{p,s_\mathrm{E}} = 1$) will be the most limiting ones since the aggregated complexity in these cases will consider all the elementary sectors that form the operating sectors (since they are all successors of the first elementary sector in the sector path), hence, ensuring capacity limit.

VI.3.6 Linearisation

In this model, the constraint (VI.58) is non-linear because $C_{\mathrm{A}_k}^{t,s_\mathrm{E}}$ is non-linear (see Equation (VI.57)). The linearisation of this equation will be done by the introduction of two real valued auxiliary variables: Firstly, $C_{\mathrm{P}_{k,k'}}^{t,s_\mathrm{E}}$ as the chosen pairwise complexity that the trajectory k' induces on the trajectory k at time instant t when the trajectory k is in the elementary sector s_E or in one of its successors. This auxiliary variable can be constrained as follows:

$$C_{\mathrm{P}_{k,k'}}^{t,s_\mathrm{E}} \geq 0, \quad \forall k \in \mathcal{K}, \forall k' \in \mathcal{K} \setminus \{k\}, \forall t \in \mathcal{T}, \forall s_\mathrm{E} \in \mathcal{S}_\mathrm{E}, \tag{VI.59}$$

$$\begin{aligned} C_{\mathrm{P}_{k,k'}}^{t,s_\mathrm{E}} \geq C_{k,k'}^{t} B_k^{t,s_\mathrm{E}} + \sum_{s'_\mathrm{E} \in \mathcal{S}_\mathrm{E} | s_\mathrm{E} < s'_\mathrm{E}} C_{k,k'}^{t} B_k^{t,s'_\mathrm{E}} w^{p,s_\mathrm{E},s'_\mathrm{E}} + M_1(z_{k'} - 1) \\ \forall k \in \mathcal{K}, \forall k' \in \mathcal{K} \setminus \{k\}, \forall p \in \mathcal{P}, \forall t \in \mathcal{T}^p, \forall s_\mathrm{E} \in \mathcal{S}_\mathrm{E}, \end{aligned} \tag{VI.60}$$

where M_1 is a given parameter that represents the highest pairwise complexity that a trajectory can receive in a sector and it is calculated as:

$$M_1 \geq \max \left(C_{k,k'}^{t} B_k^{t,s_\mathrm{E}} + \sum_{s'_\mathrm{E} \in \mathcal{S}_\mathrm{E} | s_\mathrm{E} < s'_\mathrm{E}} C_{k,k'}^{t} B_k^{t,s'_\mathrm{E}} w^{p,s_\mathrm{E},s'_\mathrm{E}} \right). \tag{VI.61}$$

Secondly, the auxiliary variable $C_{\mathrm{A}_k}^{*t,s_\mathrm{E}}$ is introduced, which represents a chosen value of complexity for the trajectory k at time instant t considering the elementary sector s_E and its successors. It is constrained by:

$$C_{\mathrm{A}_k}^{*t,s_\mathrm{E}} \geq 0, \quad \forall k \in \mathcal{K}, \forall t \in \mathcal{T}, \forall s_\mathrm{E} \in \mathcal{S}_\mathrm{E}, \tag{VI.62}$$

$$C_{\mathrm{A}_k}^{*t,s_\mathrm{E}} \geq \sum_{k' \in \mathcal{K} \setminus \{k\}} C_{\mathrm{P}_{k,k'}}^{t,s_\mathrm{E}} + M_2(z_k - 1), \quad \forall k \in \mathcal{K}, \forall t \in \mathcal{T}, \forall s_\mathrm{E} \in \mathcal{S}_\mathrm{E}, \tag{VI.63}$$

where M_2 is a big positive value that is greater that any possible value of $C_{\mathrm{A}_k}^{t,s_\mathrm{E}}$. Thus, Equation (VI.58) can be linearised as:

$$\sum_{k \in \mathcal{K}} C_{\mathrm{A}_k}^{*t,s_\mathrm{E}} \leq H^t, \quad \forall t \in \mathcal{T}, \forall s_\mathrm{E} \in \mathcal{S}_\mathrm{E}. \tag{VI.64}$$

VI.3.7 Flexibility of the sector shape

The definition of the decision variable $w^{p,s_\mathrm{E},s'_\mathrm{E}}$ (where $s_\mathrm{E} < s'_\mathrm{E}$, see Equation VI.43) together with constraint (VI.53) (each elementary sector, except the first one in a given sector path, must have at least one predecessor which is his direct neighbour) limit the feasible set of sector paths and, hence, the resulting sectors. This issue is illustrated in Figure VI-2(a). The blue sector is perfectly feasible since the sector path s_{E1}-s_{E2}-s_{E4} satisfies the ascending order imposed by the definition of $w^{t,s_{\mathrm{E}},s'_{\mathrm{E}}}$ and also verify the constraint (VI.53), since s_{E2} has the predecessor s_{E1}, which is his neighbour; and s_{E4} has s_{E1} as neighbour. Contrary, the orange sector is not feasible, although perfectly operational. The ascending order imposed in the definition of $w^{t,s_{\mathrm{E}},s'_{\mathrm{E}}}$ makes the sector path s_{E3}-s_{E5}-s_{E6} the only possible solution that defines orange sector. However, this sector path does not satisfy constraint (VI.53), since the elementary sector s_{E3} is the only predecessor of s_{E5} and they are not neighbours, hence, it is infeasible.

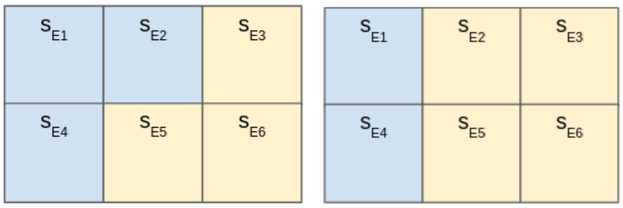

(a) Infeasible configuration (b) Feasible configuration

Figure VI-2: *Illustrative example of feasible and infeasible sectors*

Although this limitation makes impossible to represent some sector shapes[1], one can find similar sectors that could be modeled. For example, the sector path s_{E3}-s_{E5}-s_{E6} is infeasible, but these elementary sectors could be collapsed together by simply including s_{E2} in the sector path, like s_{E2}-s_{E3}-s_{E5}-s_{E6}. Hence, Figure VI-2(b) illustrates a feasible configuration, provided that the other constraints are satisfied notably capacity constrains.

Despite this limitation on the feasible set of sector path does not represent a hard operational limitation (i.e. similar sector path can be found), the total flexibility on the sector shape could be accomplished by removing the ascending order of the sectors in the sector path that is forced by the definition of $w^{p,s_{\mathrm{E}},s'_{\mathrm{E}}}$ variables. This is achieved by increasing s_{E} and s'_{E} index domain in the variable definition. Thus, this variable $w^{p,s_{\mathrm{E}},s'_{\mathrm{E}}}$ could be defined as:

$$w^{p,s_{\mathrm{E}},s'_{\mathrm{E}}} = \begin{cases} 1, & \text{if elementary sector } s'_{\mathrm{E}} \text{ is after } s_{\mathrm{E}} \text{ in the} \\ & \text{sector path which defines an operating} \\ & \end{cases} \quad \forall p \in \mathcal{P}, \forall s_{\mathrm{E}}, s'_{\mathrm{E}} \in \mathcal{S}_{\mathrm{E}} | s_{\mathrm{E}} \neq s'_{\mathrm{E}}. \quad \text{(VI.65)}$$

This new definition demands the update of the index domains of certain constrains. In addition, two new constraints are required to guarantee the connectivity:

- If two elementary sectors s_{E} and s'_{E} have the same predecessor s''_{E} in the sector path, then either s'_{E} is after s_{E} or s_{E} is after s'_{E}:

$$w^{p,s''_{\mathrm{E}},s_{\mathrm{E}}} + w^{p,s''_{\mathrm{E}},s'_{\mathrm{E}}} - 1 \leq w^{p,s_{\mathrm{E}},s'_{\mathrm{E}}} + w^{p,s'_{\mathrm{E}},s_{\mathrm{E}}}, \quad \forall p \in \mathcal{P}, \forall s_{\mathrm{E}}, s'_{\mathrm{E}}, s''_{\mathrm{E}} \in \mathcal{S}_{\mathrm{E}} | s_{\mathrm{E}} \neq s'_{\mathrm{E}} \neq s''_{\mathrm{E}}. \quad \text{(VI.66)}$$

- If one elementary sector s'_{E} is successor of s_{E} in the sector path, then s_{E} cannot be successor of s'_{E}:

$$w^{p,s_{\mathrm{E}},s'_{\mathrm{E}}} + w^{p,s'_{\mathrm{E}},s_{\mathrm{E}}} \leq 1, \quad \forall p \in \mathcal{P}, \forall s_{\mathrm{E}}, s'_{\mathrm{E}} \in \mathcal{S}_{\mathrm{E}} | s_{\mathrm{E}} \neq s'_{\mathrm{E}}. \quad \text{(VI.67)}$$

Note that this alternative formulation increases the number of decision variables and constraints considerably. In addition, it introduces a symmetry problem since the same elementary sector

[1]It is worth noting that the orange sector in Figure VI-2(a) could be represented with sector path s_{E5}-s_{E6}-s_{E3} that perfectly satisfies the constraint (VI.53) but this sector path can not be modeled due to definition of decision variable $w^{t,s_{\mathrm{E}},s'_{\mathrm{E}}}$.

grouping could be represented with multiple sector paths (solutions). For example, the orange sector in Figure VI-2(a) can be represented by following sector paths:

s_{E3}-s_{E5}-s_{E6}, s_{E3}-s_{E6}-s_{E5}, s_{E5}-s_{E3}-s_{E6}, s_{E5}-s_{E6}-s_{E3}, s_{E6}-s_{E3}-s_{E5}, s_{E6}-s_{E5}-s_{E3}

The increased size and symmetry issue make this alternative formulation much more difficult to solve with exact methods.

VI.3.8 MILP formulation for Model IV

Wrapping up, and for the sake of completeness, this section summarises the full MILP formulation for this model.

$$\min J = J_{\Delta A} + J_O + J_S = \sum_{k\in\mathcal{K}} (J_k - \bar{J}_k) z_k + \sum_{p\in\mathcal{P}} \psi^p \sum_{s_E\in\mathcal{S}_E} d^{p,s_E} + \rho \sum_{p\in\mathcal{P}\setminus\{1\}} \sum_{s_E\in\mathcal{S}_E} \sum_{s'_E\in\mathcal{S}_E | s_E < s'_E} l^{p,s_E,s'_E} \tag{VI.68}$$

s.t.

$$\sum_{k\in\mathcal{K}_f} z_k = 1, \quad \forall f \in \mathcal{F} \tag{VI.69}$$

$$\sum_{s'_E\in\mathcal{S}_E | s_E > s'_E} w^{p,s'_E,s_E} A^{s'_E,s_E} \geq 1 - d^{p,s_E}, \quad \forall p \in \mathcal{P}, \forall s_E \in \mathcal{S}_E \tag{VI.70}$$

$$(1 - d^{p,s_E})|\mathcal{S}_E| \geq \sum_{s'_E\in\mathcal{S}_E | s_E > s'_E} w^{p,s'_E,s_E}, \quad \forall p \in \mathcal{P}, \forall s_E \in \mathcal{S}_E \tag{VI.71}$$

$$w^{p,s_E,s'_E} + w^{p,s'_E,s''_E} - 1 \leq w^{p,s_E,s''_E}, \quad \forall p \in \mathcal{P}, \forall s_E, s'_E, s''_E \in \mathcal{S}_E | s_E < s'_E, s'_E < s''_E \tag{VI.72}$$

$$w^{p,s_E,s''_E} + w^{p,s'_E,s''_E} - 1 \leq w^{p,s_E,s'_E}, \quad \forall p \in \mathcal{P}, \forall s_E, s'_E, s''_E \in \mathcal{S}_E | s_E < s'_E, s'_E < s''_E \tag{VI.73}$$

$$l^{p,s_E,s'_E} \geq w^{p,s_E,s'_E} + w^{p,s'_E,s_E}, \quad \forall p \in \mathcal{P} \setminus \{1\}, \forall s_E, s'_E \in \mathcal{S}_E | s_E < s'_E \tag{VI.74}$$

$$l^{p,s_E,s'_E} \geq w^{p-1,s_E,s'_E} + w^{p-1,s'_E,s_E}, \quad \forall p \in \mathcal{P} \setminus \{1\}, \forall s_E, s'_E \in \mathcal{S}_E | s_E < s'_E \tag{VI.75}$$

$$C_{P_{k,k'}}^{t,s_E} \geq 0, \quad \forall k \in \mathcal{K}, \forall k' \in \mathcal{K} \setminus \{k\}, \forall t \in \mathcal{T}, \forall s_E \in \mathcal{S}_E \tag{VI.76}$$

$$C_{P_{k,k'}}^{t,s_E} \geq C^t_{k,k'} B_k^{t,s_E} + \sum_{s'_E\in\mathcal{S}_E | s_E < s'_E} C^t_{k,k'} B_k^{t,s'_E} w^{p,s_E,s'_E} + M_1(z_{k'} - 1)$$
$$\forall k \in \mathcal{K}, \forall k' \in \mathcal{K} \setminus \{k\}, \forall p \in \mathcal{P}, \forall t \in \mathcal{T}^p, \forall s_E \in \mathcal{S}_E$$

$$C_{A_k}^{*t,s_E} \geq 0, \quad \forall k \in \mathcal{K}, \forall t \in \mathcal{T}, \forall s_E \in \mathcal{S}_E \tag{VI.77}$$

$$C_{A_k}^{*t,s_E} \geq \sum_{k'\in\mathcal{K}\setminus\{k\}} C_{P_{k,k'}}^{t,s_E} + M_2(z_k - 1), \quad \forall k \in \mathcal{K}, \forall t \in \mathcal{T}, \forall s_E \in \mathcal{S}_E \tag{VI.78}$$

$$\sum_{k\in\mathcal{K}} C_{A_k}^{*t,s_E} \leq H^t, \quad \forall t \in \mathcal{T}, \forall s_E \in \mathcal{S}_E \tag{VI.79}$$

$$z_k \in \{0,1\}, \quad \forall k \in \mathcal{K} \tag{VI.80}$$

$$w^{p,s_E,s'_E} \in \{0,1\}, \quad \forall p \in \mathcal{P}, \forall s_E, s'_E \in \mathcal{S}_E | s_E < s'_E \tag{VI.81}$$

$$d^{p,s_E} \in \{0,1\}, \quad \forall p \in \mathcal{P}, \forall s_E \in \mathcal{S}_E \tag{VI.82}$$

$$l^{p,s_E,s'_E} \in \{0,1\}, \quad \forall p \in \mathcal{P} \setminus \{1\}, \forall s_E, s'_E \in \mathcal{S}_E | s_E < s'_E \tag{VI.83}$$

A verification example of this formulation is presented in Annex B.

VI.3.9 Relation with previous research

The Model IV introduces an additional level of capacity management where elementary sectors are dynamically collapsed to build operating sectors at every period of time. From the demand side, the problem is still focused on the selection of the "best" trajectory for each flight.

The level of capacity management proposed here, however, was considered in the literature only as an isolated problem (with no demand management). Some examples are found in Sergeeva *et al.* (2017, 2015) or Treimuth (2018).

The definition of an holistic problem similar to the one corresponding to our Model IV was discussed in Xu *et al.* (2020b), but the problem was not modeled. Thus, to the best of the author's knowledge, this is the first time such an holistic problem is formulated, which combines the selection of alternative trajectories provided by the Airspace Users (AUs) and a DAC based on the elementary sectors combination, while including a generic complexity metric at trajectory level and a penalisation of big differences between consecutive configurations.

VI.4 Discussion on holistic DCB models

Nowadays, the ATC controllers are trained for deploying the ATC services on sectors which are well known for them. In other words, the controllers need to be familiar with the major traffic flows in a sector in order to provide separation with a sufficient level of safety. Moreover, the sectors are operated in configurations in a way that the controllers are aware of the surrounding sectors.

Hence, the current organisation of the capacity matches perfectly with the Model II. The Model III still uses predefined operating sectors, so the controllers could be trained on them, but the coordination load could increase since the sectors around may change. With respect to Model IV, although it is the most promising from the point of view of capacity management, it is very far away from the operational feasibility since the sector shape might be different every time period and the controllers may deal with traffic flows and sector shapes for which they are not trained. In addition, some uncommon sector shapes may appear as solution of Model IV as illustrated in Appendix B.

Hence, the Model II has been identified as the most suitable to be tackled in this PhD since the capacity management level still uses predefined configurations (what fits with what could be nowadays accepted for ATCs), but in addition uses complexity metric for the traffic load assessment.

VII

Solution for Model II: selection of sector configurations

After examining the difficulty of the Mixed Integer Linear Programming (MILP) formulation of Model II, this chapter proposes an adapted solution approach that could scale to solve a realistic scenario. A hybrid approach, based on the integration of heuristic and exact optimisation methods, is introduced. Furthermore, three validation case studies are presented.

VII.1 Solution approach

A linear formulation for Model II has been presented in Section VI.1. Since the model contains integer (binary) variables, the exact method to solve is Branch and Bound (B&B). The size of the problem when facing real large-scale scenarios, however, may be impracticable for this kind of methods. For this reason, a new heuristic is proposed as a hybrid method between Simulated annealing and Dynamic programming.

VII.1.1 Hybrid method: Simulated annealing and Dynamic programming

In this hybrid method, the demand management and the capacity management is decoupled. The simulated annealing acts as the main evolutionary engine and it is responsible of the demand side, i.e. choosing which is the trajectory to be used per each flight. The dynamic programming is used to tackle the capacity side and it is dedicated only to propose the best sector opening scheme given a traffic condition.

The state vector of the simulated annealing algorithm is $\overrightarrow{x} = [x_1, x_2, x_3, ..., x_{N_F}]$. There is one element of the vector (x_i) for every flight and it indicates the selected trajectory ($k \in \mathcal{K}_f$) for the specific flight f. Note that the vector $\overrightarrow{x}$ has N_F (number of flights) positions and represents by itself one possible solution of the demand side. Then, the contribution of the Airspace Users (AUs) $J_{\Delta A}$ in the objective function (IV.2) can be computed.

With respect to the capacity side, for a given traffic situation provided with $\overrightarrow{x}$ it is possible to obtain the optimum sector opening scheme. One decision (used configuration) has to be taken at each time period, hence the problem could be separatet into subproblems based of the principle of Dynamic programming. This Dynamic programming algorithm is provided by the Ecole Nationale de l'Aviation Civile (ENAC) and it is based on the work published by Vidosavljevic & Delahaye (2017). The optimum sectorisation is obtained by the minimisation of three costs:

- Cost of open sectors, J_O as in equation (VI.8).
- Penalisation cost for having differences in consecutive configurations, J_S as in equation (VI.9).
- Penalisation cost for having overloaded sectors.

This last penalty cost is the consequence of the relaxation of the constraint (VI.12) that ensures that the demand can not exceed the capacity (in terms of complexity) in any active sector s and in any instant of time t. Hence, the Dynamic programming will provide always an opening scheme although the demand solution $\overrightarrow{x}$ may be infeasible from the capacity side point of view. When the solution is not feasible, the cost of the Air Navigation Service Providers (ANSPs) is penalised.

The Dynamic programming, dealing with the capacity side, is embedded in the overall engine based on Simulated annealing, dealing with the demand side, but minimising the global costs (AUs and ANSPs costs). The following lines describe the pseudo-code of the hybrid method proposed to solve the Model II:

$T \leftarrow$ Initial temperature
$T_{min} \leftarrow$ Final temperature
$N \leftarrow$ Number of transitions
$\alpha \leftarrow$ Cooling rate (<1)
$\overrightarrow{x} \leftarrow$ Initial random trajectory allocation
$\overrightarrow{y} \leftarrow$ Opening scheme from dynamic programming for demand $\overrightarrow{x}$
$f(\overrightarrow{x}, \overrightarrow{y}) \leftarrow$ Objective function for demand $\overrightarrow{x}$ and sectorisation $\overrightarrow{y}$
while $T > T_{min}$ **do**
    while $n < N$ **do**
        $\overrightarrow{x}^* \leftarrow \overrightarrow{x}$
        $i \leftarrow$ Random selection of a flight (bias to flights with more complexity)
        $x_i^* \leftarrow$ Random selection of new trajectory for flight i
        $\overrightarrow{y}^* \leftarrow$ Opening scheme from dynamic programming for demand $\overrightarrow{x}^*$
        $f(\overrightarrow{x}^*, \overrightarrow{y}^*) \leftarrow$ Objective function for demand $\overrightarrow{x}^*$ and sectorisation $\overrightarrow{y}^*$
        if $f(\overrightarrow{x}^*, \overrightarrow{y}^*) < f(\overrightarrow{x}, \overrightarrow{y})$ **then**
            $\overrightarrow{x} \leftarrow \overrightarrow{x}^*$
        else
            if $\exp(-\frac{f(\overrightarrow{x}^*, \overrightarrow{y}^*) - f(\overrightarrow{x}, \overrightarrow{y})}{T}) > rand()$ **then** $\overrightarrow{x} \leftarrow \overrightarrow{x}^*$
    $T \leftarrow \alpha T$

VII.1.2 Heating loop

As explained in Section II.3.2.3, the simulated annealing process emulates the annealing process of a metal from a high temperature to a lower temperature. The selection of the initial temperature is important in order to allow a good exploration. A low initial temperature may result in a low performance local minima. This is because with low temperature the probability of accepting degradation of the solution is low, hence the simulated annealing could be stuck in a local minima prematurely.

In this context, a *heating loop* is proposed in order to establish the initial temperature of the *cooling loop* that is adapted to the difficulty of the problem. In this *heating loop*, the temperature is increased until the number of solutions accepted at this temperature level reaches a required threshold (Delahaye *et al.*, 2019). The pseudo-code for the heating loop is:

$T \leftarrow$ Initial temperature
$A \leftarrow$ Minimum number of accepted solutions
$N \leftarrow$ Number of transitions
$\alpha \leftarrow$ Heating rate (>1)
$a \leftarrow 0$ (Number of accepted solutions)
while $a < A$ **do**
  $a \leftarrow 0$
  while $n < N$ **do**
    $\overrightarrow{x} \leftarrow$ Initial random trajectory allocation
    $\overrightarrow{y} \leftarrow$ Opening scheme from dynamic programming for demand $\overrightarrow{x}$
    $f(\overrightarrow{x}, \overrightarrow{y}) \leftarrow$ Objective function for demand $\overrightarrow{x}$ and sectorisation $\overrightarrow{y}$
    $\overrightarrow{x}^* \leftarrow \overrightarrow{x}$
    $i \leftarrow$ Random selection of a flight (bias to flights with more complexity)
    $x_i^* \leftarrow$ Random selection of new trajectory
    $\overrightarrow{y}^* \leftarrow$ Opening scheme from dynamic programming for demand $\overrightarrow{x}^*$
    $f(\overrightarrow{x}^*, \overrightarrow{y}^*) \leftarrow$ Objective function for demand $\overrightarrow{x}^*$ and sectorisation $\overrightarrow{y}^*$
    if $f(\overrightarrow{x}^*, \overrightarrow{y}^*) < f(\overrightarrow{x}, \overrightarrow{y})$ **then**
      $a \leftarrow a + 1$
    else
      if $exp(-\frac{f(\overrightarrow{x}^*, \overrightarrow{y}^*) - f(\overrightarrow{x}, \overrightarrow{y})}{T}) > rand()$ **then** $a \leftarrow a + 1$
  $T \leftarrow \alpha T$

VII.2 Validation case studies: General setup

Three validation case studies are described in this chapter. The first one consists of a performance assessment that aims to compare the exact method to solve the MILP problem, i.e. the B&B algorithm, with the proposed Hybrid method. The second case study consists of a sensitivity analysis of the penalty cost for different consecutive configurations (ρ in Equation (VI.9)). The third validation exercise is a big scale case study solved with the Hybrid method aiming at demonstrating the applicability of the method in an hypothetical use in operations.

The day analysed in these case studies is July 28th 2016. All trajectories crossing the Functional Airspace Block Europe Central (FABEC) are computed, since the initial idea was to study this geographical area. Nevertheless, and due to the computation time limitations encountered with the proposed models, the geographical scope of the three validations was later on constrained to the upper airspace of Germany. In particular, two Area Control Centers (ACCs) are considered in the first two case studies (performance assessment and sensitivity study) and are shown in Figure VII-1(a); while all seven German ACCs are analysed in the third case study (big scale case study), which are shown in Figure VII-1(b).

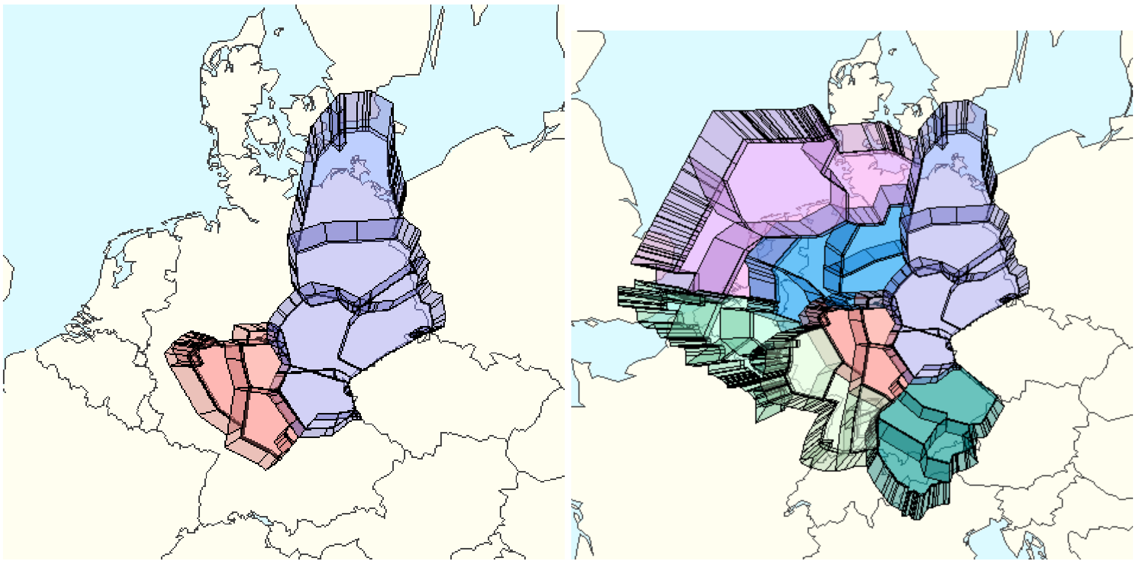

(a) First and second case study (b) Third case study

Figure VII-1: *Geographical scope of the validation case studies*

Differently than the case study of Section V.4, the historical regulations are not used. The idea is to regulate where and when the demand complexity exceeds the capacity threshold.

Next, the general setup and assumptions which are common in the three validation case studies are introduced and the results of each validation are presented in sections VII.3, VII.4 and VII.5, respectively.

VII.2.1 Generation of nominal and alternative trajectories

The preferred trajectories for the AUs are the optimum trajectories obtained with the DYNAMO tool (Dalmau *et al.*, 2018) minimising the direct operating costs. Considering the origin and destination airports, the aircraft types, the meteorological conditions and the airspace routes, DYNAMO provides the optimum 4D trajectories. A total of 15,994 flights crossing the FABEC airspace are identified and simulated with DYNAMO. These are considered as nominal trajectories.

For the alternative trajectories it is important to note that since there are not historical regulations, it is not possible to avoid directly the overloaded sectors. In order to identify the potential airspace regions to avoid, the complexity is calculated using the nominal trajectories. The alternative trajectories are then obtained by optimisation (also with DYNAMO), while satisfying one of the following constraints:

- Avoiding laterally the elementary sector with more complexity among those crossed by the nominal trajectory.
- Avoiding vertically the elementary sector with more complexity among those crossed by the nominal trajectory.

Hence, each flight has its nominal trajectory and up to 2 alternative trajectories, since alternative trajectories cannot be provided by all the flights. For instance, there are cases where the complex elementary sectors (regions to avoid) are over the airport and, in this case, they cannot be

Table VII-1: *Summary of nominal and alternative trajectories*

Type	Number of trajectories
Nominal	15,994
Lateral	13,301
Vertical	11,469
Total	40,764
Total (with delay options)	203,820

avoided. In other situations, the elementary sector to be avoided is defined over all the available altitudes, making the vertical avoidance impossible.

The number of each type of alternative trajectory is summarised in Table VII-1. Recall that the previous table and the following figures consider all trajectories crossing the FABEC airspace, although some trajectories will not eventually be used due to the reduced geographical scope of both case studies.

Figure VII-2 depicts a comparison between the lateral alternative trajectories and nominal trajectories. Typically, the lateral alternative options are longer, consume more fuel and need more trip time, but some negative values are obtained in very few situations. The same behaviour is found when analysing the cost of trajectories. Yet, the extra total cost is always higher in the alternative trajectories. Note that the nominal trajectories were the optimum ones, so having more expensive alternative trajectories is an expected outcome. With respect to the vertical alternative trajectories, the comparison with the nominal trajectories is shown in Figure VII-3. The same behaviour is observed in time and fuel. Since the lateral track is the same (there are only changes in the vertical profile of trajectories), the distance and the route charges of the vertical re-routed options are the same as the nominal trajectories.

Finally, the delay options are considered as new trajectories since the pairwise complexity must be calculated in advance. The delay discretisation is set to 10 minutes having the options: 0, 10, 20, 30 and 120 minutes. This leads to a total of 203,820 trajectories.

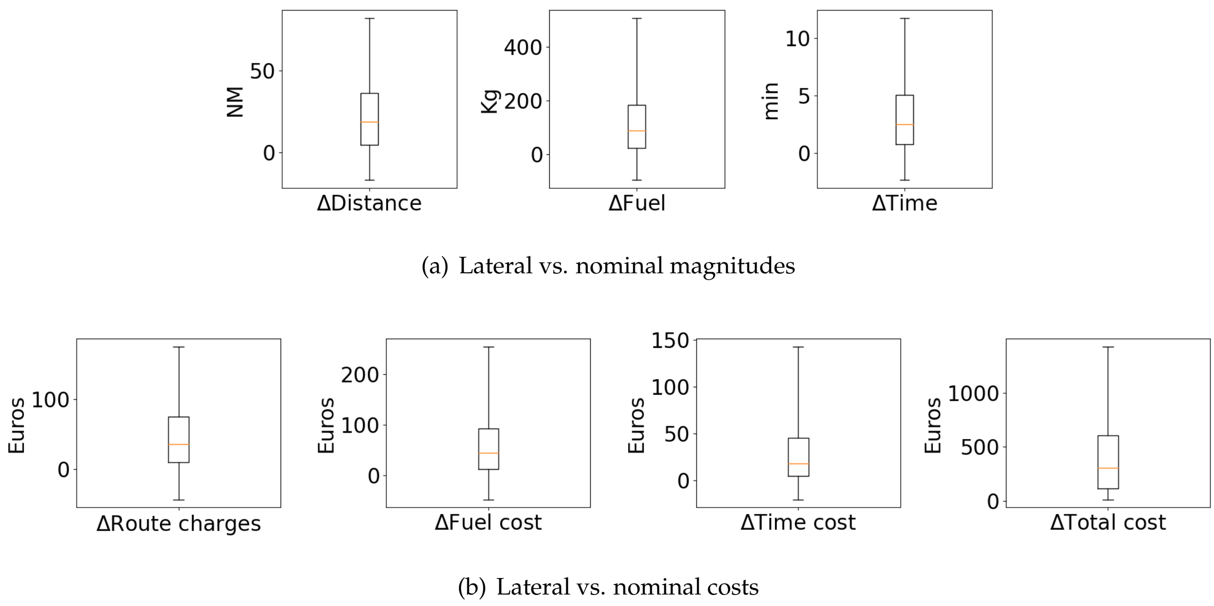

Figure VII-2: *Comparison between lateral and nominal trajectories*

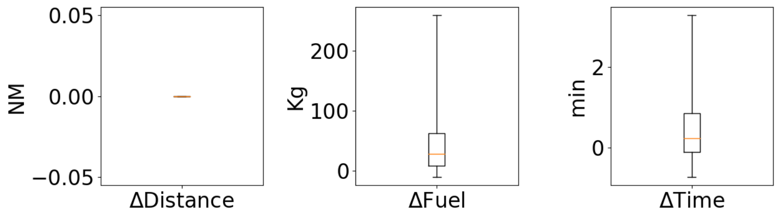

(a) Vertical vs. nominal magnitudes

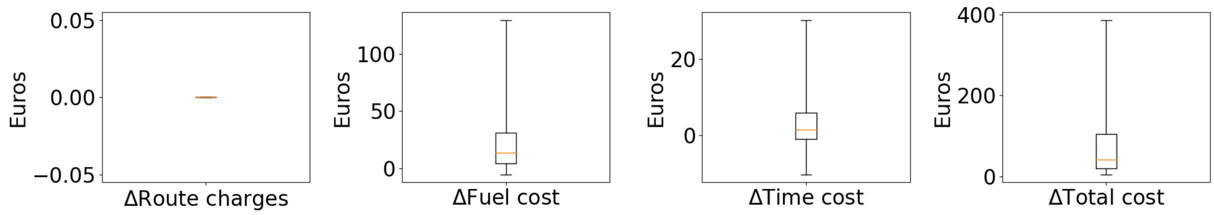

(b) Vertical vs. nominal costs

Figure VII-3: *Comparison between vertical and nominal trajectories*

VII.2.2 Complexity threshold establishment

In this study, the original geometric complexity metric described in Delahaye & Puechmorel (2000); Vidosavljevic *et al.* (2017) is used as a measure of traffic load. It is worth noting that this choice may provide ’null’ complexity in case of diverging and widely distributed traffic without regard to the aircraft quantity.

First, it is necessary to identify the capacity threshold using this complexity metric. The main hypothesis of the traffic complexity is that the same level of complexity induces the same difficulty to solve that situation regardless of the number of involved flights and the sector in which Air Traffic Control (ATC) provision occurs. The following approach is used to determine the maximum level of complexity that one controller can manage.

The regulations of the day due to ATC capacity are analysed using the data of the EUROCONTROL’s Demand Data Repository 2 (DDR2). The rationale behind is that if a regulation was implemented in one sector for this reason, it would indicate that the ATC controller was overloaded. In some occasions, the regulations are deployed on non-open sectors or at ACC level. These regulations are not considered since no ATC controller was in charge of the airspace region. The rest of the regulated sectors are analysed in terms of entry counts and complexity. These metrics are measured before and after the regulations in order to compare the effect of the regulation.

An example of such sector analysis is given in Figure VII-4 where the sector LFFFUZ, which is open from 6:00 to 20:00 and it is regulated from 11:20 to 14:00, is analysed. The top figures VII-4(a) and VII-4(b) contain the complexity and entry counts before the regulation. On the contrary, the information after the regulation is shown in the figures below VII-4(c) and VII-4(d). The two left figures VII-4(a) and VII-4(c) provide the traffic complexity evolution and, in the right figures VII-4(b) and VII-4(d), the same traffic demand is evaluate using entry counts. The red color indicates the period when the sector is regulated, while the green line indicates the proposed threshold in complexity and entry counts respectively.

The complexity threshold is set such that it is violated only in the regulated period and the demand is below during the active periods that are not regulated as well as after the regulation. It contrasts with the case using entry counts, since the regulations are not systematically applied when the demand is higher than the capacity. The Flow Management Positionss (FMPs) verify other traffic parameters before applying a regulation. This is something that is not longer necessary with the use of a complexity metric that directly takes into account those criteria.

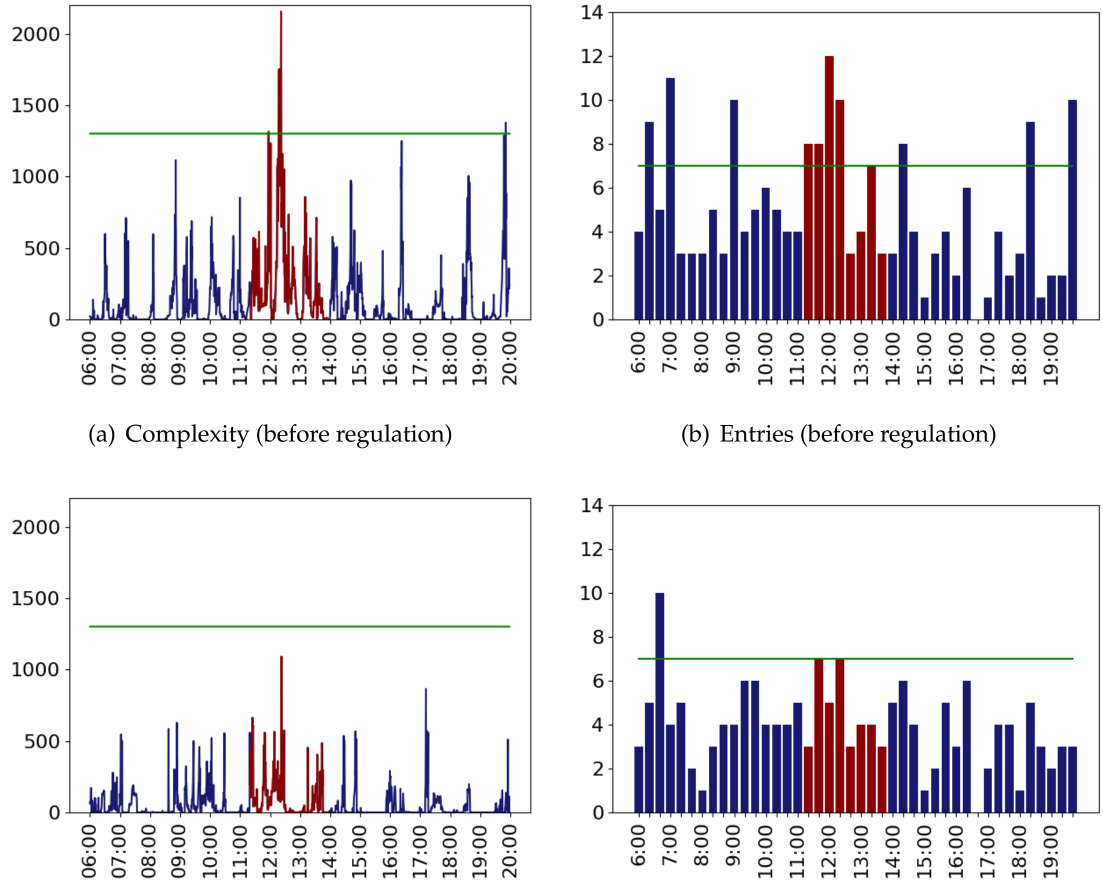

(a) Complexity (before regulation)

(b) Entries (before regulation)

(c) Complexity (after regulation)

(d) Entries (after regulation)

Figure VII-4: *Complexity/Entry count assessment of sector LFFFUZ.*

Another example is the sector LECBP1U analysed in Figure VII-5. In this case, the sector is regulated from 8:20 to 12:00 with an entry count threshold a slightly higher than the nominal. In terms of complexity, the regulated period contains a big peak of complexity and this explains the regulation. It is important to note that, after the regulation, the complexity remains under the value of the threshold. The regulation is also explained when looking at at the entry counts. After the regulation, however, the entry counts still remain a bit higher the threshold.

There are, however, examples where the explained approach does not give satisfactory results. This is the case of sector EDYYBOLN (see Figure VII-6). The sector is open from 04:30 to 05:00 and regulated from 05:20 to 06:40. Note that the regulation is extended more than the time the sector is really opened. Furthermore, the demand entries do not produce any overloaded periods prior to the implementation of the regulations, which supports the idea that the Network Manager (NM) considers additional factors when executing a regulation. This is particularly represented by the high values of complexity before the regulation in comparison with the values of entry counts. However, what it is difficult to explain and justify are the high values of complexity after the regulation. A possible explanation could be that additional traffic goes trough the sector as a consequence of other regulations. Another explanation could be that the complexity metric is sensible to the traffic patterns and does not depend only on the number of flights. Hence, the regulations that delay some flights may theoretically create more difficult situations.

Another example of unexpected behaviour is sector EDYYDWST analysed in Figure VII-7.

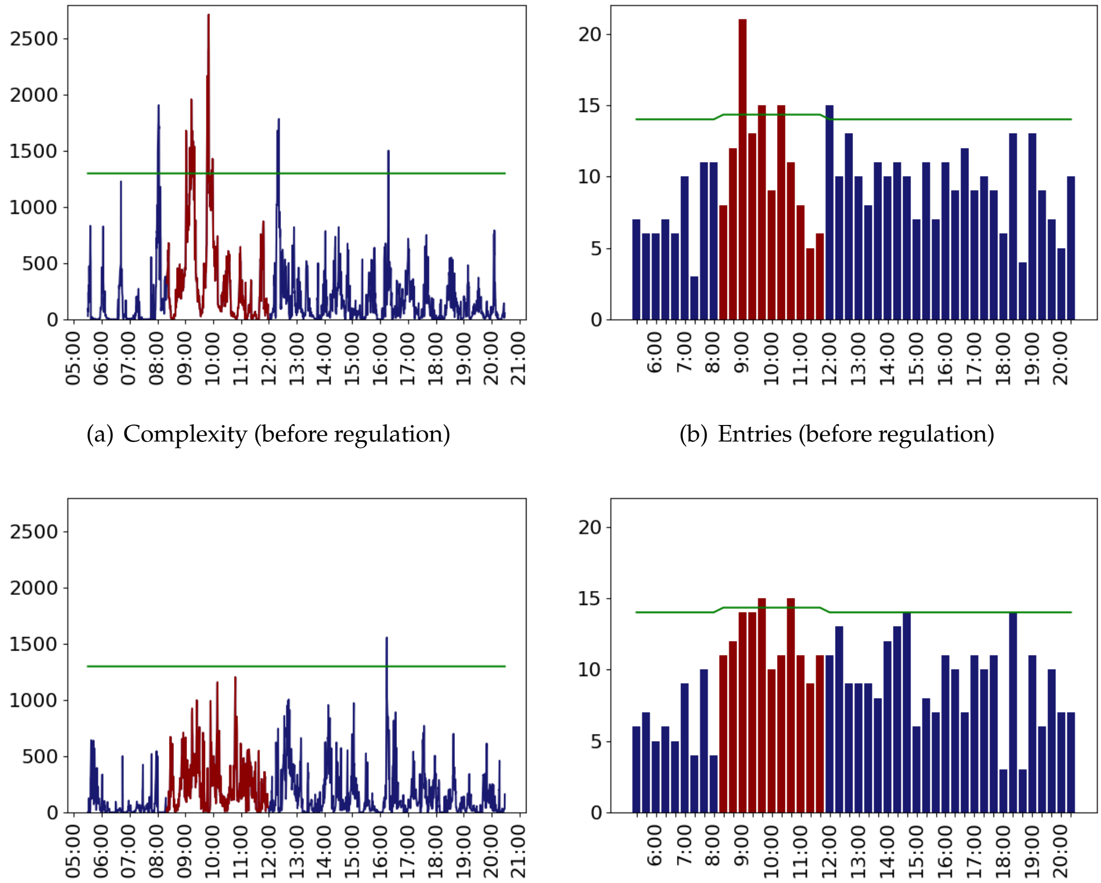

(a) Complexity (before regulation)

(b) Entries (before regulation)

(c) Complexity (after regulation)

(d) Entries (after regulation)

Figure VII-5: *Complexity/Entry count assessment of sector LECBP1U.*

The sector is used from 08:30 to 21:00 and regulated from 8:40 to 21:40. Again the regulation is applied even after closing the sector. This sector is particularly interesting because the are overloads in entry counts after the regulation, but the traffic demand has low complexity. In other words, considering only the values of complexity, this regulation was not even necessary. Besides this, the resulting values of complexity and entry counts after the regulation remains above the respective thresholds. Hence, the reason for this regulation remains unexplained.

Wrapping up, the method used in order to determine the complexity threshold has its limits and further research is needed on it. In particular, the experience of air traffic controllers or experts from NM would be very helpful, specially when assessing the cases difficult to explain. With these limitations, the complexity threshold is set to 1,300 such that provides statistically the best value considering the considered regulations.

VII.2.3 Algorithms setup

The B&B algorithm used in the first case study is applied using Gurobi 9.5.0, which is a commercial solver (Gurobi, 2023). Gurobi offers many calibration options that change the behaviour of the solver, for instance, the *Presolve* and the *Heuristics*. *Presolve* transforms the model into an equivalent model that is smaller and easier to solve. Although Gurobi performs the B&B algorithm, it allows some level of heuristics. The *Heuristics* value controls the time spent in Mixed Integer Program (MIP) heuristics. Larger values produce more and better feasible solutions, at a cost of slower progress in the best bound. Different combinations of *Presolve* and *Heuristics* are explored

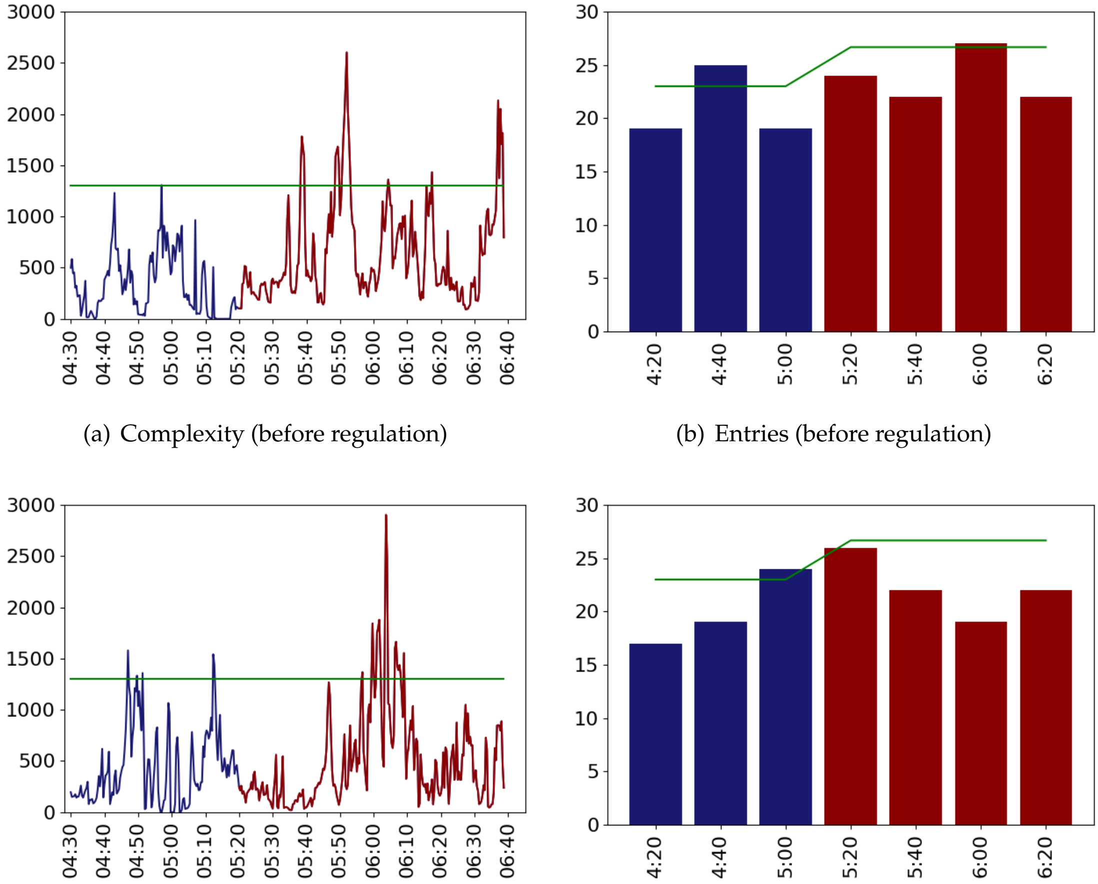

(a) Complexity (before regulation) (b) Entries (before regulation)

(c) Complexity (after regulation) (d) Entries (after regulation)

Figure VII-6: *Complexity/Entry count assessment of sector EDYYBOLN.*

Table VII-2: *Gurobi configuration setup used in analysis*

Presolve	Heuristics
Off	5%
Auto	0%
Auto	5%
Auto	50%
Auto	75%

as summarised in Table VII-2. The Gurobi simulations are limited at a maximum of 5 hours. The option of computing in parallel is available. This is particularly important when Gurobi is working with heuristics.

For the Hybrid method, the calibration parameters are:

- $\alpha = 0.995$ (Cooling rate).
- $N = 2000$ (Number of transitions).
- $T_{min} = T_{initial} \cdot 10^{-4}$.
- $A = 0.8N$ (Minimum number of accepted solutions in the heating loop).

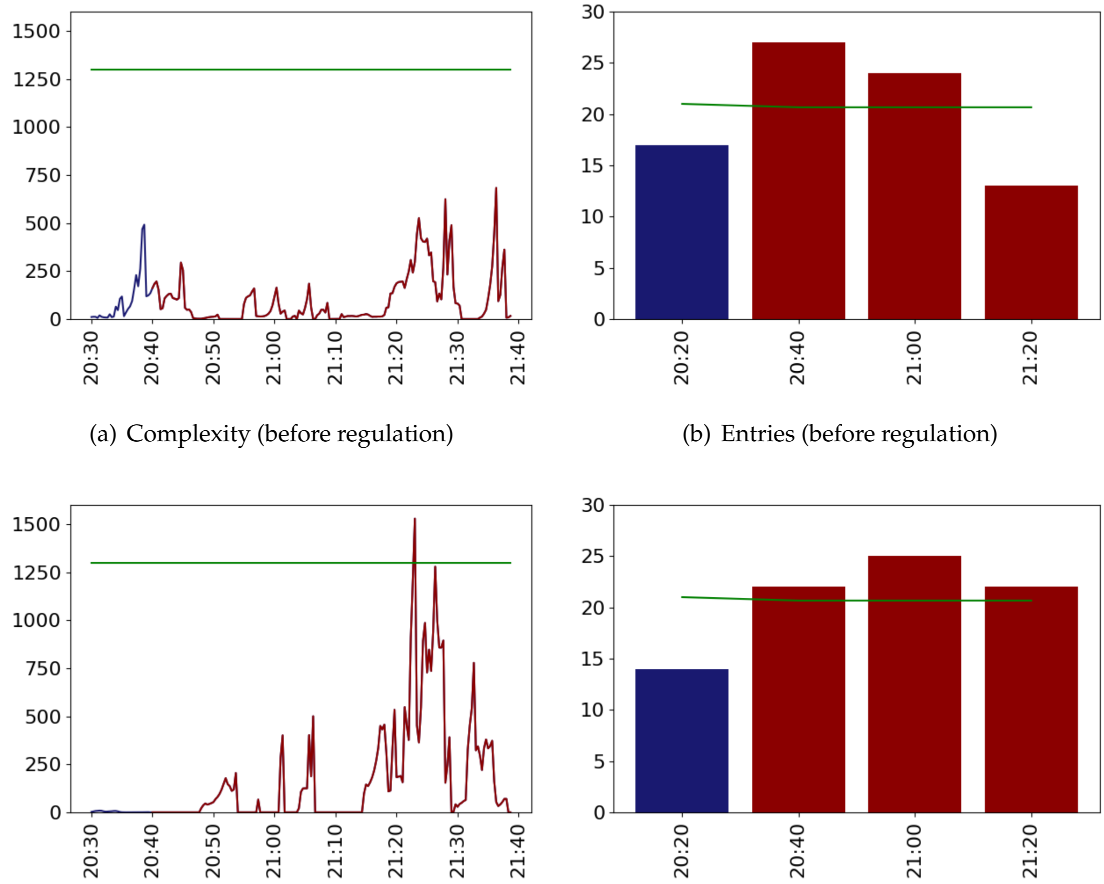

(a) Complexity (before regulation)

(b) Entries (before regulation)

(c) Complexity (after regulation)

(d) Entries (after regulation)

Figure VII-7: *Complexity/Entry count assessment of sector EDYYDWST.*

The simulated annealing component of the Hybrid method works linearly but the dynamic programming part finds the sector opening scheme of the different ACCs with parallel computing.

VII.2.4 Time considerations

The complexity of the traffic demand is evaluated in samples of 20 seconds. Hence, there is an instant of time every 20 seconds. The reason of such small discretisation is that the considered complexity metric provides instantaneous information of the traffic load.

A period of time is linked with the capacity management. The sector configuration can change at the beginning of each period, but the capacity limitation is verified for every instant of time of the period. The period duration is set to 15 minutes in order to provide high flexibility in terms of capacity management.

VII.3 Performance assessment case study: Branch and Bound vs. Hybrid method

A validation study is proposed in order to compare the performance of the Hybrid method introduced in Chapter VII.1 against the exact method solved with Gurobi.

VII.3.1 Computation setup

The computer used for the performance assessment case study contains two Intel(R) Xeon(R) CPU E5-2695 v3 @ 2.30GHz. The combination of both gives 28 cores with 56 threats. The simulations, however, were launched with a maximum of 18 cores. The available RAM is 256GB.

VII.3.2 Definition of scenarios

The goal of this analysis is to benchmark the performances of the two methods with problem instances of different difficulty. Two instruments have been used to generate the problem instances of different difficulty: cumulative (total) complexity of the instance and the instance duration. Figure VII-8 illustrates the number of nominal flights, the number of trajectories (note that one flight might have more than one alternative trajectory) and the total value of aggregated complexity over two ACCs in Germany (EDUUUTAC and EDUUUTAE) in 28th July of 2016 (see Figure VII-1(a)). The complexity is aggregated because it is calculated over the two ACCs (with no differentiation of sectors). Only two ACCs are considered in order to limit the computation time at a maximum of 5h.

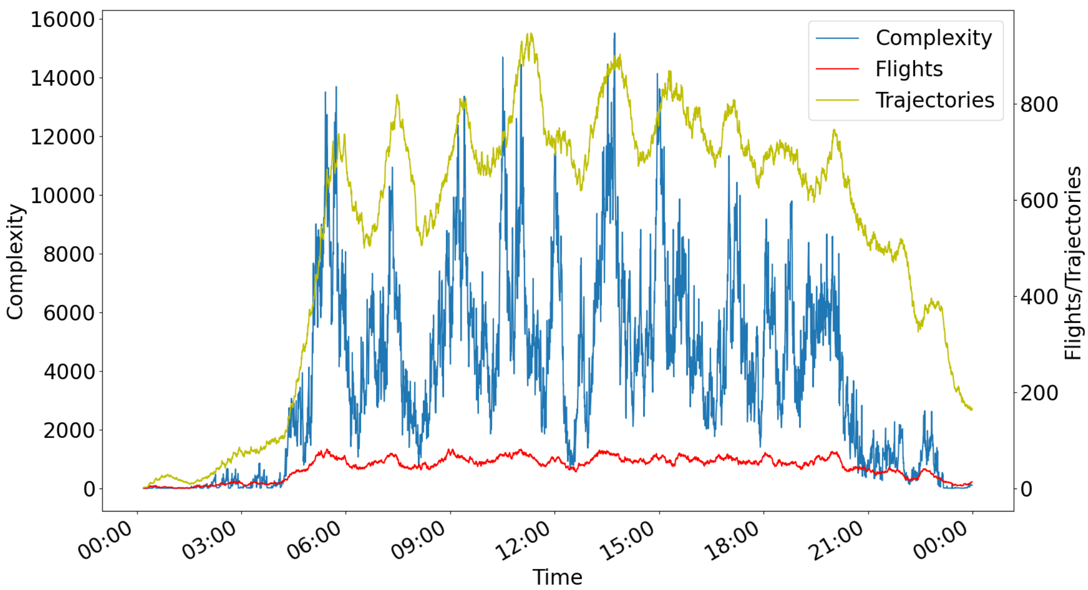

Figure VII-8: *Number of flights, number of trajectories and aggregated complexity*

In order to assess the effects of the level of complexity and the time duration, six scenarios are defined and detailed in Table VII-3. Note that these scenarios are selected only to compare the computation performance of the two solution methods. In the generation of the scenarios, the following rules are considered:

- Only the flights, which nominal trajectory crosses the scenario geographic area in the scenario time duration are considered.
- Only the trajectories in the scenario geographic area selected are considered. In other words, if one alternative trajectory is not crossing the selected geographic area it is not considered.
- Only the trajectories in the scenario time duration are considered. It implies that, in the scenarios of 1h duration it is not possible to have more than 1h of delay.
- The demand and capacity balance is only ensured during the scenario duration, regardless what it may happen after.

Table VII-3: *Summary of scenarios*

	Low complexity	Medium complexity	High complexity	1h duration	2h duration	3h duration
Duration	1h	1h	1h	1h	2h	3h
Start time	01:00	06:00	10:00	00:00	00:00	00:00
End time	02:00	07:00	11:00	01:00	02:00	03:00
Periods	4	4	4	3	7	11
Instants	180	180	180	135	315	495
Flights	18	228	295	13	28	70
Trajectories	67	1630	2200	67	131	354
Sectors	40	40	40	40	40	40
Elementary sectors	21	21	21	21	21	21
Configurations	62	62	62	62	62	62

Table VII-4: *B&B computation times for the Low complexity scenario*

Presolve	Heuristics	Computation time [s]
Off	5%	2.12
Auto	0%	0.97
Auto	5%	1.07
Auto	50%	1.03
Auto	75%	1.11

In both cases, Gurobi and Hybrid method, the penalty for different configurations of the Model II is set to 0 ($\rho = 0$).

VII.3.3 Methods benchmark for different scenario complexity

The scenarios with different complexity are assessed in the following lines.

VII.3.3.1 Low complexity scenario

The Low complexity scenario has been solved with all the Gurobi setups listed in Table VII-2. Although the problem seems easy to be solved with Gurobi, different computation times are observed depending on the setup (see Table VII-4).

The same scenario is solved using the Hybrid method. The Hybrid method is launched three times in order to check if there are differences due to the stochastic behaviour of the heuristics. The optimal solution is obtained for each Hybrid method repetition. With respect to the resolution time, it has been 21.69 minutes, 21.79 minutes and 22.29 minutes in each instance of the Hybrid method. Although the resolution time is higher than in Gurobi, very good solutions are obtained much before the end time as it can be seen in Figure VII-9. Yet, the use of the Hybrid method in low complexity scenarios is not justified when Gurobi provides the optimum solution very fast.

VII.3.3.2 Medium complexity scenario

The Medium complexity scenario is more ambitious than the Low complexity scenario. Gurobi does not find the optimum solution in 5 hours with any of the Gurobi setups. In fact, it is particularly relevant that with no Presolve, no feasible solution is found in 5 hours. The time evolution of the different algorithms is shown in Figure VII-10.

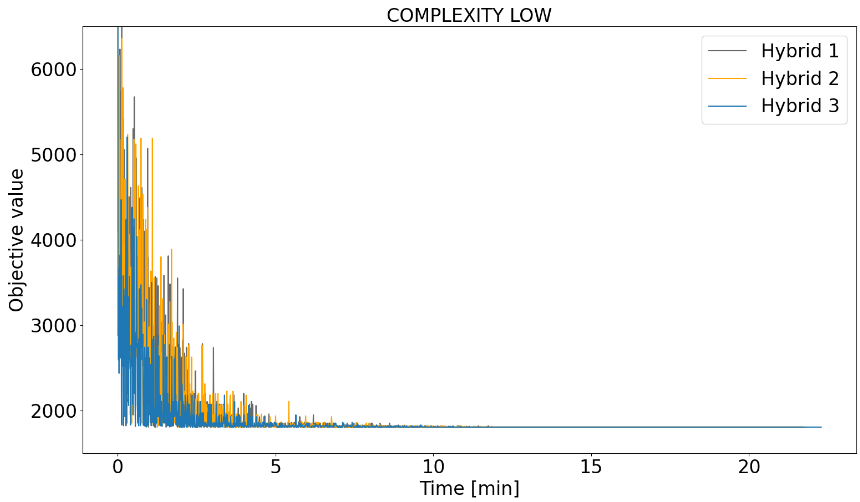

Figure VII-9: *Objective function evolution with Hybrid Method in Low complexity scenario*

The Upper Bound (UB) in the B&B algorithm indicates the objective function value of the best integer feasible solution found. The Lower Bound (LB), by definition, indicates that the optimum solution must have an objective function value higher or equal to it. The optimality gap indicates the difference between the upper and the lower bounds and it is defined as follows:

$$\text{gap} = \frac{\text{UB} - \text{LB}}{\text{UB}} \tag{VII.1}$$

The optimum solution is found when the upper and lower bounds are coincident and the gap is null.

Hence, according to what is shown in Figure VII-10, Gurobi provides feasible solutions but not the optimum one. The different Gurobi setups have different behaviours in terms of how fast the first feasible solution is found and in the quality of the feasible solution found. Considering the best upper and lower bounds, the gap with Gurobi is 39.09%.

With respect to the Hybrid method, it was launched three times in order to study its stochastic behaviour. The computation times were 2.16 hours, 2.15 hours and 2.17 hours. In all instances, the Hybrid method provides better feasible solutions than Gurobi (better objectives than the B&B upper bound and closer to the lower bound) with a considerable reduction in the computation time. In fact, considering the best lower bound obtained with Gurobi, the gap with the Hybrid method is 29.23%. Hence, the Hybrid method performs much better than Gurobi when dealing with the Medium complexity scenario.

VII.3.3.3 High complexity scenario

This scenario is too diffcult to be solved using Gurobi. No feasible solution is found in any of the Gurobi setups and the solution is only lower bounded. Hence, no gap can be provided for the Gurobi cases.

Three different repetitions are launched with the Hybrid method and the computation times have been 2.40 hours, 2.43 hours and 2.46 hours. The solutions obtained are feasible and no big time differences are observed with respect to the medium complexity scenario. The evolution of the objective in time of the methods is shown in Figure VII-11. Considering the best lower bound obtained with Gurobi and the best solution of the Hybrid method, the gap of the Hybrid method is 68.90%. It is worth noting that the solution obtained with the Hybrid method might be close to

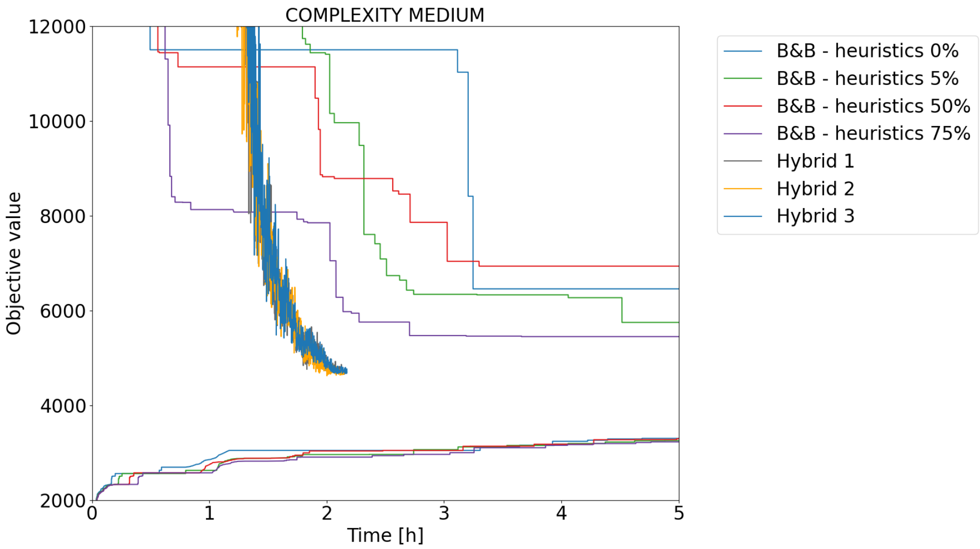

Figure VII-10: *B&B vs Hybrid method in Medium complexity scenario*

the optimum solution, but the big value of gap obtained may be the consequence of a low value obtained in the lower bound.

Comparing Gurobi and the Hybrid method, the high complexity scenario is intractably with B&B but it can be addressed easily with the Hybrid method.

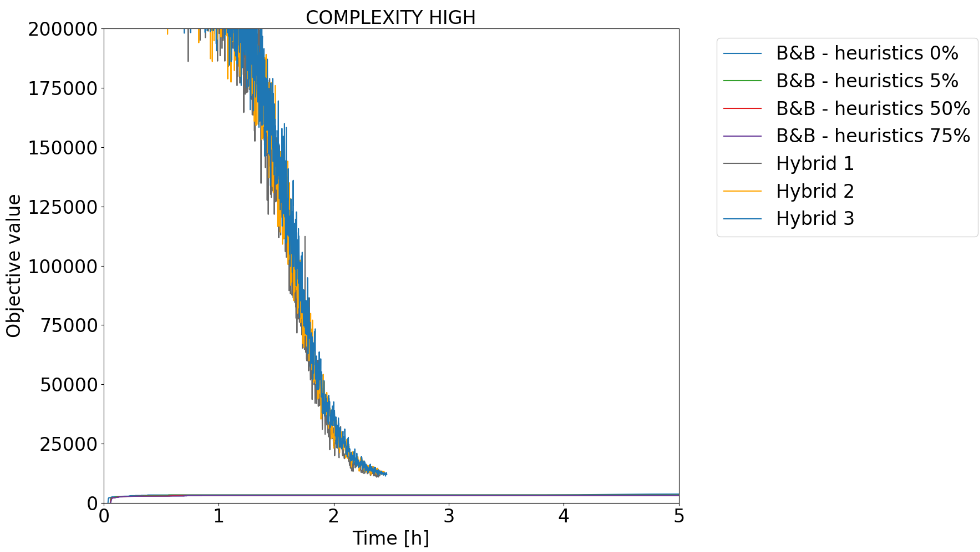

Figure VII-11: *B&B vs Hybrid method in Medium complexity scenario*

VII.3.4 Methods benchmark for different scenario durations

This section aims at comparing the Gurobi and the Hybrid methods when dealing with scenarios with different time duration. The scenarios were selected during the night hours in order to avoid inferences due to big changes of complexity or in the number of flights or trajectories. Since the difficulty of the scenarios remains moderate in terms of complexity, number of flights and trajectories, the optimum solution has been found with Gurobi for all the Gurobi setups given in Table VII-2. With respect to the Hybrid method, three repetitions are considered in order to evaluate the stochastic behaviours. All the scenarios are solved with Gurobi and the Hybrid method and the resolution times are summarised in Table VII-5.

Table VII-5: *Summary of the resolution times for different temporal scenarios*

	1h	2h	3h
B&B Presolve Off Heuristics 5%	2.31 s	14.78 s	534.69 s
B&B Presolve Auto Heuristics 0%	1.12 s	4.12 s	25.82 s
B&B Presolve Auto Heuristics 5%	1.16 s	4.66 s	27.74 s
B&B Presolve Auto Heuristics 50%	1.17 s	4.64	28.75 s
B&B Presolve Auto Heuristics 75%	1.18 s	4.72 s	28.61 s
Hybrid 1	22.42 min	34.66 min	74.70 min
Hybrid 2	23.08 min	37.74 min	77.50 min
Hybrid 3	21.86 min	34.06 min	76.31 min

The resolution times are better with Gurobi but this is because the complexity is very low in all the scenarios. It was already concluded in the previous section that with low complexity and low number of flights/trajectories Gurobi performs very well. The purpose of this study is to evaluate how the methods behaves when the scenario duration increases and consequently the difficulty of the problem. The resolution times when using Gurobi look to have an exponential trend while the resolution times with the Hybrid method are comparatively less impacted by the increase of the scenario difficulty.

The average ratio between the computation time for the 3h scenario and the 1h scenario is 3.38. In the case of the B&B algorithm, this ratio is 23.96. This can be observed in Figure VII-12 (the case with Presolve off is disregarded because of its bad performance). Hence, the Hybrid method is much more scalable and more suitable for real scale scenarios.

VII.4 Sensitivity case study: penalty for sector configuration changes

A sensitivity analysis case study is proposed to assess the impact of the penalty cost for different consecutive configurations in the resulting solution. This sensitivity analysis consists of the exploration of different values of the parameter ρ in Equation (VI.9).

VII.4.1 Definition of the scenarios

This sensitivity study is conduced on the medium complexity scenario defined previously in Table VII-3. The 1 hour duration scenario covers two ACCs in Germany (EDUUUTAC and EDUUUTAE) and, since the period duration is 15 minutes, there are 4 potential changes of sector configurations.

The Demand and Capacity Balancing (DCB) problem is solved in these conditions with four

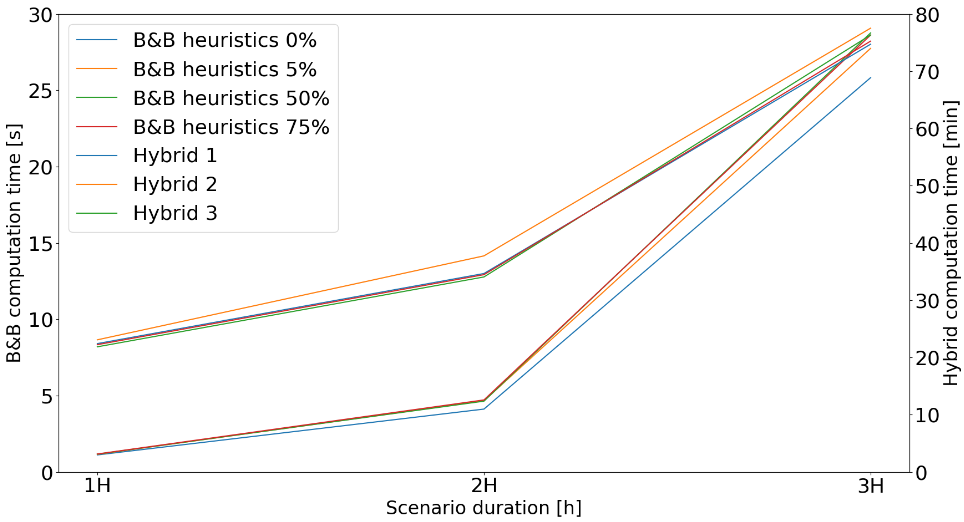

Figure VII-12: *B&B vs Hybrid method resolution times*

different values of ρ: 0, 15, 30 and 50 € per elementary sector change.

Only the Hybrid method is used in order solve the DCB problem.

VII.4.2 Results

The different costs for the different values of ρ are summarised in Table VII-6, while the resulting sector opening schemes are illustrated in Figure VII-13. Each item of Figure VII-13 describes in grey the open configuration during each period and in white the open operating sectors. Looking at the figures horizontally (i.e. rows of the table), one can see how the sectors are split and collapsed. For example, in Figure VII-13(c), the configuration C3 is open from 6:00 to 6:30 containing the three sectors EDUUFFM1F, EDUUFUL1U and EDUUWUR1Z. Then, from 6:30 to 7:00 the open configuration is C1 such that the sectors EDUUFFM1F, EDUUFUL1U and EDUUWUR1Z are collapsed together to form sector EDUUCNTR.

With $\rho = 0$, there is no penalty for different consecutive configurations. This is specially visible in the ACC EDUUUTAC where the configuration C4C with 4 sectors is open from 6:00 to 6:15. Then, the number of sectors is progressively reduced by using the configuration C3 with 3 sectors from 6:15 to 6:30 and the configuration C1 with one sector from 6:30 to 7:00. The ACC EDUUUTAE, however, is managed with 2 sectors from 6:30 to 6:30 and with 4 sectors from 6:30 to 7:00. A total of 25 elementary sectors changed from operating sector at some period, but with no effect in the penalty cost due to the value of ρ. With $\rho = 0$, the capacity provision is better adapted to the demand needs providing the lowest extra costs for the AUs.

With $\rho = 15$, the configuration C3 in EDUUUTAC is open from 6:00 to 6:30, avoiding the use of 4 sectors at the beginning and reducing the number of elementary sectors that change. In fact, this solution saves the penalty of collapsing the sectors EDUUFFM1C and EDUUFFM3C to EDUUFFM1F. In EDUUUTAE, the increment of open sectors with the time is now more progressive with the use of the configuration E3 from 6:30 to 6:45. With respect to the penalty for different consecutive configurations in EDUUUTAE, it is the same than with $\rho = 0$, since the number of sector changes is the same. The overall number of elementary sectors that changed from operating sector at some period with $\rho = 15$ is 21. Regarding the extra cost for the AUs, it is higher than with $\rho = 0$, which is an expected consequence due to the use of less open sectors. Since the capacity provided is lower, the demand side initiatives have a greater impact.

The opening scheme obtained with $\rho = 30$ in EDUUUTAC is the same as the obtained with

$\rho = 15$. In EDUUUTAE, the sector EDUUERL1R remains open during all periods avoiding the penalty for dividing the sector EDUUERL1R in the sectors EDUUERL12 and EDUUERL22. The sector EDUUOHAP, however, is divided 3 sectors. The total number of elementary sectors that changes in this case is 19, which is lower than before. Note that the number of controller hours is higher than with $\rho = 15$ because of the use of 4 sectors instead of 3 from 6:30 to 6:45. This explains why the extra cost for the AUs is lower than the case of $\rho = 15$.

Finally, the penalty cost for different consecutive configuration becomes predominant with $\rho = 50$. Note that the opening schemes obtained are static avoiding changes of elementary sectors. Hence, the penalty obtained in that case is null. The capacity provision can not adapt to the demand needs and therefore, the extra extra cost for the AUs is the highest of the analysed values of ρ.

<table>
<tr><th>6:00</th><th>6:15</th><th>6:30</th><th>6:45</th></tr>
<tr><td>C4C</td><td>C3</td><td colspan="2">C1</td></tr>
<tr><td>EDUUFFM1C</td><td rowspan="2">EDUUFFM1F</td><td colspan="2" rowspan="4">EDUUCNTR</td></tr>
<tr><td>EDUUFFM3C</td></tr>
<tr><td colspan="2">EDUUFUL1U</td></tr>
<tr><td colspan="2">EDUUWUR1Z</td></tr>
</table>

(a) EDUUUTAC ($\rho = 0$)

<table>
<tr><th>6:00</th><th>6:15</th><th>6:30</th><th>6:45</th></tr>
<tr><td colspan="2">E2</td><td colspan="2">E4B</td></tr>
<tr><td colspan="2" rowspan="2">EDUUERL1R</td><td colspan="2">EDUUERL12</td></tr>
<tr><td colspan="2">EDUUERL22</td></tr>
<tr><td colspan="2" rowspan="2">EDUUOHAP</td><td colspan="2">EDUUOH</td></tr>
<tr><td colspan="2">EDUUAP</td></tr>
</table>

(b) EDUUUTAE ($\rho = 0$)

<table>
<tr><th>6:00</th><th>6:15</th><th>6:30</th><th>6:45</th></tr>
<tr><td colspan="2">C3</td><td colspan="2">C1</td></tr>
<tr><td colspan="2">EDUUFFM1F</td><td colspan="2" rowspan="3">EDUUCNTR</td></tr>
<tr><td colspan="2">EDUUFUL1U</td></tr>
<tr><td colspan="2">EDUUWUR1Z</td></tr>
</table>

(c) EDUUUTAC ($\rho = 15$)

<table>
<tr><th>6:00</th><th>6:15</th><th>6:30</th><th>6:45</th></tr>
<tr><td colspan="2">E2</td><td>E3</td><td>E4B</td></tr>
<tr><td colspan="3" rowspan="2">EDUUERL1R</td><td>EDUUERL12</td></tr>
<tr><td>EDUUERL22</td></tr>
<tr><td colspan="2" rowspan="2">EDUUOHAP</td><td colspan="2">EDUUAP</td></tr>
<tr><td colspan="2">EDUUOH</td></tr>
</table>

(d) EDUUUTAE ($\rho = 15$)

<table>
<tr><th>6:00</th><th>6:15</th><th>6:30</th><th>6:45</th></tr>
<tr><td colspan="2">C3</td><td colspan="2">C1</td></tr>
<tr><td colspan="2">EDUUFFM1F</td><td colspan="2" rowspan="3">EDUUCNTR</td></tr>
<tr><td colspan="2">EDUUFUL1U</td></tr>
<tr><td colspan="2">EDUUWUR1Z</td></tr>
</table>

(e) EDUUUTAC ($\rho = 30$)

<table>
<tr><th>6:00</th><th>6:15</th><th>6:30</th><th>6:45</th></tr>
<tr><td colspan="2">E2</td><td colspan="2">E4</td></tr>
<tr><td colspan="4">EDUUERL1R</td></tr>
<tr><td colspan="2" rowspan="3">EDUUOHAP</td><td colspan="2">EDUUOH</td></tr>
<tr><td colspan="2">EDUUSAL1A</td></tr>
<tr><td colspan="2">EDUUSPE1P</td></tr>
</table>

(f) EDUUUTAE ($\rho = 30$)

<table>
<tr><th>6:00</th><th>6:15</th><th>6:30</th><th>6:45</th></tr>
<tr><td colspan="4">C3</td></tr>
<tr><td colspan="4">EDUUFFM1F</td></tr>
<tr><td colspan="4">EDUUFUL1U</td></tr>
<tr><td colspan="4">EDUUWUR1Z</td></tr>
</table>

(g) EDUUUTAC ($\rho = 50$)

<table>
<tr><th>6:00</th><th>6:15</th><th>6:30</th><th>6:45</th></tr>
<tr><td colspan="4">E3</td></tr>
<tr><td colspan="4">EDUUERL1R</td></tr>
<tr><td colspan="4">EDUUOH</td></tr>
<tr><td colspan="4">EDUUAP</td></tr>
</table>

(h) EDUUUTAE ($\rho = 50$)

Figure VII-13: *Sector opening schemes for EDUUUTAC and EDUUUTAE with different values of ρ (Euros per elementary sector change).*

Table VII-6: *Summary of costs (ρ given in € per elementary sector change)*

	$\rho = 0$	$\rho = 15$	$\rho = 30$	$\rho = 50$
Extra AU cost [€]	1,428	1,726	1,639	1,753
ANSPs cost [€]	3,161	2,860	3,011	3,613
Penalty cost [€]	0	315	570	0
Total cost [€]	5,016	5,106	5,153	5,311

VII.4.3 Discussion on the results

As expected, when the value of ρ is low, the number of changes of configurations is higher and the capacity can be better adapted to the demand needs, what is reflected in a low value of extra cost for the AUs. When ρ has intermediate values the sectors are open for longer time, reducing the number of elementary sectors that change. With greater values of ρ, the opening schemes become static and the capacity provision is not adapted to the traffic demand leading to high values of extra cost for the AUs.

Choosing among the the values of ρ would require expert judgement regarding the operational feasibility of the resulting opening schemes at ACC level. The feedback of experienced controllers in the corresponding ACCs would be very valuable in this type of assessment. High values of ρ are not desirable in order to avoid too rigid (i.e., static) opening schemes, but low values may result in too many changes that might be difficult to operate.

VII.5 Big scale case study

The aim of this section is to assess a realistic case in order to check the operational feasibility of the proposed concept of operations introduced in Section IV.1 and the Hybrid method. Furthermore, a benchmark between the proposed Model II and the best setup of the current system (where demand and capacity management are deployed separately and using entry counts) is provided.

This big scale case study addresses the traffic over the upper airspace in Germany (7 ACCs) during the first wave of aggregated complexity from 06:00 to 12:00 (Figure VII-1(b)). The number of flights/trajectories and the aggregated complexity over the considered airspace is shown in Figure VII-14. According with the aggregated complexity, there are two waves of aggregated complexity, having one period of low complexity at midday.

The problem is solved first with no penalty cost associated to sector configuration changes ($\rho = 0$ in Equation (VI.9)). This allows for fair comparison with the baseline scenario that is presented below in section VII.5.2. Then, a repetition of the same scenario is given for $\rho = 15$ € per elementary sector change.

VII.5.1 Computation setup

The computer used for the big scale study contains two CPUs Intel(R) Xeon(R) Gold 6230 CPU @ 2.10GHz. The combination of both gives 40 cores with 80 threats. The simulations, however, were launched with a maximum of 30 cores. The available RAM is 1TB.

VII.5.2 Baseline scenario

The baseline scenario is defined in order to compare the results obtained with the Model II and solved using the Hybrid method. Differently than what it is done in Section V.4, the historical regulation data is not used. The main reason is to avoid having regulations with diverse motivation

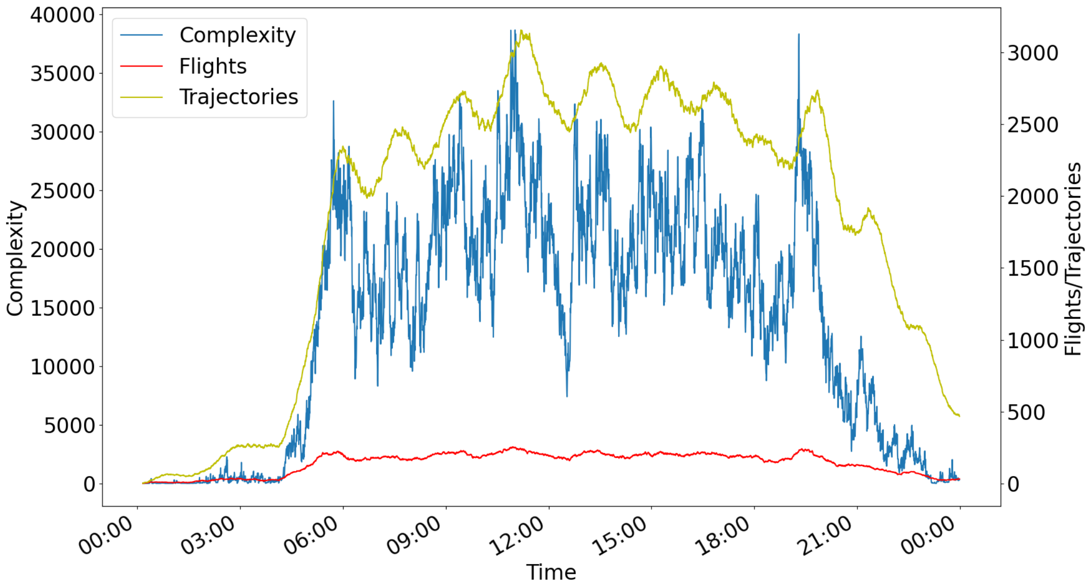

Figure VII-14: *Number of flights, number of trajectories and aggregated complexity*

that may not be covered by the use of complexity metrics. Hence, the baseline scenario is created from scratch using NEST v1.6 in four steps:

1. Import the trajectories. The initial traffic demand consists of the trajectories optimised with DYNAMO. Those trajectories are imported to NEST.

2. Optimisation of the capacity side. The opening schemes of the 7 ACCs considered are optimised with the Dynamic Airspace Configurations (DAC) tool embedded in NEST based on the Improved Configuration Optimizer (ICO) algorithm (Verlhac, C. and Manchon, S., 2005). This optimisation of the capacity side is done measuring the demand and the capacity in entry counts. The minimum configuration duration is set to 15 minutes and no limit on the available number of controllers is considered. In addition, no operational limit is considered between consecutive configurations. The idea behind is to create a baseline scenario where the capacity side is optimised with the best possible conditions. The resulting cost for the ANSPs during the studied period is 174,922€.

3. Identification of regulations. Once the opening scheme is defined, the regulations are created where the traffic demand is higher that the capacity in entry counts. The regulations are simulated with NEST considering that the minimum duration of a regulation is 20 minutes. Consecutive regulations in less than 60 minutes are merged. The regulation are only identified in the 7 ACCs and from 06:00 to 12:00. A total number of 62 regulations are created.

4. Allocation of delay. The delay is allocated with the Computer-Assisted Slot Allocation (CASA) based on Ration-by-Schedule (RBS) algortihm. A total of 28,285 minutes of delay is given to 1,154 flights, what represents a cost for the AUs of 2,291,085€. The average delay is 25 minutes, being the maximum 71 minutes. The median is 20 minutes, and the standard deviation 17.6 minutes. These values for CASA are summarised in Table VII-7.

There are some considerations to be taken when comparing the baseline scenario with the Model II scenario. The first consideration is that the regulations in the baseline scenario are identified considering entry counts. This means that some regulations may be applied in regions/periods with low complexity. On the contrary, there may be regions/periods with high complexity not regulated because there is a low number of entry counts. This phenomenon, however, is part of the justification for the use of complexity metrics instead of entry counts.

Another consideration is the use of regulations by itself. The delay allocation is done to maintain the demand below the capacity during the regulations what does not prevent overloads after the delay allocation in the non regulated areas. In fact, the baseline scenario has some overloads after the delay allocation process.

These considerations contrast with the scenario with Model II, where the concept of *regulation* is not used since the demand is maintained below the capacity (in complexity metric) in all open sectors, so there are no remaining overloads after the DCB process.

The purpose of comparing the baseline scenario with the scenario with Model II is threefold:

- Study the impact of considering the demand and capacity management into the same optimisation problem. The baseline scenario is sequential. First, the capacity side is optimised and then the demand side is considered by the allocation of delay.
- Study the impact of using complexity metrics instead of entry counts.
- Study the impact of the use of alternative trajectories together with delay allocation as demand management measure.

VII.5.3 Results with the Hybrid method

This section is focused on the results obtained with the resolution of the Model II with the Hybrid method proposed in Section VII.1. The cooling loop of the method needed 30.17 hours to finish and provided a feasible solution.

For $\rho = 0$, the opening schemes for all the considered ACCs and periods is shown in Figures VII-15-VII-21. The open configurations are indicated in grey and the open sectors in white for each time period. Reading horizontally (i.e., rows in the table), one can see how the sectors are split and collapsed. When one sector is not directly obtained by collapsing the sectors it has immediately to the left of this table it is indicated with a *. For example, in Figure VII-21(b), at 6:50 the airspace delimited by sectors EDYYHMNS, EDYYHRHR and EDYYHSOL is reallocated to sectors EDYYH5MH, EDYYH5RH, EDYYH5SH, EDYYH5SL and EDYYH5WL. The * indicates that the sector EDYYHMNS is not divided directly to EDYYH5MH and EDYYH5RH and the sector EDYYHRHR is not divided directly to EDYYH5SH and EDYYH5SL.

Although, there is variability in terms of open sectors, in general, the Model II solution opens less sectors than the solution obtained in the baseline scenario. In fact, the cost of the open sectors with Model II is 122,260€, which contrasts with the 174,922€ of the baseline scenario (representing a 28.47% less). In both cases, baseline and Model II scenarios, the capacity management is done with no limits in the number of controllers and in consecutive configurations aiming at providing the best capacity management possible (independently on the operational feasibility of the opening scheme).

With respect to the demand side, the results are summarised in Table VII-7. The total ground delay obtained with the Hybrid method is 6,410 minutes, which represents a 77.34% less than the baseline scenario with CASA. The number of flights with ground delay is reduced by 58.32% with the Hybrid method. Since Model II has re-routing possibility, the arrival delay is different than the ground delay because the trip time of the used alternative trajectories is different. The total amount of arrival delay is lower (a 74.01% less) in the Hybrid solution which is translated into a cost of 595,339€. The number of flights with arrival delay is a 17.38% lower than in the baseline scenario.

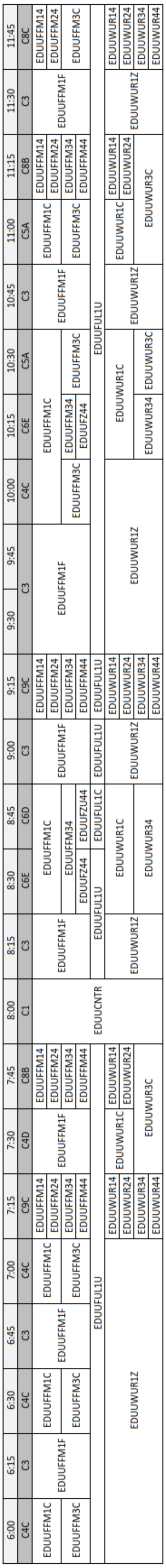

(a) Hybrid method

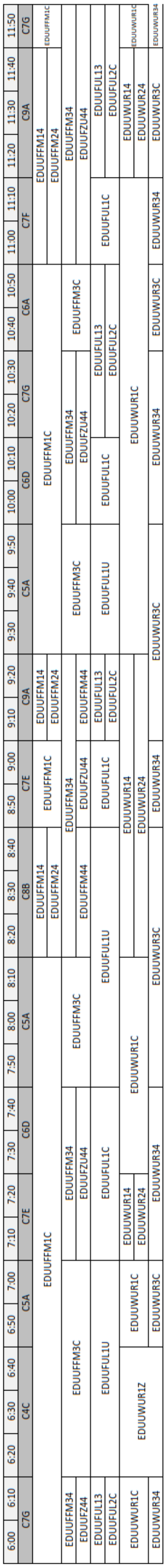

(b) ICO

Figure VII-15: *Sector opening schemes for EDUUTAC*

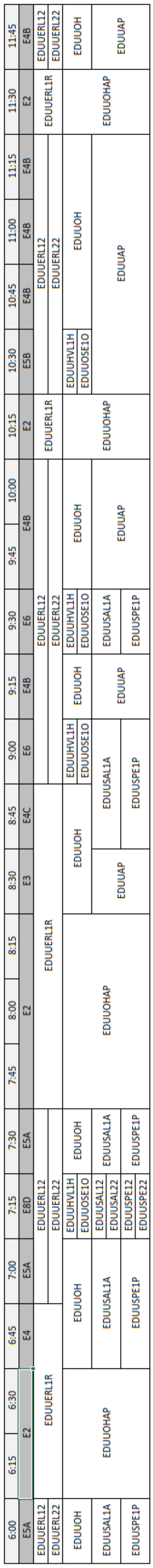

(a) Hybrid method

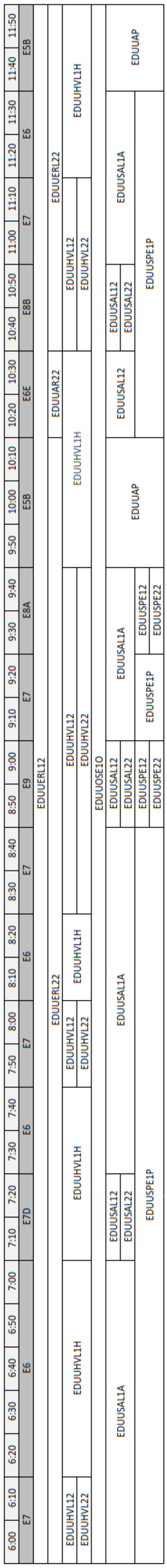

(b) ICO

Figure VII-16: *Sector opening schemes for EDUUTAE*

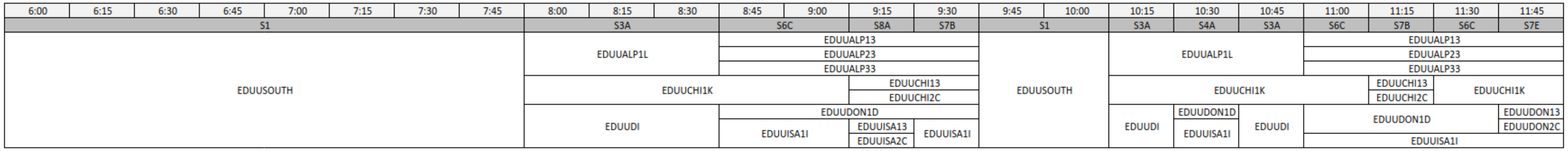

(a) Hybrid method

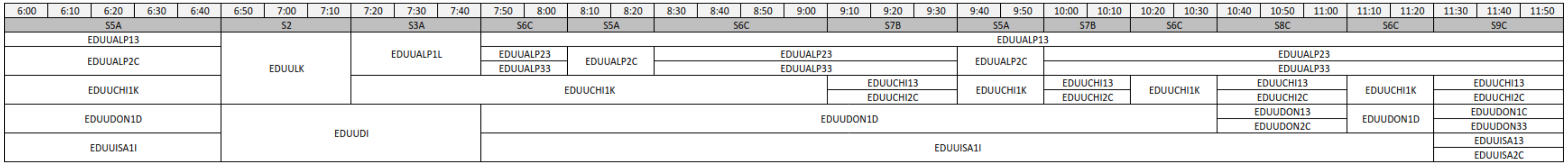

(b) ICO

Figure VII-17: *Sector opening schemes for EDUUTAS*

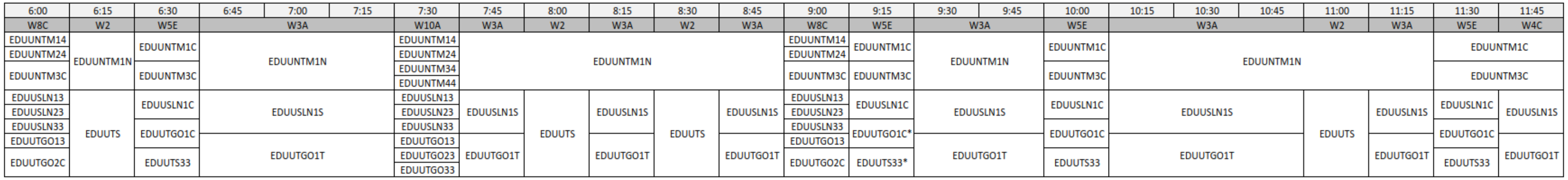

(a) Hybrid method

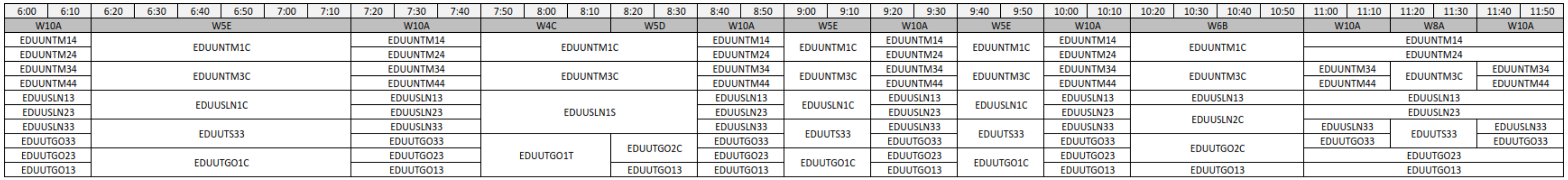

(b) ICO

Figure VII-18: *Sector opening schemes for EDUUTAW*

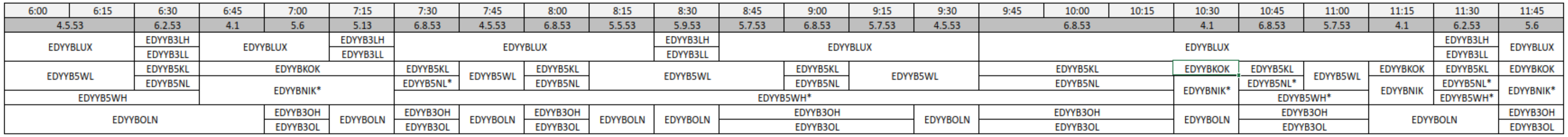

(a) Hybrid method

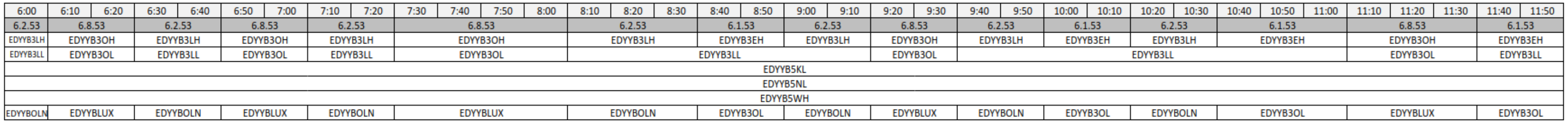

(b) ICO

Figure VII-19: *Sector opening schemes for EDYYBUTA*

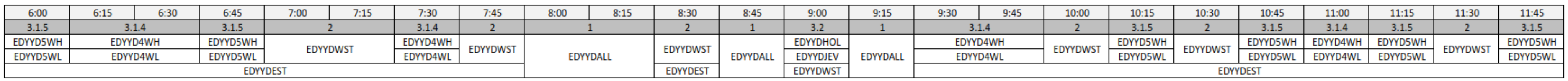

(a) Hybrid method

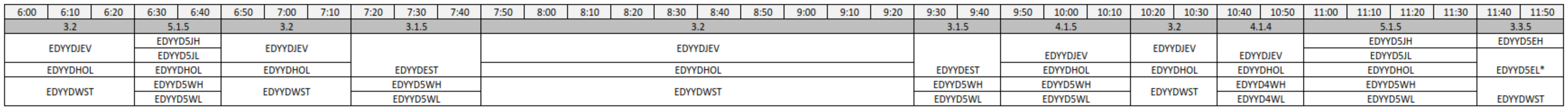

(b) ICO

Figure VII-20: *Sector opening schemes for EDYYDUTA*

6:00	3.2	EDYYHEST, EDYYHMNS, EDYYHRHR
6:15, 6:30	2	EDYYHEST, EDYYHWST
6:45	4.2.3	EDYYH3CL, EDYYH3EH, EDYYH3SL, EDYYHWST
7:00	4.1	EDYYHCEL, EDYYHSOL, EDYYHMNS, EDYYHRHR
7:15	2	EDYYHEST, EDYYHWST
7:30	4.9.5	EDYYH5EH, EDYYH5EL, EDYYHMNS, EDYYHRHR
7:45, 8:00	3.3.3	EDYYHEST, EDYYH3WH, EDYYH3WL
8:15	5.7.5	EDYYH5CH, EDYYH5CL, EDYYH5SL, EDYYH5SH, EDYYHWST
8:30	7.6.5	EDYYH5CH, EDYYH5EL, EDYYH5SH, EDYYH5MH, EDYYH5ML, EDYYH5RH, EDYYH5RL
8:45	4.9.3	EDYYH3EH, EDYYH3EL, EDYYHMNS, EDYYHRHR
9:00	4.8.5	EDYYH5CH, EDYYH5EL, EDYYH5SH, EDYYHWST
9:15, 9:30	5.6.5	EDYYH5EH, EDYYH5EL, EDYYH5RL, EDYYHMNS, EDYYH5RH
9:45	2	EDYYHEST, EDYYHWST
10:00	3.3.5	EDYYHEST, EDYYH5WH, EDYYH5WL
10:15	4.12.5	EDYYHEST, EDYYH5MH, EDYYH5RH, EDYYH5WL
10:30	5.5.5	EDYYH5CH, EDYYH5CL, EDYYHSOL, EDYYHMNS, EDYYHRHR
10:45	4.11.5	EDYYH5EH, EDYYH5EL, EDYYH5WH, EDYYH5WL
11:00	5.6.5	EDYYH5EH, EDYYH5EL, EDYYH5RL, EDYYHMNS, EDYYH5RH
11:15	5.16.3	EDYYHCEL, EDYYHSOL, EDYYH3MH, EDYYH3WL, EDYYH3RH
11:30	3.3.5	EDYYHEST, EDYYH5WH, EDYYH5WL
11:45	3.2	EDYYHEST, EDYYHMNS, EDYYHRHR

(a) Hybrid method

6:00, 6:10, 6:20	3.2	EDYYHMNS, EDYYHRHR, EDYYHEST
6:30, 6:40	4.1	EDYYHMNS, EDYYHRHR, EDYYHSOL, EDYYHCEL
6:50, 7:00	6.17.5	EDYYH5MH*, EDYYH5RH*, EDYYH5SH*, EDYYH5SL*, EDYYH5WL, EDYYHCEL
7:10, 7:20, 7:30	3.3.3	EDYYH3WH*, EDYYH3WL*, EDYYHEST*
7:40, 7:50	4.7.3	EDYYHMNS, EDYYH3RH, EDYYH3RL, EDYYHEST
8:00, 8:10	5.5.3	EDYYHMNS, EDYYH3CH*, EDYYH3CL*, EDYYHSOL*, EDYYHRHR*
8:20, 8:30	5.8.5	EDYYH5EH, EDYYH5EL, EDYYH5ML, EDYYH5RL, EDYYH5WH
8:40, 8:50	6.19.5	EDYYH5MH*, EDYYH5RH*, EDYYH5RL, EDYYH5ML, EDYYHSOL, EDYYHCEL
9:00, 9:10	6.13.3	EDYYHMNS, EDYYH3CH, EDYYH3EL, EDYYH3RH, EDYYH3RL, EDYYH3SH
9:20, 9:30	5.11.3	EDYYH3MH, EDYYH3ML*, EDYYHRHR, EDYYHCEL, EDYYHSOL
9:40, 9:50	4.1	EDYYHMNS, EDYYHRHR, EDYYHCEL, EDYYHSOL
10:00, 10:10	5.17.5	EDYYH5MH, EDYYH5RH, EDYYH5SH, EDYYH5SL, EDYYHEST
10:20, 10:30	6.20.5	EDYYH5MH, EDYYH5RH, EDYYH5EH, EDYYH5EL, EDYYH5ML*, EDYYH5RL*
10:40, 10:50, 11:00	6.13.3	EDYYHMNS, EDYYH3CH, EDYYH3EL, EDYYH3RH, EDYYH3RL, EDYYH3SH
11:10, 11:20, 11:30	4.9.5	EDYYHMNS, EDYYH5EH, EDYYH5EL, EDYYHRHR*
11:40, 11:50	3.2	EDYYHMNS, EDYYHEST, EDYYHRHR

(b) ICO

Figure VII-21: *Sector opening schemes for EDYYHUTA*

Table VII-7: *Summary of the results for the AUs*

		CASA	Model II	Δ
Cost	Total AUs regulation cost [€]	2,291,085	643,873	-71.90%
	Arrival delay cost [€]	2,291,085	595,339	-74.01%
	Δ Fuel cost [€]	0	20,074	-
	Δ Route charges cost [€]	0	26,569	-
	Δ Trip time cost [€]	0	1,891	-
Delay	Total ground delay [min]	28,282	6,410	-77.34%
	Delayed flights (ground)	1,154	481	-58.32%
	Total arrival delay [min]	28,282	7,350	-74,01%
	Delayed flights (arrival)	1,154	988	-14.38%
	Max. arrival delay [min]	71	35.3	-50.34%
	Average arrival delay [min]	25	7.4	-69.65%
	Median arrival delay [min]	20	5.3	-73.70%
	Std. Dev. arrival delay [min]	17.6	7.5	-57.27%
Trip data	Δ Fuel [Tn]	0	40	-
	Δ Trip time [min]	0	689	-
	Δ Distance [NM]	0	2,273	-
Traj. options	Nominal	2,992	2,059	-
	Lateral	0	423	-
	Vertical	0	510	-

The maximum value of arrival delay is 35.3 minutes which is lower than the value obtained with CASA. This is clearly represented in Figure VII-22 where the boxplot of the arrival delay for Model II is presented. In fact, the average arrival delay is 7.4 minutes (69.65% less) and the median is 5.3 minutes (73.70% less), being the standard deviation 7.5 (52.27% less).

Such reduction in the value of arrival delay is due to holistic optimisation of the demand and capacity sides together with the use of alternative trajectories. In addition, the use of complexity metric allows to solve the DCB imbalance by cherry peaking the trajectories that contribute the most to the imbalance and modify them accordingly. Indeed, 2,059 flights used their nominal or original trajectories (with or without delay), 423 flights used their lateral avoidance trajectories and 510 used their vertical avoidance trajectories. The use of alternative trajectories, however, incurs with additional costs due to the extra fuel burned, 20,074€; the extra route charges, 26,569€; and the extra trip time flown, 1,891€. The overall cost for the AUs of the solution provided by Hybrid method is 643,873€, what represents a 71.90% less than in the baseline scenario.

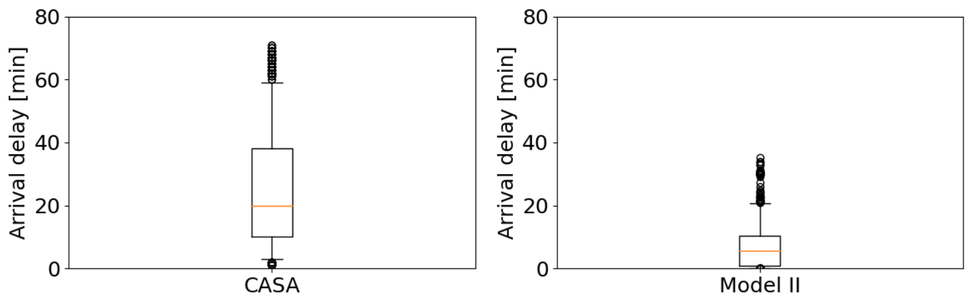

Figure VII-22: *Arrival delay boxplot with outliers*

Although the previous scenario has been solved with no penalty in consecutive configurations ($\rho = 0$) in order to be compared with the baseline scenario, other values of ρ may be con-

Table VII-8: *Summary of costs for different values of ρ (given in Eur per elementary sector change).*

		$\rho = 0$	$\rho = 15$	Δ
Cost	**Total AUs regulation cost [€]**	643,873	654,287	1.6%
	Arrival delay cost [€]	595,339	603,084	1.3%
	Δ Fuel cost [€]	20,074	21,601	7.6%
	Δ Route charges cost [€]	26,569	26,049	-2%
	Δ Trip time cost [€]	1,891	3,553	87.9%
Delay	**Total ground delay [min]**	6,410	6,460	0.8%
	Delayed flights (ground)	481	479	-0.4%
	Total arrival delay [min]	7,350	7,445	1.3%
	Delayed flights (arrival)	988	980	-0.8%
	Max. arrival delay [min]	35.3	120	239.9%
	Average arrival delay [min]	7.4	7.60	2.7%
	Median arrival delay [min]	5.3	6.18	16.6%
	Std. Dev. arrival delay [min]	7.5	8.24	9.9%
Trip data	**Δ Fuel [Tn]**	40	43	7.5%
	Δ Trip time [min]	689	706	2.5%
	Δ Distance [NM]	2,273	2,505	10.2%
Traj. options	**Nominal**	2,059	2,051	-0.4%
	Lateral	423	432	2.1%
	Vertical	510	509	-0.2%
ANSP costs	**Cost sectors**	122,260	126,688	3.6%
	Penalty	0	10,320	-

sidered in real operations, specially for avoiding fast changes of configurations. As an illustrative example, one repetition of the same scenario but with $\rho = 15$ € per elementary sector change has also been solved.

The summary of the results with $\rho = 0$ and $\rho = 15$ are given in Table VII-8. As concluded in Section VII.4, the opening schemes obtained with $\rho = 0$ are the best adapted to the demand needs and this is why the cost for the AUs is higher with $\rho = 15$. The maximum arrival delay increases considerably from 35.3 to 120 minutes, but such big differences are explained due to the discretisation of the delay (recall that only 10, 20, 30 ans 120 minutes were given as delay options).

VII.5.4 Discussion on the obtained results

The Hybrid method has demonstrated its capability for solving a scenario significantly big in terms of time and geographical area covered. The resolution time, however, was 30 hours and, although it is sufficient for addressing scenarios in the pre-tactical phase, further research may be done in order to speed up the algorithm (specially if bigger scenarios are considered). One possible option could be the parallelisation of the Hybrid method algorithm. With the current version of the method, the dynamic programming part (which deals with the capacity management) is executed in parallel, but the overall simulated annealing algorithm run sequentially. Although the simulated annealing algorithm is not amenable to be computed in parallel, some parts may be re-considered.

Analysing the outcomes, the results obtained with Model II are significantly better than the results of the baseline scenario and even better solutions may be obtained with more granularity in the delay discretisation.

The baseline scenario represents the best one can do with the current system, i.e. optimisation of the opening scheme (with unlimited ATC resources) and allocation of delay in the regulated periods/areas using entry counts. Note that the baseline scenario is facing remaining overloads even when the DCB process is finished.

On the contrary, the scenario with Model II maintains the demand below the capacity (measured with complexity metric) in all open sectors and times. The use of complexity metrics makes that not all flights contributes in the same way to the traffic demand. Hence, when a hotspot is detected it can be solved by modifying the flight or flights (if needed) that contribute the most (cherry picking). Furthermore, the consideration of the demand and capacity management together in the same problem allows a better use of the resources. Moreover, the use of alternative trajectories gives flexibility in the traffic demand management that helps to reduce significantly the amount of allocated delay.

Hence, the results show that the concept of operations proposed in this PhD and the Model II improves considerably the current system, even when it is optimised with no ATC limitations.

In real operations, however, the value of ρ might be different than 0 in order to avoid fast changes of configuration. The use of expert judgement would be required in order to establish the adequate value of ρ for each ACC.

VIII

Concluding Remarks

The recovery of the air traffic demand to values close to before the COVID-19 pandemic requires the improvement of the Air Traffic Flow and Capacity Management (ATFCM) models and methodologies in order to protect the Air Traffic Management (ATM) systems from overloaded situations.

The current ATFCM processes deploy the capacity management initiatives and the demand management measures independently, leading to airspace sectorisations that may be not optimal after the demand management initiatives are deployed. Moreover, the demand and capacity are evaluated using entry counts as proxy of the Air Traffic Control (ATC) workload. This metric, however, does not properly evaluate the harmonisation of the traffic and the difficulty to control certain traffic patterns, what leads to capacity buffers. In addition, the demand management initiatives are based on delay allocation with a limited flexibility for the Airspace Users (AUs). This PhD aimed at addressing the limitations of the current system by studying the introduction of complexity metrics in order to evaluate the demand and the capacity in the ATFCM processes, the holistic integration of the demand and capacity management into the same optimisation problem and the use of alternative re-route options in order to give more flexibility to the AUs.

During the execution of this PhD, some questions were raised and were evaluated; some of these questions remain unsolved and might be the subject of future research.

VIII.1 Summary of conclusions and contributions

The following lines contain the main conclusions achieved in this PhD, along with a brief summary of the principal scientific contributions:

- The integration of the Dynamic Airspace Configurations (DAC) and Flight Centric Air Traffic Control (FCA) capacity management solutions, while using complexity metrics, was studied in Chapter III. A novel delineation method to identify when/where DAC and FCA shall be applied was also presented. Results showed that the integration of DAC and FCA has benefits in the cost-effectiveness area when the dynamic integration is proposed. The static integration of DAC/FCA is penalised by the the lack of a trajectory reallocation mechanism in the FCA algorithm leading to a big increase of underloads and consequently need of more controller hours.

- A new concept of operations was presented in Chapter IV where the Network Manager (NM) and the Air Navigation Service Providers (ANSPs) functions are integrated into the same optimisation problem and the AUs are involved into the ATFCM process with the possibility of submitting re-route options. This concept of operations represents a significant paradigm shift since the NM takes part of the current ANSP functions and it responsible for the airspace sectorisation (capacity management) and for the allocation of delay and choice of the final trajectory used (demand management).

- Two Demand and Capacity Balancing (DCB) models dealing with demand management were detailed in Chapter V. The Model 0 uses entry counts at Traffic Volume (TV) level as a first attempt to consider the ATC workload. The use of TVs allows to regulate particular traffic flows instead of deploying a regulation to the full sector. The Model I is an evolution and considers a generic complexity metric instead of entry counts. The linear formulation of two models was also provided. A 24h scenario over the full ECAC area was analysed with Model 0 and compared with the current system. Results showed that the introduction of alternative trajectories as a demand measure together with the optimisation of the delay allocation could reduce the total amount of ground delay by a 78.19% and the total cost of the regulations was reduced by 76.20% proving that the model presented has enormous advantages in terms of delay and cost with respect to the current system. Significant big values of remaining overloads were identified after the regulations with the current system and with Model 0, what highlights that entry counts are not a good proxy of ATC complexity.

- Three additional DCB models dealing with the holistic demand and capacity management using complexity metrics are provided in Chapter VI. The diference between the models is the level of capacity management allowed. A simple verification is provided in Annex B in order to complement the definition of the models and verify their formulations.

- A new Hybrid method, which combines Simulated annealing with Dynamic programming, was proposed in Chapter VII in order to address the Model II (optimisation of the opening scheme given a set of available configurations). A performance assessment was done in order to benchmark the Hybrid method and the exact method using Gurobi. The Hybrid method performed better with scenarios with medium and high difficulty, where Gurobi could not find the optimum solution. Moreover, the Branch and Bound (B&B) was more sensitive against the scenario duration in comparison with the Hybrid method. Moreover, a sensitivity study of the parameter that models the penalty for different consecutive configurations was assessed. Low values of such parameter provided sector opening schemes better adapted to the traffic demand while high values of such parameters were translated to static sectorisations. Finally, a 6h scenario over the upper airspace of Germany is analysed with Model II and compared with a baseline scenario, which reflects the best that can be achieved with the current system based on entry counts. The resulting opening schemes were a 28.47% cheaper and the resulting cost for the AUs was a 71.90% lower proving the advantages of the proposed Model II.

VIII.2 Future work

New questions and areas of research have been identified during the realisation of this PhD. Considering the presented contributions and, in line with the scope and limitations of the PhD, some future work is proposed:

- The lack of reallocation mechanism in the used FCA algorithm leaded to a big amount of underloads. Hence, the inclusion of this mechanism should be considered in future research.
- The maximum complexity or threshold that an ATC controller can accept safely requires further research. Some human-in-the-loop experiments should be done with trained controllers in order to collect feedback and define a consolidated threshold.
- The models presented in this PhD may have fairness issues. In future work, the models require improvements in order to protect the DCB solution against equity imbalances.
- Uncertainty factors should be considered in order to propose models and methods more robust.
- A Hybrid resolution method was proposed for Model II. Further research is required for proposing resolution methods for Models III and IV.
- The computation performance of the Hybrid method requires further improvements. Although the Simulated annealing algorithm works sequentially by definition, some parts of the algorithm may be computed in parallel.
- The proposed formulation for Model IV does not guaranty the operational feasibility of the resulting sector shapes (see Annex B). Further research is required in the formulation in order to avoid isolated sectors.

A

Illustrative example of complexity aggregation at sector level

A simple illustrative example (see Figure A-1) is provided in order to facilitate the comprehension of the process of calculation of the complexity at sector level from the complexity at trajectory level. This example refers to only one instant of time t_1. An hypothetical airspace is divided in four elementary sectors (s_{E1}, s_{E2}, s_{E3}, s_{E4}), which can be collapsed into two operating sectors (s_1 and s_2). This grouping is provided through the set $\mathcal{E}^s$. For this particular example, the set $\mathcal{E}^s$ is defined as: $\mathcal{E}^{s_1} = [s_{\mathrm{E1}}, s_{\mathrm{E2}}]$ and $\mathcal{E}^{s_2} = [s_{\mathrm{E3}}, s_{\mathrm{E4}}]$.

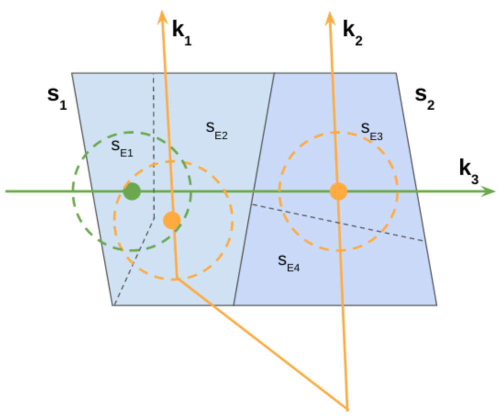

Figure A-1: *Illustrative example of complexity calculation at sector level.*

Furthermore, there are two flights, f_1 and f_2; and f_1 has also two alternative trajectories, i.e.

Table A-1: *Complexity per pairs of trajectory for the illustrative example of Fig. A-1*

Receiver (k)	**Generator (k′)**	$\mathbf{C^{t_1}_{k,k'}}$
k_1	k_3	1
k_2	k_3	0
k_3	k_1	1
k_3	k_2	0

Table A-2: *Complexity at trajectory level and at sector level for the illustrative example of Fig. A-1*

Sector (s)	**Receiver (k)**	$\mathbf{C_{T_k}^{t_1,s}}$		$\mathbf{C_S^{t_1,s}}$	
		$z_{k_1}=1$, $z_{k_2}=0$	$z_{k_1}=0$, $z_{k_2}=1$	$z_{k_1}=1$, $z_{k_2}=0$	$z_{k_1}=0$, $z_{k_2}=1$
s_1	k_1	1	0	2	0
	k_2	0	0		
	k_3	1	0		
s_2	k_1	0	0	0	0
	$k2$	0	0		
	k_3	0	0		

k_1 and k_2, while f_2 has only the trajectory k_3. Recall that the pairwise complexity is precomputed for all possible combinations of flights and their alternative trajectories regardless if the trajectories are finally retained by the DCB algorithm or not.

In this example, a very simple complexity metric is used for illustrative purposes only: a value of 1 will be given if two aircraft are *close* to each other and 0 if not. These values are summarised in Table A-1, while Figure A-1 shows with a small circle the position of each aircraft and with a dotted circle what is considered the "vicinity" environment of each aircraft.

The complexity $C_{T_k}^{t,s}$ associated to trajectory k in sector s and at time t_1 depends on whether trajectory k is inside sector s at time t, but also on which trajectory is finally used (and it is reflected through variables z_k and $z_{k'}$):

$$C_{T_k}^{t,s} = \sum_{s_E \in \mathcal{E}^s} B_k^{t,s_E} \sum_{k' \in \mathcal{K} \setminus \{k\}} C^t_{k,k'} z_{k'} z_k, \quad \forall k \in \mathcal{K}, \forall t \in \mathcal{T}, \forall s \in \mathcal{S}. \tag{A.1}$$

In this example there are only two options: either trajectory k_1 or trajectory k_2 can be selected. Trajectory k_3 is going to be always selected since there is only one possible trajectory for flight f_2. Table A-2 provides the values of $C_{T_k}^{t,s}$ when trajectory k_1 is used (z_{k_1} = 1) and when trajectory k_2 is used (z_{k_2} = 1).

With these values it is easy to obtain the complexity at sector level $C_S^{t,s}$ using the following equation:

$$C_S^{t,s} = \sum_{k \in \mathcal{K}} C_{T_k}^{t,s}, \quad \forall t \in \mathcal{T}, \forall s \in \mathcal{S}. \tag{A.2}$$

When trajectory k_1 is used (z_{k_1} = 1) the complexity of sector s_1 is 2 and the complexity of sector s_2 is 0. On the other hand, when trajectory k_1 is selected (z_{k_1} = 1), the complexity is zero in all sectors. These results are summarised in Table A-2.

B

Simple verification example

For the sake of illustration and to verify the proposed models, a simple example is presented and solved in this appendix. The models are solved using an Intel(R) Xeon(R) CPU X5355 @ 2.66GHz using 4 cores (8 threads). The solver used is Gurobi 9.1.1.

B.1 Scenario setup

The example comprises 4 flights, each having two different trajectory options, flying in an airspace defined by 25 elementary sectors during 5 different periods of time and the period duration is 1 instant of time t. This example is illustrated in Figure B-1, where the flights, f_1, f_2, f_3 and f_4, and their trajectory options, k_1, k_2, k_3, k_4, k_5, k_6, k_7 and k_8, are coloured in green, yellow, blue and red, respectively. Hence, the trajectories are linked with the flights as follows:

$$\begin{aligned}\mathcal{K}_{f_1} &= \{k_1, k_2\}\\ \mathcal{K}_{f_2} &= \{k_3, k_4\}\\ \mathcal{K}_{f_3} &= \{k_5, k_6\}\\ \mathcal{K}_{f_4} &= \{k_7, k_8\}\end{aligned} \tag{B.1}$$

where the initial and preferred trajectories by the AUs are k_1, k_3, k_5 and k_7, since the choice of k_2, k_4, k_6 and k_8, inquire an assumed extra cost of 250€ for them. All trajectories follow a straight line and are flown at constant speed, such that they change one elementary sector every time period (the trajectory evolution is shown in Figure B-1).

In this example, a simple complexity metric is used for illustrative purposes. The complexity that trajectory k' generates on trajectory k at time t, $C^t_{k,k'}$, takes the value of 1 when trajectories

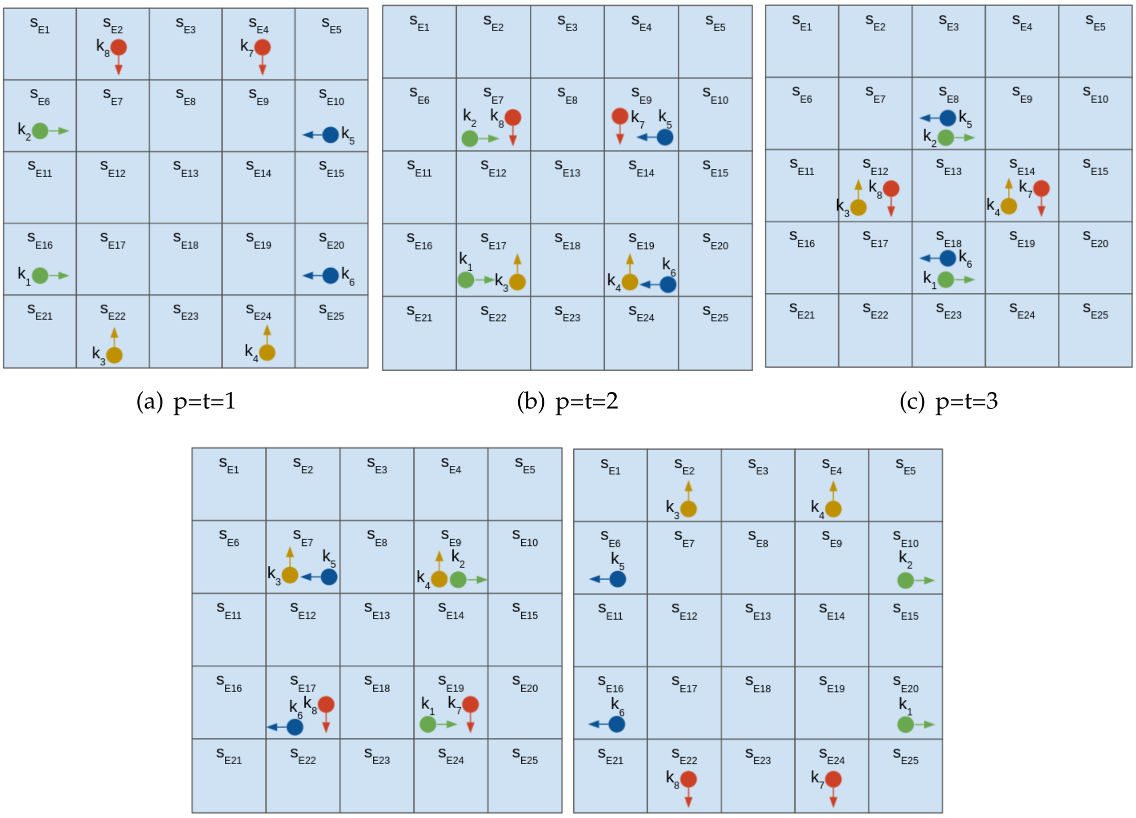

(d) p=t=4 (e) p=t=5

Figure B-1: *Evolution of trajectories.*

k and k' are in the same elementary sector and 0 in all other cases. Hence, in the case where one operating sector s contains an elementary sector with two trajectories inside (k and k'), the complexity at trajectory level, $C_{\mathrm{T}_k}^{t,s}$ and $C_{\mathrm{T}_{k'}}^{t,s}$, will take the value of 1 and, as a consequence, the complexity at sector level, $C_{\mathrm{S}}^{t,s}$, will be 2.

Figure B-2 shows how the airspace can be organised in configurations, operating sectors and elementary sectors. The airspace elements known at the beginning of the problem depend on the model assessed and they will be indicated in the corresponding sections below.

With this initial setup, the solution of this problem is provided considering different levels of capacity management.

B.2 Model I: Fixed sectorisation

In this case, the model considers a given capacity of the airspace system with a fixed sectorisation as shown in Figure B-2(b). The same two sectors will be open during all 5 time periods of the example.

In a first study, the sector complexity threshold is fixed at 2, which means that in an operating sector, only two trajectories can be in the same elementary sector. The problem is solved in $1.74 \cdot 10^{-2}$ seconds and the chosen trajectories are: k_1, k_3, k_5 and k_7. Note that they are the initial trajectories and the resulting extra cost is 0. The sector complexity is 2 in both sectors at times 2 and 4, and 0 otherwise.

In a second study, the sector complexity threshold is set at 1, which means that only one tra-

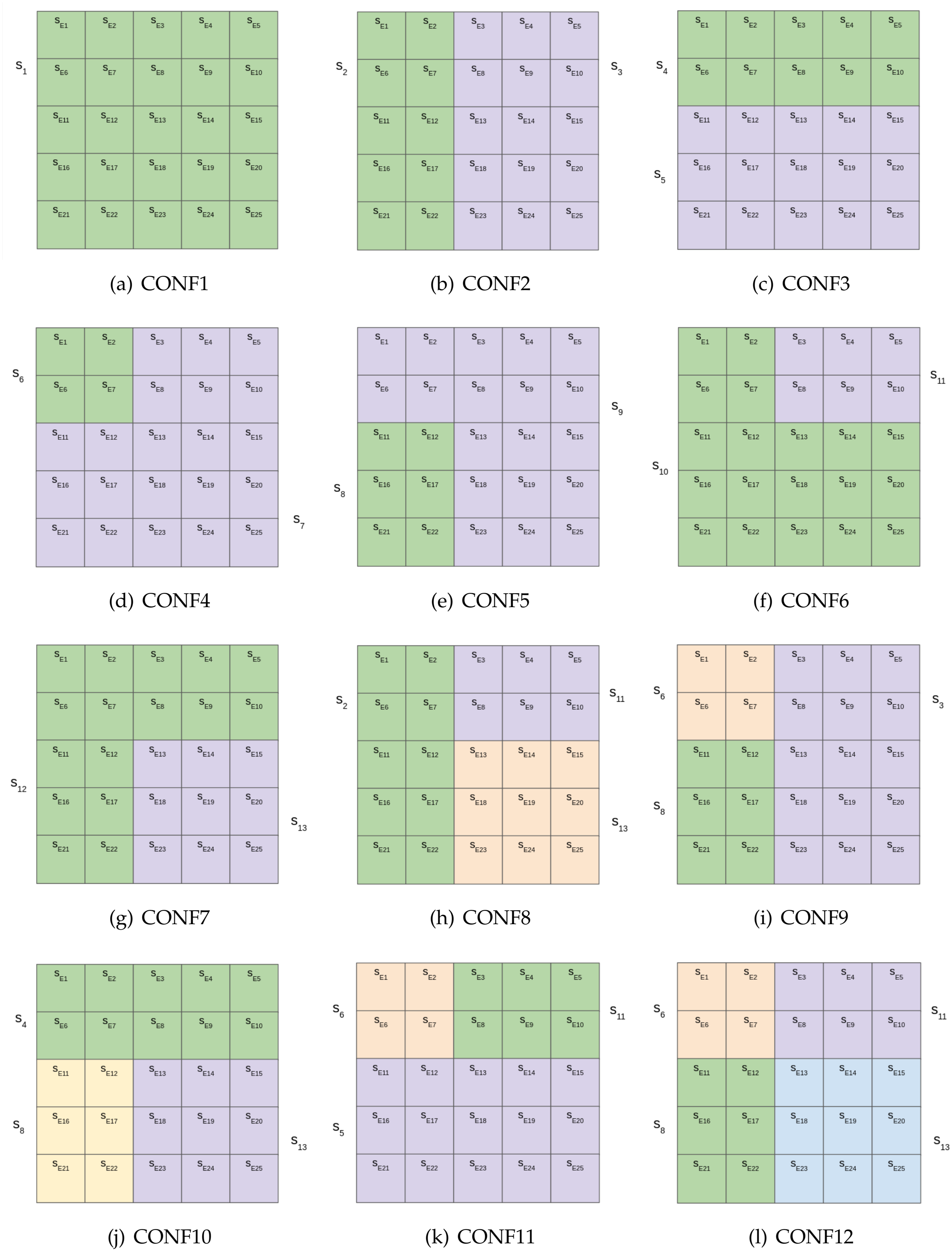

(a) CONF1 (b) CONF2 (c) CONF3

(d) CONF4 (e) CONF5 (f) CONF6

(g) CONF7 (h) CONF8 (i) CONF9

(j) CONF10 (k) CONF11 (l) CONF12

Figure B-2: *Set of configurations and sectors.*

jectory is allowed to be in one elementary sector. This subscenario is designed aiming at pushing the solver to choose some of the alternative trajectories. The problem is solved in $1.29 \cdot 10^{-2}$ seconds by choosing trajectories k_2, k_3, k_6 and k_7. This represents and extra (total) cost of 500€ (250€ for each chosen alternative) but ensures that the sector complexity is 0 in all time periods.

B.3 Model II: Selection of the best configuration opening scheme

Differently than Model I, the Model II includes the capacity management into the optimisation problem. As described in Section VI.1, the problem consists on selecting one trajectory for every flight and on choosing the sectorisation opening scheme given a set of available configurations. Figure B-2 shows the set of 12 configurations (given from B-2(a) to B-2(l)), available in model II.

A first subscenario is performed considering a sector complexity threshold of 2. Recall that in addition to trajectory cost, now the cost of opening sectors and the penalty cost for having different consecutive configurations are considered in the objective function. The cost of opening one sector during one time period, $\theta^{p,s}$, is set to 100€ for all sectors and time periods. The penalty cost of allocating one elementary sector to a different operating sector in two consecutive time periods, ρ, is set to 10€.

The problem is solved in $7.93 \cdot 10^{-2}$ seconds by choosing CONF1 (only one sector) during all time periods and trajectories k_1, k_3, k_6 and k_7. Note that flight f_3 takes its alternative trajectory k_6 instead of the initial k_5. This represents an extra cost of 250€ but guarantees a sector complexity of 2 at time periods 2, 3 and 4. The sector complexity is 0 in the first and last periods considered. The cost of open sectors is 500€ due to the fact that only 1 sector is open during 5 time periods.

Although opening two sectors in periods 2 and 4 (extra cost of 200€) would be enough to select the initial trajectories k_1, k_3, k_5 and k_7 and to maintain the complexity below the threshold, the introduction of the penalty cost for configuration changes makes this solution more expensive than choosing an alternative trajectory k_6 and keeping only one sector opened during all time.

For the sake of illustration, another subscenario is defined where the penalty cost is set to zero ($\rho = 0$). The solution is found in $2.92 \cdot 10^{-2}$ seconds by choosing trajectories k_1, k_3, k_5 and k_7 (no extra cost for AUs), and CONF1 (1 sector) in periods 1, 3 and 5 and CONF2 (2 sectors) in periods 2 and 4. The overall cost of the solution is 700€ basically due to the sectors opened.

B.4 Model III: Dynamic configurations

The Model III considers the capacity management by choosing among a set of operating sectors. The 13 available operating sectors are represented with different colours in Figures B-2(a)-B-2(g) (the ones used to create CONF1-CONF7).

The penalty cost of allocating one elementary sector to a different operational sector, ρ, is set to 10€; and the cost of opening one sector during one time period, $\theta^{p,s}$, is set to 100€ for all sectors and time periods. The sector complexity threshold remains at 2.

The problem is solved in $8 \cdot 10^{-2}$ seconds by choosing trajectories k_1, k_3, k_6 and k_7; and the operating sector s_1 during all time periods. It is worth noting that this solution is the same obtained in the previous model where CONF1 was chosen for all times. Since all configurations used in the previous model were defined with the same operating sectors used in Model III, it is then expected to obtain the same result.

In order to fully compare the results obtained with the previous model, a new subscenario is provided by neglecting the penalty cost ρ. The problem is solved in $3 \cdot^{-2}$ seconds choosing trajectories k_1, k_3, k_5 and k_7 with no extra cost for AUs. The opened sectors are s_1 for time periods 1, 3 and 5; and s_4 and s_5 for time periods 2 and 4. This is particularly interesting, because s_4 and s_5 correspond to CONF3 (instead of CONF2 chosen in model II). Nevertheless, these solutions are equivalent since both configurations have two sectors and therefore the same opening cost.

B.5 Model IV

In Model IV, the problem consists of selecting one trajectory for every flight and dynamically collapsing the available elementary sectors.

As done previously, the cost of opening one sector during one time period, $\theta^{p,s}$, is set to 100€ for all sectors and time periods, the penalty cost of allocating one elementary sector to a different operating sector, ρ, is set to 10€, and the sector complexity threshold is 2. The problem is solved in 10.1982 seconds what represents a significant increase in comparison with previous models resolution time . The solution selects trajectories k_2, k_3, k_5 and k_7, which represent an extra cost for the AUs of 250€. With respect to the capacity side, i.e. chosen sectorisation, only one sector is open during all time periods with a cost of 500€, that is in correspondence to solutions of model II and III.

As done with the previous models, an additional subscenario is provided ignoring the penalty cost, ρ, in order to compare the findings. The problem is solved in 2.07 seconds and the solution selects the trajectories k_1, k_3, k_5 and k_7 what represents a null extra cost for the AUs. The chosen sectorisation is illustrated in Figure B-3.

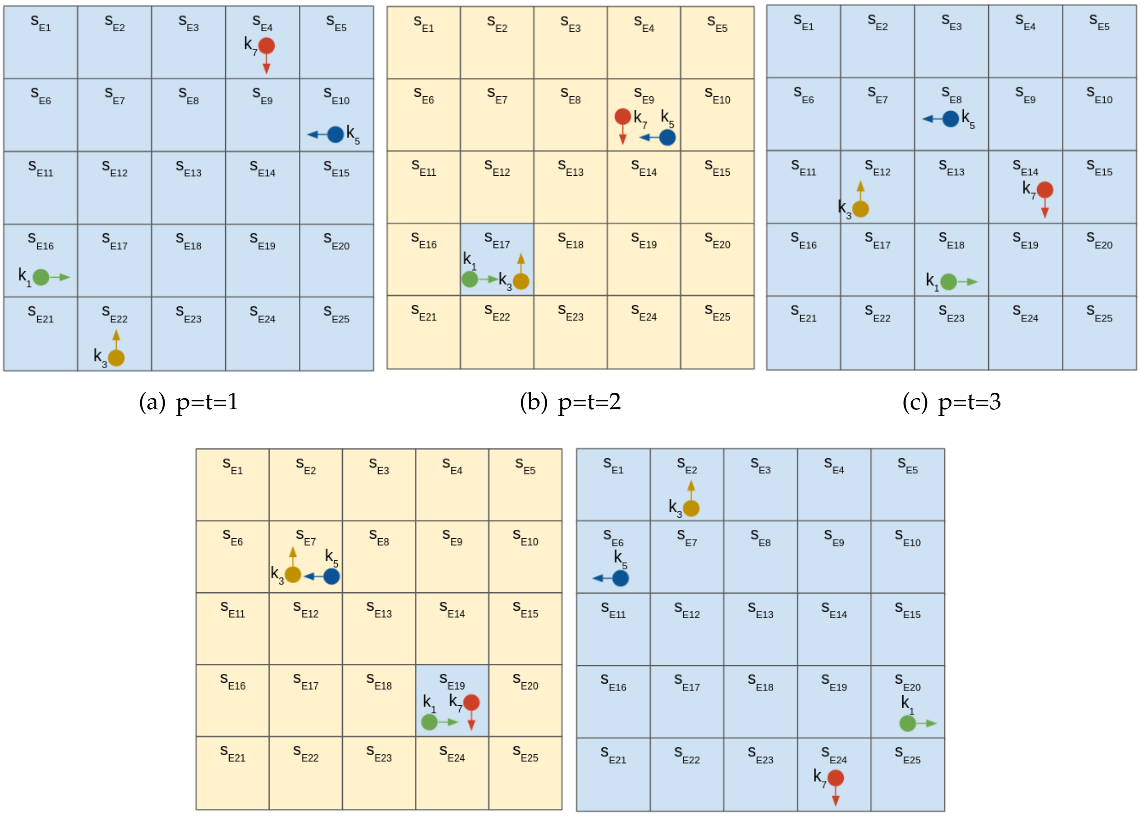

(a) p=t=1 (b) p=t=2 (c) p=t=3

(d) p=t=4 (e) p=t=5

Figure B-3: *Solution for model IV.*

The cost of opening sectors is 700€ since there is one opened sector in periods 1, 3 and 5, but there are two open sectors in periods 2 and 4. Note that the demand is below the capacity (in complexity) since s_{E9} and s_{E17} are part of different operating sectors in time 2 and s_{E7} and s_{E19} belong to different operating sectors in time 4.

As acknowledged, this model formulation does not have a direct control of the operational feasibility of the resulting sectorisation. This can be observed at periods 2 and 4, where s_{E17} and s_{E19} are operating as isolated sectors and are fully surrounded by a single operating sector (the second one). Based on the current operational standards this is not an operationally feasible sectorisation. Nevertheless, those isolated sectors are surrounded by empty elementary sectors that have complexity equal to zero, that explains such "strange" groupings. In real situations with traffic demand (trajectories) spread in the airspace, it would be less probable to get such solutions. With some post-processing, however, it would be easy to obtain a mathematically equivalent solution (same sector complexity, same number of sectors) for periods 2 and 4 as shown in Figure B-4.

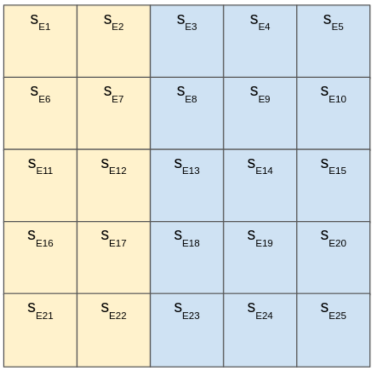

Figure B-4: *Equivalent configuration for configurations not operationaly feasible.*

Bibliography

Abdul Rahman, Siti Mariam, Borst, Clark, Mulder, Max, & Van Paassen, Marinus M. 2012. *Measuring sector complexity: Solution space-based method*. Pages 11–34. 15

Airbus. 1998. *Airbus Flight Operations Support & Line Assistance*. Tech. rept. Blagnac, France. 53

Airline Business. 2016. *Reed Business Information, Colchester*. Tech. rept. ISSN 0268-7615. 53

Andreatta, Giovanni, Odoni, Amedeo R., & Richetta, Octavio. 1993. Models for the ground holding problem. *Pages 125–168 of:* Bianco, Lucio, & Odoni, Amedeo R. (eds), *Large scale computation and information processing in air traffic control*. Berlin, Heidelberg: Springer Berlin Heidelberg. 12, 51

Ball, Michael O, Hoffman, Robert, Lovell, David, & Mukherjee, Avijit. 2005. Response mechanisms for dynamic air traffic flow management. *In: Proceedings of the 6th USA/Europe ATM R&D Seminar*. 4, 11

Barnhart, Cynthia, Bertsimas, Dimitris, Caramanis, Constantine, & Fearing, Douglas. 2012. Equitable and efficient coordination in traffic flow management. *Transportation science*, **46**(05). 42

Bellman, Richard. 1957. *Dynamic programming*. Princeton, New Jersey: Princeton University press. 18

Bellman, Richard, & Dreyfus, Stuart. 1962. *Applied dynamic programming*. Princeton University Press. 18

Bertsekas, Dimitri. 1995. *Dynamic programming and optimal control*. Vol. 1. 18

Bertsimas, Dimitris, & Gupta, Shubham. 2016. Fairness and collaboration in network air traffic flow management: An optimization approach. *Transportation science*, **50**(1), 57–76. 42

Bertsimas, Dimitris, & Patterson, Sarah. 2000. The traffic flow management rerouting problem in air traffic control: A dynamic network flow approach. *Transportation science*, **34**(08), 239–255. 12, 52

Bertsimas, Dimitris, & Patterson, Sarah Stock. 1998. The air traffic flow management problem with enroute capacities. *Operations research*, **46**(3), 406–422. 12, 48, 49, 52

Brinton, C., Atkins, S., Cook, L., Lent, S., & Prevost, T. 2010 (May). Ration by schedule for airport arrival and departure planning and scheduling. *Pages I3–1–I3–9 of: 2010 integrated communications, navigation, and surveillance conference proceedings*. 3, 4, 11

CADENZA Consortium. 2021. *D2.1-Initial TB concept and ADCB options*. Tech. rept. 53

CAÑAS, JOSÉ JUAN, FERREIRA, PEDRO, PUNTERO, EVA, LÓPEZ, PATRICIAL, LÓPEZ, ELENA, & GÓMEZ, FERNANDO. 2017 (September 26-29). An air traffic controller psychological model with automation. *In: 37th easn international conference*. 14

CAPIOT, KEVIN, MARTINS, ANA, & WEBER, MARA. 2022 (Dec). Performance review of non-nominal scenarios in a validation exercise of the flight centric air traffic control concept. *In: Proceedings of the 12th sesar innovation days (sids)*. 35

CHEN, YANGZHOU, BI, HONG, DEFU, ZHANG, & SONG, ZHUOXI. 2013. Dynamic airspace sectorization via improved genetic algorithm. *Journal of modern transportation*, **21**(06). 12

COOK, ANDREW J, & TANNER, GRAHAM. 2015. *European airline delay cost reference values: Updated and extended values*. Tech. rept. 10, 53

COTTON CONSORTIUM. 2018a. *D2.1 - Impact of trajectory's uncertainty in existing complexity methodologies*. Tech. rept. 5

COTTON CONSORTIUM. 2018b. *D2.2 - Innovative complexity and workload assessment to support future Capacity Management processes in TBO*. Tech. rept. 5

COTTON CONSORTIUM. 2019. *D4.2 - Validation Report*. Tech. rept. 29

DALMAU, RAMON, MELGOSA, MARC, VILARDAGA, SANTI, & PRATS, XAVIER. 2018. A fast and flexible aircraft trajectory predictor and optimiser for ATM research applications. *In: Proceedings of the 8th international congress on research in air transportation (ICRAT)*. Castelldefels, Spain: Eurocontrol and FAA. 78

DELAHAYE, D., & PUECHMOREL, S. 2000 (June 13-16). Air traffic complexity: towards intrinsic metrics. *In: 3rd usa/europe air traffic management research and development seminar*. 16, 25, 80

DELAHAYE, DANIEL, & PUECHMOREL, STÉPHANE. 2015 (Apr). Air traffic complexity versus control workload. *In: Eurognc, european aerospace guidance, navigation and control conference*. 16

DELAHAYE, DANIEL, ALLIOT, JEAN-MARC, SCHOENAUER, MARC, & FARGES, J.L. 1995. Genetic Algorithms for Automatic Regroupment of Air Traffic Control Sector. *In: Proceeding of the 4th Annual Conference on Evolutionary Programming*. 12, 13, 66

DELAHAYE, DANIEL, SCHOENAUER, MARC, & ALLIOT, JEAN-MARC. 1998 (May). Airspace sectoring by evolutionary computation. *Pages pp 218 – 223 of: IEEE 1998, International Conference on Evolutionary Computation*. 12

DELAHAYE, DANIEL, PUECHMOREL, STEPHANE, HANSMAN, R., & HISTON, JONATHAN. 2003 (Jun). Air traffic complexity based on non linear dynamical systems. *In: 5th usa/europe air traffic management research and development seminar*. 16

DELAHAYE, DANIEL, CHAIMATANAN, SUPATCHA, & MONGEAU, MARCEL. 2019. Simulated annealing: From basics to applications. *Pages 1–35.ISBN 978–3–319–91085–7 of:* GENDREAU, MICHEL, & POTVIN, JEAN-YVES (eds), *Handbook of Metaheuristics*. International Series in Operations Research & Management Science (ISOR), vol. 272. Springer. 77

DELGADO, LUIS. 2015. European route choice determinants. *In: Proceedings of the 11th usa/europe air traffic management research and development seminar*. 5

D'ENGELBRONNER, JURRIAAN, BORST, CLARK, ELLERBROEK, JOOST, VAN PAASSEN, MARINUS M., & MULDER, MAX. 2015. Solution-space-based analysis of dynamic air traffic controller workload. *Journal of aircraft*, 04. 15

EUROCONTROL. *Phare - back to the future*. *https://www.eurocontrol.int/phare/*. Accessed: 11-02-2023. 14

EUROCONTROL. 2014. *ATFCM operating procedures for flow management position, Edition N°: 18.1.1*. Tech. rept. 2

EUROCONTROL. 2017. *ATFCM operations manual - network operations handbook*. Tech. rept. Ed. 21.0. 1, 3, 4, 11, 51

EUROCONTROL. 2018 (May). *Performance review report*. Tech. rept. 1

EUROCONTROL. 2019. *Rad - route availability document*. *https://ansperformance.eu/acronym/rad/*. Accessed: 08-07-2019. 5

EUROCONTROL. 2020a (June). *Performance review report*. Tech. rept. 1

EUROCONTROL. 2020b. *RNEST: Powerful modelling and analysis tool for ecac-wide performance assessment*. *https://simulations.eurocontrol.int/solutions/rnest-powerful-modelling-and-analysis-tool-for-ecac-wide-performance-assessment/*. Accessed: 13-02-2020. 29

EUROCONTROL. 2022. *Forecast update 2022-2028. european flight movements and service units. after covid-19, russian invasion of ucraine and europe's energy crisis*. Tech. rept. 1

FAA. 2009. *Traffic Flow Management in the National Airspace System*. Tech. rept. FAA-2009-AJN-251. Federal Aviation Administration. 4

FAA. 2014. *Collaborative Trajectory Options Program (CTOP): Document Information.* Tech. rept. AC 90-115. Federal Aviation Administration. 4, 12

FERREIRA, PEDRO, AÑAS, JOSÉ JUAN, NETJASOV, FEDJA, MIRKOVIC, BOJANA, PUNTERO, EVA, RODRIGUEZ, SARA, CRESCENZIO, FRANCESCA DE, & COMENDADOR, FERNANDO. 2017 (May 24-26). Understanding the impacts of enhanced automation in future atm. *In: Framily*. 14

FISCHETTI, MATTEO, TOTH, PAOLO, & VIGO, DANIEL. 1994. A branch-and-bound algorithm for the capacitated vehicle routing. problem on directed graphs. *Operations research*, **42**(5), 846–859. 18

GIANAZZA, DAVID. 2010. Forecasting workload and airspace configuration with neural networks and tree search methods. *Artificial intelligence*, **174**(7), 530 – 549. 12, 13, 64

GIANAZZA, DAVID. 2019 (June). Optimizing Successive Airspace Configurations with a Sequential A * Algorithm. *In: ATM 2019, 13th USA/Europe Air Traffic Management Research and Development Seminar*. ATM Seminar 2019. 12, 13, 64

GIANAZZA, DAVID, & DURAND, NICOLAS. 2020. Ant Colony Systems for Optimizing Sequences of Airspace Partitions. *Pages ISBN: 978–1–7281–5381–0 of: AIDA-AT 2020, 1st conference on Artificial Intelligence and Data Analytics in Air Transportation*. 2020 International Conference on Artificial Intelligence and Data Analytics for Air Transportation (AIDA-AT). Singapour, Singapore: IEEE. 12, 13, 64

GOMEZ COMENDADOR, VICTOR, VALDÉS, ROSA, VIDOSAVLJEVIC, ANDRIJA, CIDONCHA, SANCHEZ, & ZHENG. 2019. Impact of trajectories' uncertainty in existing atc complexity methodologies and metrics for dac and fca sesar concepts. *Energies*, **12**(04), 1559. 5

GOMORY, RALPH E. 1958. Outline of an algorithm for integer solutions to linear programs. *Bulleting of the american mathematical society*, **64**(5), 275–278. 18

GUROBI. 2023. *Gurobi optimization*. *https://www.gurobi.com/*. Accessed: 16-01-2023. 82

HERMES, P., MULDER, M., VAN PAASSEN, M. M., L. BOERING, J. H., & HUISMAN, H. 2009. Solution-space-based complexity analysis of the difficulty of aircraft merging tasks. *Journal of aircraft*, **46**(6), 1995–2015. 15

HISTON, J., LI, L., & HANSMAN, R. J. 2010 (Oct). Airspace structure, future atc systems, and controller complexity reduction. *Pages 4.A.4–1–4.A.4–14 of: 29th digital avionics systems conference*. ix, 14, 15

HOLLAND, JOHN. 1992. *Adaptation in natural and artificial systems : an introductory analysis with applications to biology, control, and artificial intelligence*. 1st MIT press ed. edn. Cambridge Mass.: MIT Press. 19

ICAO. 2001. *Air Traffic Services: Air Traffic Control Service, Flight Information Service, Alerting Service*. Tech. rept. 2

ICAO. 2016. *Doc 4444. Air Traffic Management: Procedures for Air Navigation Services*. Tech. rept. 1

IDRIS, H., VIVONA, R., GARCIA-CHICO, J., & WING, D. 2007 (Oct). Distributed traffic complexity management by preserving trajectory flexibility. *Pages 3.B.6–1–3.B.6–13 of: 2007 ieee/aiaa 26th digital avionics systems conference*. 15

IDRIS, HUSNI, DELAHAYE, DANIEL, & WING, DAVID. 2009 (Jun). Distributed trajectory flexibility preservation for traffic complexity mitigation. *In: 8th usa/europe air traffic management research and development seminar*. 15

IVANOV, NIKOLA, JOVANOVIĆ, RADOSAV, FICHERT, FRANK, STRAUSS, ARNE, STARITA, STEFANO, BABIĆ, OBRAD, & PAVLOVIĆ, GORAN. 2019. Coordinated capacity and demand management in a redesigned air traffic management value-chain. *Journal of air transport management*, **75**, 139 – 152. 13

KENNEDY, J., & EBERHART, R. 1995. Particle swarm optimization. *Pages 1942–1948 vol.4 of: Proceedings of icnn'95 - international conference on neural networks*, vol. 4. 19

KIRKPATRICK, S., GELATT, C. D., & VECCHI, M. P. 1983. Optimization by simulated annealing. *Science*, **220**(4598), 671–680. 20

KOPARDEKAR, PARIMAL, BILIMORIA, KARL, & SRIDHAR, BANAVAR. 2007 (Sep). Initial concepts for dynamic airspace configuration. *In: 7th aiaa aviation technology, integration and operation conference*. 12

KORN, BERND, EDINGER, CHRISTIANE, KÜGLER, DIRK, PÜTZ, THOMAS, HASSA, OLIVER, & MOHRHARD, BERND. 2009 (Oct). Is sectorization really required for efficient en-route air traffic control? *In: Ceas 2009 european air and space conference*. 13

KÜNNEN, JAN-RASMUS, & STRAUSS, ARNE K. 2022. The value of flexible flight-to-route assignments in pre-tactical air traffic management. *Transportation research part b: Methodological*, **160**, 76–96. 13, 64

LAND, A. H., & DOIG, A. G. 1960. An automatic method of solving discrete programming problems. *Econometrica*, **28**(3), 497–520. 18

LAUDEMAN, SHELDEN, STEPHEN G., BRANSTROM, ROBERT B., & BRASIL, CONNIE L. 1998 (Apr). *Dynamic density: An air traffic management metric*. Tech. rept. 19980210764. NASA Ames research center. 16

LEE, K., FERON, E., & PRITCHETT, A. 2007 (July). Air traffic complexity: An input-output approach. *Pages 474–479 of: 2007 american control conference*. 16

L.R. FORD, JR., & D.R. FULKERSON. 1958. A suggested computation for maximal multi-commodity network flows. *Management science*, **5**(1), 97–101. 18

LULLI, GUGLIELMO, & ODONI, AMEDEO. 2007. The european air traffic flow management problem. *Transportation science*, **41**(11), 431–443. 12

MARCOS, RODRIGO, HERRANZ, RICARDO, RODRÍGUEZ VÁZQUEZ, RITA, GARCÍA-ALBERTOS, PEDRO, & CANTÚ ROS, OLIVA G. 2018 (Dec). Application of machine learning for atm performance assessment - identification of sources of en-route flight inefficiency. *In: Proceedings of the 8th sesar innovation days (sids)*. 5

MARTINEZ, STEPHANE, CHATTERJI, GANO, SUN, DENGFENG, & BAYEN, ALEXANDRE. 2007 (Aug). A weighted-graph approach for dynamic airspace configuration. *In: Aiaa guidance, navigation and control conference and exhibit*. 12

MARTINS, ANA, FINCK, TOBIAS, MOLLWITZ, VILMAR, KLING, FANNI, & ROHÁCW, DÁNIEL. 2019 (Dec). Feasibility study of flight centric mode of operations: A human performance approach. *In: Proceedings of the 9th sesar innovation days (sids)*. 24

MATEOS, MANUEL, MARTÍN, IGNACIO, GARCÍA, PEDRO, HERRANZ, RICARDO, CANTÚ-ROS, OLIVA GARCÍA, & PRATS, XAVIER. 2020 (September). Full-scale pre-tactical route prediction - machine learning to increase pre-tactical demand forecast accuracy. *In: Proceedings of the 9th international congress on research in air transportation (ICRAT)*. 2

MECKIFF, COLIN, CHONE, RENAUD, & NICOLAON, JEAN-PIERRE. 1998. The tactical load smoother for multi-sector planning. *In: 2nd usa/europe air traffic management r&d seminar*. 14

MONDOLONI, STEPHANE, & LIANG, DIANA. 2001. Airspace fractal dimensions and applications. *In: 3rd usa/europe atm r&d seminar*. 14

NETWORK MANAGER. 2018. *ATFCM users manual*. Tech. rept. 2

ODONI, AMEDEO R. 1987. The flow management problem in air traffic control. *Pages 269–288 of: Flow control of congested networks*. Springer. 12, 51

PERFORMANCE REVIEW COMMISSION. 2020. *ATM Cost-Effectiveness (ACE) 2018 Benchmarking Report*. Tech. rept. Federal Aviation Administration. 10

PILON, NADINE, COOK, ANDREW, RUIZ, SERGIO, BUJOR, ANDRADA, & CASTELLI, LORENZO. 2016 (8-10 November). Improved flexibility and equity for airspace users during demand-capacity imbalance - an introduction to the user-driven prioritisation process. *In: Proceedings of the 6th sesar innovation days (sids)*. 5, 12

POURTAKLO, NASIM VAKILI, & BALL, MICHAEL. 2009. Equitable allocation of enroute airspace resources. *In: Proceedings of the 8th USA/Europe ATM R&D Seminar*. 4

PRANDINI, MARIA, PIRODDI, LUIGI, PUECHMOREL, STEPHANE, & BRÁZDILOVÁ, SILVIE LUISA. 2009. *ifly deliverable d3.1 complexity metrics applicable to autonomous aircraft*. Tech. rept. Project no. TREN/07/FP6AE/S07.71574/037180 IFLY, Brussels. 16

PRANDINI, MARIA, PUTTA, VAMSI, & HU, JIANGHAI. 2012. Air traffic complexity in future air traffic management systems. *Journal of aerospace operations*, **1**(3), 281–299. 16

PREVOT, THOMAS, & LEE, PAUL. 2011. Trajectory-based complexity (tbx): A modified aircraft count to predict sector complexity during trajectory-based operations. *2011 ieee/aiaa 30th digital avionics systems conference*, 10. 15

PUECHMOREL, STÉPHANE, & DELAHAYE, DANIEL. 2009 (Mar). New trends in air traffic complexity. *In: Enri international workshop on atm/cns, eiwac*. 16

RICHETTA, OCTAVIO, & ODONI, AMEDEO R. 1993. Solving optimally the static ground-holding policy problem in air traffic control. *Transportation science*, **27**(3), 228–238. 12, 51

RUIZ, SERGIO, GUICHARD, LAURENT, PILON, NADINE, & DELCOURTE, KRIS. 2019. A new air traffic flow management user-driven prioritisation process for low volume operator in constraint: Simulations and results. *Journal of advanced transportation*, **2019**, 21. Article ID 1208279. 5, 12

SERGEEVA, MARINA, DELAHAYE, DANIEL, ZERROUKI, LEILA, & SCHEDE, NICK. 2015. Dynamic airspace configurations generated by evolutionary algorithms. *Pages 1–14 of: Proceedings of the 34th ieee/aiaa digital avionics systems conference (dasc)*. IEEE and AIAA. 12, 13, 74

SERGEEVA, MARINA, DELAHAYE, DANIEL, MANCEL, CATHERINE, & VIDOSAVLJEVIC, ANDRIJA. 2017. Dynamic airspace configuration by genetic algorithm. *Journal of traffic and transportation engineering (english edition)*, **4**(3), 300 – 314. 12, 13, 74

SESAR JOINT UNDERTAKING. 2012. *SESAR Concept Of Operations Step 1*. Tech. rept. Brussels. 8

SESAR JOINT UNDERTAKING. 2014. *SESAR Concept Of Operations Step 2, Edition 2014*. Tech. rept. Brussels. 8

SESAR JOINT UNDERTAKING. 2015. *European ATM Master Plan. The roadmap for delivering high performing aviation for Europe*. Tech. rept. SESAR, Brussels. 8

SESAR JOINT UNDERTAKING. 2016. *STEP1 V3 Final Complexity Management OSED*. Tech. rept. Brussels. 5, 14

SESAR JOINT UNDERTAKING. 2020. *European ATM master plan*. Tech. rept. Brussels. 7, 8

SESAR JOINT UNDERTAKING. 2021. *SESAR solutions catalogue 2021*. Tech. rept. Brussels. 8

SESAR PJ08 CONSORTIUM. 2019. *AAM Project - SESAR Solution PJ.8-01 FINAL SPR-INTEROP/OSED for V2*. Tech. rept. 7, 13, 39

SESAR PJ09 CONSORTIUM. 2019. *D1.2 Final Project Report*. Tech. rept. 39

SESAR PJ10-01B CONSORTIUM. 2019. *PROSA Project - SESAR Solution PJ10-01b Final SPR-INTEROP/OSED for V2, Ed 00.03.02*. Tech. rept. 7, 13, 26

SESAR PJ19 CONSORTIUM. 2019 (May). *SESAR Concept of Operations (CONOPS 2019)*. Tech. rept. Deliverable D2.5. Edition 01.00.00. 39

SRIDHAR, BANAVAR, SHETH, KAPIL S., & GRABBE, SHON. 1998 (December 1-4). Airspace complexity and its application in air traffic management. *In: 2nd usa/europe air traffic management research and development seminar*. 16

STARITA, STEFANO, JOVANOVIC, RADOSAV, IVANOV, NIKOLA, STRAUSS, ARNE, & FRANK, FICHERT. 2021. Strategic cross-border capacity planning under uncertainty. *In: Proceedings of the 11th sesar innovation days (sids)*. 13, 64

TANG, JIANGJUN, ALAM, SAMEER, LOKAN, CHRIS, & ABBASS, HUSSEIN A. 2012. A multi-objective approach for dynamic airspace sectorization using agent based and geometric models. *Transportation research part c: Emerging technologies*, **21**(1), 89 – 121. 12

TERRAB, MOSTAFA, & ODONI, AMEDEO R. 1993. Strategic flow management for air traffic control. *Operations research*, **41**(1), 138–152. 12, 51

TOGA PROJECTS. 2018. *Cost index database v1.3.1*. Tech. rept. Available from: https://www.togaprojects.com/documentation. 53

TOSIC, VOJIN, & BABIC, OBRAD. 1995. Air route flow management — problems and research efforts. *Transportation planning and technology*, **19**, 63–72. 42

TRANDAC, H., & VU DUONG. 2002. A constraint-programming formulation for dynamic airspace sectorization. *Pages 1C5–1C5 of: Proceedings. the 21st digital avionics systems conference*, vol. 1. 12

TREIMUTH, TAMBET. 2018 (1). *Dynamic optimization of airspace sector grouping*. Ph.D. thesis, Université de Toulouse. 3, 12, 13, 64, 66, 74

VERLHAC, C. AND MANCHON, S. 2005. *Improved Configuration Optimiser Methodology to use a Decision Support Tool, EEC Technical/Scientific Report No. 2005-015*. Tech. rept. Brussels. 12, 13, 27, 64, 93

VIDOSAVLJEVIC, ANDRIJA, & DELAHAYE, DANIEL. 2017. Decision support tool for airspace configuration. *Dac journée*, February. 12, 13, 64, 76

VIDOSAVLJEVIC, ANDRIJA, DELAHAYE, DANIEL, & TOŠIĆ, VOJIN. 2017. Homotopy Route Generation Model for Robust Trajectory Planning. *Pages pp 69–88 of:* ENRI (ed), *Air Traffic Management and Systems II*. Lecture Notes in Electrical Engineering, vol. 420. Springer. 25, 80

VRANAS, PETER, BERTSIMAS, DIMITRIS, & ODONI, AMEDEO. 1992. The multi-airport ground-holding problem in air trafic control. *Massachusetts institute of technology (mit), sloan school of management, working papers*, **42**(01). 12, 51

VRANAS, PETER, BERTSIMAS, DIMITRIS, & ODONI, AMEDEO. 1994. Dynamic ground-holding policies for a network of airports. *Transportation science*, **28**(11). 12, 51

WALTER, LEIF, PUSCH, MANUEL, HOLZAPFEL, FLORIAN, & KNORR, DAVE. 2010. Quantifying trajectory uncertainty using a sensitivity-based complexity metric component. *In: Proceedings of the 4th international congress on research in air transportation (ICRAT)*. Budapest, Hungary: Eurocontrol and FAA. 16

WEISE, THOMAS. 2009. *Global optimization algorithms - theory and application*. 19

XU, YAN, & PRATS, XAVIER. 2017. Including linear holding in air traffic flow management for flexible delay handling. *Journal of air transportation*, **25**(4), 123–137. 52

XU, YAN, DALMAU, RAMON, MELGOSA, MARC, MONTLAUR, ADELINE, & PRATS, XAVIER. 2018a. Alternative trajectory options for delay reduction in demand and capacity balancing. *In: Proceedings of the 8th international congress on research in air transportation (ICRAT)*. Castelldefels, Spain: Eurocontrol and FAA. 12, 52, 57

XU, YAN, PRATS, XAVIER, & DELAHAYE, DANIEL. 2018b. Synchronization of traffic flow and sector opening for collaborative demand and capacity balancing. *In: Proceedings of the 37th digital avionics systems conference (dasc)*. IEEE/AIAA. 6, 13, 64

XU, YAN, DALMAU, RAMON, MELGOSA, MARC, MONTLAUR, ADELINE, & PRATS, XAVIER. 2020a. A framework for collaborative air traffic flow management minimizing costs for airspace users: Enabling trajectory options and flexible pre-tactical delay management. *Transportation research part b: Methodological*, **134**, 229 – 255. 12, 52

XU, YAN, PRATS, XAVIER, & DELAHAYE, DANIEL. 2020b. Synchronised demand-capacity balancing in collaborative air traffic flow management. *Transportation research part c: Emerging technologies*, **114**(Mar), 359 – 376. 6, 13, 64, 66, 74